12-2012

GENETIC ANALYSIS OF THE HIPPO PATHWAY IN MOUSE LIVER

Li Lu

Approval Sheet page

GENETIC ANALYSIS OF THE HIPPO PATHWAY IN MOUSE LIVER

GENETIC ANALYSIS OF THE HIPPO PATHWAY IN MOUSE LIVER

by

Li Lu, M.S.

APPROVED:

_____

Randy L. Johnson, Ph.D., Supervisory Professor

_____

Richard R. Behringer, Ph.D.

_____

Michelle C. Barton, Ph.D.

_____

Pierre D. McCrea, Ph.D.

_____

Milton J. Finegold, M.D.

APPROVED:

_____

Dean, The University of Texas

Graduate School of Biomedical Sciences at Houston

GENETIC ANALYSIS OF THE HIPPO PATHWAY IN MOUSE LIVER

A

DISSERTATION

Presented to the Faculty of

The University of Texas

Health Science Center at Houston,

The University of Texas

M.D. Anderson Cancer Center,

and

Baylor College of Medicine

In Fulfillment

of the Requirements

for the Degree of

DOCTOR OF PHILOSOPHY

by

Li Lu, M.S.

Houston, Texas

July 2012

DEDICATION

I dedicate this work to my family whose love supported me in every way.

ACKNOWLEDGMENTS

I have had much help and support during my PhD study and would like to sincerely thank those who have greatly impacted my personal and professional life. First and foremost, I would like to thank my supervisor, Dr. Randy Johnson, for giving me the opportunity to study and work in his lab, and supporting my PhD education through providing material and financial supports. I definitely would not be in the position I am in today had I selected another advisor. Our lab's senior research assistant, Guijin Lu has been very helpful with mouse genotyping and he always been ready to assist me. Previous lab members Ying Li and Pu Liu also helped me a lot when I just joined the lab.

I want to sincerely thank all the faculty members who have served on my committees, especially Dr. Richard Behringer and Dr. Georg Halder (moved to K.U.Leuven, Belgium). I appreciate being invited to participate in Dr. Behringer's Mouse Club. It is not only a place for scientific communication, but also a wonderful training opportunity full of fun. Dr. Halder's lab was our best neighbor that generously shared reagents and instruments, as well as helpful thoughts. The other advisory committees members were: Dr. Jeffrey Rosen (Baylor college of Medicine) and Dr. Khandan Keyomarsi. Although they were replaced in my other two committees due to the change in direction of my project, I truly appreciate their support on my previous work. Dr. Rosen was always very responsive and open to talk, and his lab has greatly helped on my experimental techniques.

Words cannot express my gratitude for all the help and support that Dr. Milton Finegold (Texas Children's Hospital) has given to me. Besides spending lot of time on

going through slides and teaching me liver pathology, Dr. Finegold also taught me about successful personality and professional performance. Dr. Michelle Barton is the only women scientist in my supervisory committee. I sincerely appreciate Dr. Barton's effort in training my scientific thinking by asking inspiring questions, and her comments are always helpful and encouraging. I would also like to thank Dr. Pierre McCrea for serving on my supervisory committee after Dr. Halder moved to Belgium for his new position.

So many friends have helped me during this PhD journey that unfortunately I do not have enough room here to thank them all individually. I will miss the private talks with Dr. Aimee Anderson, who is not only a nice person but also an enthusiastic scientist who inspired me a lot. I appreciate her helpful discussions on both science and art.

I would like to thank Aimee Anderson, Sarah Woodfield, Jeannette Tucker, Patty Dimarco, Kathleen Gajewski, Elisabeth Lindheim and Patricia Lopez for their kindly help with editing my writings during their busy schedules.

Additionally, I would like to thank our department and G&D program for establishing a wonderful research and training environment. I greatly appreciate Jodie and Hank for their training on microscopy. Elisabeth arranged fantastic students' activities and events, and has always been very caring and helpful for students' lives away from lab.

Last but not the least, I want to thank UT-HSC, MD Anderson, GSA, SIC, and GSBS for their support on my PhD training. Our GSBS has the best team that supports students' training by paying close attention to their concerns and issues. I

would like to give my special gratitude and thanks to Dr. Victoria Knutson who always listens to students and offers kindly help.

GENETIC ANALYSIS OF THE HIPPO PATHWAY IN MOUSE LIVER

Publication No. _____

Li Lu

Supervisory Professor: Randy L. Johnson, Ph.D.

Cancer therapy and tumor treatment remain unsolved puzzles. Genetic screening for tumor suppressor genes in *Drosophila* revealed the Hippo-signaling pathway as a kinase cascade consisting of five core components. Disrupting the pathway by deleting the main component genes breaks the balance of cell proliferation and apoptosis and results in epithelial tissue tumorigenesis. The pathway is therefore believed to be a tumor suppressor pathway. However, a corresponding role in mammals is yet to be determined. Our lab began to investigate the tumor suppression function of the potent mammalian Hippo pathway by putting floxed alleles into the mouse genome flanking the functional-domain-expressing exons in each component (*Mst1, Mst2, Sav1, Lats1* and *Lats2*). These mice were then crossed with different cre-mouse lines to generate conditional knockout mice. Results indicate a ubiquitous tumor suppression function of these components, predominantly in the liver. A further liver specific analysis of the deletion mutation of these components, as well as the *Yap/Taz* double deletion mutation, reveals essential roles of the Hippo pathway in regulating hepatic quiescence and embryonic liver development. One of the key cellular mechanisms for the Hippo pathway's involvement in these liver biological events is likely its cell cycle regulation function. Our work will help to develop potential therapeutic approaches for liver cancer.

TABLE OF CONTENTS

TITLE PAGE iii

DEDICATION iv

ACKNOWLEDGEMENTS v

ABSTRACT viii

TABLE OF CONTENTS ix

LIST OF ILLUSTRATIONS xii

LIST OF TABLES xiv

ABBREVIATIONS xvi

APPENDIX xix

CHAPTER 1: BACKGROUND 1

1.1 *Drosophila* Hippo pathway 3

1.2 Mammalian counterparts of the Hippo pathway components 7

1.3 Liver function and liver development 12

1.4 Liver cancer 18

1.5 Organ size contol 19

1.6 Liver regeneration 22

CHAPTER 2: RESEARCH RATIONALE 25

2.1 Role of Hippo pathway in mouse liver tumorigenesis 26

2.2 Role of Hippo pathway in mouse liver regeneration 32

CHAPTER 3: MATERIAL AND METHODS 34

3.1 Breeding and generation of mice with *sav1* deletion, *mst1*;*mst2* double deletion, *lats1*;*lats2* double deletion, and *Yap;Taz* double deletion 35

3.2 Genotyping 36

3.3 Tissue processing and paraffin slides preparation 41

3.4 Immunostaining with paraffin slides 41

3.5 Frozen section and immunostaining (only for oval cell markers) 42

3.6 PAS staining 47

3.7 Quantitative PCR 47

3.8 Microarray analysis 48

3.9 Protein extraction 48

3.10 Western blot 49

3.11 Hepatocytes enrichment (liver perfusion) 50

3.12 Partial hepatectomy 51

3.13 Statistical Analysis 52

CHAPTER 4: RESULTS 53

4.1 *Mst* and *Sav1* are required for liver tumor suppression 54

4.2 *Yap* is activated in *alb-cre;mst1/2* and *alb-cre;sav1* liver tumor tissues 59

4.3 *Lats* is required for liver development 62

4.4 Biliary hyperplasia and liver stem cell activation in *Mst, Sav1* and *Lats* mutants65

4.5 *Yap* and *Taz* are both dominant downstream inhibition targets of *Lats* 72

4.6. *Yap* increase/activation correlates with BEC expansion in *Lats* mutant 80

4.7 Notch signaling is activated in *Lats* mutant periportal area 83

4.8 *Yap* and *Taz* are activated during liver regeneration 85

4.9 *Yap/Taz* null and *Mst1/2* null livers show impaired regeneration 87

4.10 Hippo signaling regulates the timing of hepatocyte proliferation 90

CHAPTER 5: DISCUSSION 95

5.1 *Mst* in liver tumor suppression 96

5.2 *Lats* in liver development 100

5.3 The Hippo pathway in liver size control 105

CHAPTER 6: FUTURE STUDIES 109

APPENDIX 115

BIBLIOGRAPHY 119

VITA 149

LIST OF ILLUSTRATIONS

Figure 1. Normal adult mouse liver plate and portal triad structure 17

Figure 2. *Sav1* deletion in mammary gland and *Mst1/2* deletion in intestine 30

Figure 3. Hepatoma formation in *Mst* and *Sav1* mutants 55

Figure 4. Elevated hepatocytes proliferation contributes to both *Mst* and *Sav* mutants' liver enlargement 56

Figure 5. Two-month old *Mst1/2* double deleted liver 58

Figure 6. *Yap* activation in *Sav1* and *Mst* mutants 60

Figure 7. Quantitative analysis of *Lats1* and *Lats2* gene deletion efficiency mediated by *alb-cre* 62

Figure 8. PAS staining on P0 Lats mutant livers 63

Figure 9. Global gene expression profiles of the *Lats1/2* double mutants on P0 64

Figure 10. Oval cell activation and inflammatory response in *Mst* and *Sav1 mutants* 66

Figure 11. BEC hyperplasia in *Lats1/2* mutants at P0 67

Figure 12. Antibody characterization of liver oval cell 70

Figure 13. *Yap* and *Taz* deletion efficiencies by *alb-cre* 72

Figure 14. *Yap/Taz* deletion rescues *Lats1/2* mutants in a dose-dependant manner 74

Figure 15. Glycogen level comparison in the rescue experiment by PAS staining 75

Figure 16. Deletion of one allele of *Yap* decreases *Lats1/2* double mutants' ductal

hyperplasia 76

Figure 17. Increased hepatocyte turnover in *Yap/Taz* double deleted liver 78

Figure 18. Bile duct malformation in *Yap/Taz* double deleted liver 79

Figure 19. BEC proliferation in *Lats* mutants starting from E17.5 81

Figure 20. *Yap* positive cells expand in *Lats* mutant 82

Figure 21. Notch signaling activation in the periportal area of E18.5 *Lats* mutants 84

Figure 22. *Yap* and *Taz* activities during normal liver regeneration 86

Figure 23. Both *Mst1/2* double mutants and *Yap/Taz* double mutants can regenerate to about 70% of their original sizes 89

Figure 24. Cell cycle progression is delayed during *Yap/Taz* double mutants' regeneration 92

Figure 25. *STAT3* activity during regeneration 94

LIST OF TABLES

Table 1. Mammalian counterparts of the Hippo pathway core components 8

Table 2. Primer information 37

Table 3. PCR product size 39

Table 4. Antibody information 44

LIST OF DIAGRAMS

Diagram 1. *Drosophila* Hippo pathway 6

Diagram 2. Biochemical interactions between the mammalian Hippo pathway components 9

Diagram 3. Molecular signals regulating the bile duct development 14

Diagram 4. Notch signaling 15

Diagram 5. Potential Hippo pathway function in bile duct development 103

Diagram 6. Both *Akt* and *Mst* can inhibit either *mTORC* or *Yap/Taz* 108

Diagram 7. Hypothesized *Yap* function in biliary cell differentiation 112

ABBREVIATIONS

Alb	Albumin
AGS	Alagille syndrome
Ban	Bantam
BEC	Biliary epithelial cell
BrdU	Bromodeoxyuridine
CAGGS	CMV enhancer/chicken beta- actin
Cdks	Cyclin-dependent kinases
C/EBP	CCAAT/enhancer binding protein
Crb	Crumbs
Ctgf	Connective tissue growth factor
DEN	Diethylnitrosamine
DEPC	Diethylpyrocarbonate
Diap1	*Drosophila* inhibitor of apoptosis protein 1
DSB	Double strand break
Ex	Expanded
Hth	Homothrax
IHBD	Intra-hepatic bile duct

Lats	Large tumor suppressor
LCIS	Lobular carcinoma in situ
LCD	LATS conserved domains
Mad	Mothers against Dpp
Mats	Mob-as-tumor-suppressor
Mer	Merlin
Mm	Millimeter
MMTV	Mouse mammary tumor virus
Mst	Mammalian Ste20-like kinases
mTOR	Mammalian target of rapamycin
mTORC	Mammalian target of rapamycin complex
NDR	Nuclear Dbf2-related
OCT	Optimal Cutting Temperature
OSM	Oncostatin M
PBD	Protein binding domain
PCR	Polymerase chain reaction
PPxY	P, proline; X, any amino acid; Y, tyrosine
PTEN	Phosphatase and tensin homolog
RT	Room temperature

SARAH	Salvador, RASSF1, Hippo
SCID	Severe Combined Immune Deficient
Sd	Scalloped
S6K	S6 kinase (ribosomal protein p70)
STAT3	Signal transducer and activator of transcription 3
Taz	Transcriptional co-activator with PDZ-binding motif
TEB	Terminal end bud
TOR	Target of rapamycin
TSC	Tuberous sclerosis complex
PH	Partial hepatectomy
Wts	Warts
Yap	Yes Associated Protein
Yki	Yorkie

APPENDIX

APPENDIX 1. Liver phenotypes of the mutant mice from the rescue experiment 115

APPENDIX 2. Decreased phospho-*Lats1* in *Yap/Taz* double mutants 117

APPENDIX 3. *Yap* and *Taz* activities during *Mst1/2* double mutants' regeneration 118

CHAPTER 1: BACKGROUND

Genetic alteration can cause many human diseases, including developmental defects in fetus and tumor development in adults. In searching for cures, scientists have stepped into a long journey of unveiling disease mechanisms starting from identifying genes that are important for organ development and tissue homeostasis. These are the two main topics being pursued for decades. With the advances of research techniques and the discoveries of genetic modification tools, high-throughput genetic analysis has been established and many genes and pathways essential for organ development and tissue homeostasis have been identified, one of which is the Hippo pathway.

At the time we started our project, our knowledge about the Hippo pathway is limited to *Drosophila* animal model and the *in vitro* biochemical interactions between the mammalian components. For the Hippo pathway's function in the mammalian system, although biochemical studies provided valuable information on protein-protein interactions, they have limitations in addressing how these Hippo pathway main components function in a true biological environment and how they contribute to the development or homeostasis of an organ or an animal as a whole. We therefore generated genetically engineered mouse models of the main components, and started to investigate the Hippo pathway's *in vivo* function in several organs. We later focused our study on mouse liver because our preliminary data indicated a certain tissue-specificity of the Hippo pathway in liver. We found that deregulation of the Hippo pathway affected several important aspects of the liver, including inflammatory response, liver stem cell activation, liver development, and liver regeneration. Our study will help understand the Hippo pathway's tumor suppressor function in

mammals, and may put new insights into the cancer treatments, especially to the liver cancer treatments.

1.1 *Drosophila* Hippo pathway

The Hippo signaling pathway was originally identified in *Drosophila* by genetic screening for genes involved in cell growth and proliferation. The first identified pathway component is *Wts*, whose deletion results in cell autonomous proliferation and epithelium over growth [1,2]. *Warts* (*Wts*) is named for a phenotype in which mutated cells proliferate dramatically in imaginal discs and grow into wart-like mitotic clones on adult. Other pathway components were subsequently identified by similar phenotypes after gene deletion in imaginal discs. These components are: Ste20-like protein kinase *Hpo*, WW domain-containing protein *Sav*, and the adaptor protein *Mats* [2,3,4,5,6,7,8,9]. Biochemical studies further put them together as a kinase cassette (*Hpo/Sav1/Mats/Wts*): *Hpo* phosphorylates and activates *Wts* [8] in the presence of *Sav* and *Mats* that act as scaffolding proteins to facilitate the interaction between *Hpo* and *Wts*. *Hpo* and *Wts* are both *Ser/Ter* kinases capable of being activated by autophosphorylation [10,11], although *Wts* activation can also be regulated by *Hpo* phosphorylation. *Hpo* can also phosphorylate *Sav* and *Mats* [8,9], which further facilitates *Wts* binding and activation. The sequential phosphorylation and activation of the Hippo pathway components explains the similarity and also the progressive severity of mutant phenotypes. Deletion of downstream component (*Wts*) results in a similar but more severe phenotype than that of an upstream component (*Hpo* or *Sav*).

Hpo/Sav/Mats/Wts is the core kinase cassette of the Hippo pathway. It functions to sense and mediate extracellular signal transduction to the cell nuclei. Although it is yet

unknown what the extracellular signals are in a normal tissue context, some intracellular regulators upstream of *Hpo/Sav1/Mats/Wts* kinase cassette have been identified, such as *Mer-Ex-Kibra* complex [12,13,14,15], *Fat* signaling [16,17,18,19,20], and *Lethal giant larvae* (*Lgl*) complex [21]. Among these regulators, the *Mer-Ex-Kibra* complex is the most important, as it activates the Hippo pathway through both *Hpo* and *Wts* phosphorylation. *Mer*, *Ex* and *Kibra* function redundantly in regulating Hippo signaling pathway and each one can function independent of the others. In the case of cell-cell contact inhibition, cell will stop growing when the Hippo pathway is activated by *Ex*, which is activated by binding with the transmembrane protein *Crb* upon its homodimerization between two adjacent cells [22]. This is one of the mechanisms by which the Hippo pathway regulates cell growth.

Although the *Hpo/Sav1/Mats/Wts* kinase cassette functions to suppress tissue growth, none of them is a nuclear transcription factor. By yeast two-hybrid screening, the nuclear transcriptional cofactor *Yki* was identified and has been demonstrated to be a dominant *Wts*-binding protein. Activated *Wts* can phosphorylate *Yki*, and this phosphorylation enables the binding of an adaptor protein, *14-3-3,* with *Yki*, which is then followed by *Yki* cytoplasmic tethering and functional suppression [23,24,25]. While nuclear-cytoplasmic translocation is believed to be the main mechanism of regulation for *Yki* function, there is also evidence that *Wts* can inhibit *Yki* through physical binding [23]. This finding further explains why the *Wts* deletion has the most severe phenotype compared to the deletion phenotypes of other the Hippo pathway components. *Yki* activity can also be suppressed by direct protein-protein binding between its WW-domains and the proline-rich sequences within PPXY motifs. This is

evidenced by *Yki* inhibition in association with *Ex*, *Kibra*, *Hpo* or *Wts* [26,27], all of which have the *PPXY* motifs. Although several Hippo pathway upstream regulators have been identified, *Yki* is so far the only known nuclear effecter of the *Drosophila* Hippo kinase cassette that bridges the cytoplamic *Hpo/Sav1/Mats/Wts* kinase cassette with nuclear target gene transcription.

Yki itself lacks a DNA binding domain. It has to associate with DNA-binding proteins to execute its gene transcription regulation function. Several associated transcription factors have been identified, such as *Sd* (initiates *diap1* gene expression) [28,29], Mad [30] and *Hth* [31] (for ban expression). *dE2F1* can also associate with *Yk*i and function synergistically with the *Yki/Sd* complex in promoting G1-to-S phase cell cycle progression [32]. This supports the notion that the Hippo pathway regulates cell cycle and proliferation and thus controls tissue growth.

In summary, *Hpo/Sav1/Wts/Mats* kinase cassette mediates signal transduction of extracellular stimuli down to the nuclear transcription cofactor *Yki*. The diverse transcription factor binding ability of *Yki* enables the Hippo pathway to function in multiple biological processes. The observations that deletion of any component in *Hpo/Sav/Wts/Mats* cassette or over-expression of *Yki* results in tissue over-growth and organ enlargement suggests that the Hippo pathway plays fundamental roles during organ size control and may also be a suppressing pathway during tumorigenesis, an uncontrolled cell proliferation process (**Diagram 1**).

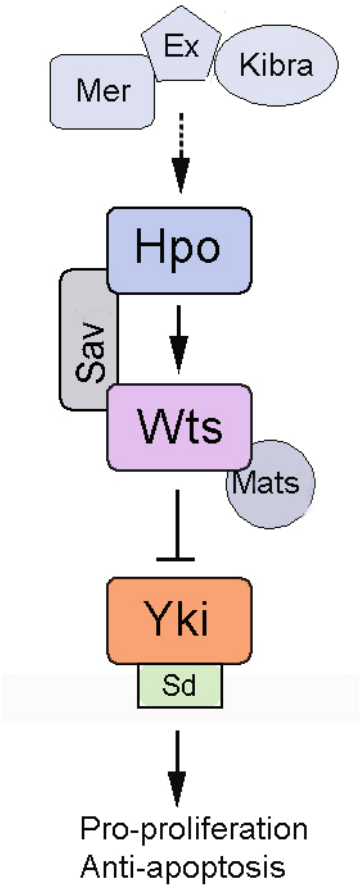

Diagram 1. *Drosophila* Hippo pathway. *Hpo* kinase is activated by *Mer/Ex/Kibra* complex). Activated *Hpo* kinase phosphorylates and activates kinase *Wts*, which is facilitated by *Sav* adaptor protein. Activated *Wts*, with another helper protein *Mats*, phosphorylates the nuclear transcription cofactor *Yki*. This phosphorylation, however, inhibits *Yki* function. Unphosphorylated *Yki* will associate with transcription factors, such as *Sd*, to initiate target-gene expression, some of which are known to be pro-proliferation and against apoptosis.

1.2 Mammalian counterparts of the Hippo pathway components.

The Hippo pathway is evolutionarily conserved. Many core components exist across species, including yeast, flies, rodents, and Homo sapiens. Most mammalian counterparts have functionally redundant paralogs as shown in **Table 1**. Biochemical interactions among mammalian counterparts are similar to those in *Drosophila* (**Diagram 2**) [8,9,23,33,34,35]. Briefly, *Mst* phosphorylates and activates *Lats* which further phosphorylates *Yap/Taz*. Phosphorylated *Yap/Taz* binds to adaptor protein *14-3-3* and is exported from the nucleus [35]. *Sav1* and *Mob1* function to facilitate the interaction between *Mst* and *Lats*.

Table1. Mammalian counterparts of the Hippo pathway core components

Drosophila	**Mouse/Human**	**References**
Hpo	*Mst1*	[36,37,38,39,40,41]
	Mst2	
Sav	*WW45/Sav1*	[42]
Warts	*Lats1*	[43,44]
	Lats2	
Mats	*Mob1*	[45,46,47]
Yki	*Yap*	[34,48,49,50,51]
	Taz/WWTR1	

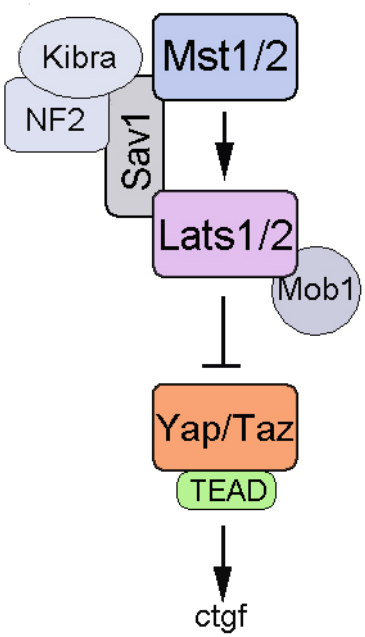

Diagram 2. Biochemical interactions between the mammalian Hippo pathway components. *Lats1/2* (*Wts* orthologs) can be activated through phosphorylation by *Mst1/2* and *Kibra/NF2* (*Mer* ortholog) complex, both of which are facilitated by the adaptor protein *Sav1* (*Sav* ortholog). Activated *Lats1/2* further phosphorylates but inhibits *Yap/Taz* (*Yki* ortholog), which is facilitated by another adaptor protein *Mob1*. Unphosphorylated *Yap/Taz* associates with the transcription factor *TEAD* and initiates the target gene expression, such as *ctgf*.

Mst1 and *Mst2* are *Ste20*-like kinases that ubiquitously expressed. The C-terminal SARAH domain mediates *Mst1* and *Mst2* self-binding and also binding with other SARAH-containing proteins such as *Sav1* and *Nore1* (a member of the Rassf tumor suppressor family). The *Mst /Sav1* complex functions as mammalian Hippo signaling that inhibits growth. *Mst/Nore1* complex plays an important role during T-cell development. *Mst* inhibitory effect on cell growth and survival is also represented by its involvement in stress-induced cell apoptosis, during which *Mst* is activated by caspase-dependent cleavage into a 36 kDa protein kinase which translocates from the cytosol to the nucleus where it contributes to chromatin condensation during apoptosis [52]. Overall, *Msts* exert a negative effect on cell growth and survival.

Lats belongs to the *NDR/Lats* kinase family and was known to be a tumor suppressor before it was related with the Hippo pathway. *Lats* expresses ubiquitously and plays essential roles in various cellular events such as proliferation, cytoskeletal dynamics, cell migration, mitotic exit, transcriptional regulation and genetic maintenance of stability maintenance [53]. The multiple functions rely on its protein structure, which contains a protein-binding domain (PBD), a catalytic domain, two *Lats* conserved domains (*LCD*), and PPxY motifs. *Lats* potentially interacts with multiple cellular regulators and is thought to be a broad governor for cellular homeostasis. However, so far *Yap* and *Taz* are the only two identified substrates of *Lats*.

Sav1 (also named *WW45*) and *Mob1* are scaffold proteins that facilitate interaction between *Mst-Lats* and *Lats-Yap/Taz*, respectively. *Sav1* biochemically binds to *Mst1*, *Mst2* and *Rassf1* [54,55]. It has two *WW*-domains, which can bind to PPXY motifs within other proteins including *Lats* and *Yap/Taz*. Evidence shows that

NF2 (Mer ortholog) together with mammalian *Kibra* can phosphorylate and activate *Lats* by binding with *Sav1* [56]. Therefore, functions of mammalian *Sav1* are thought to be very similar to its *Drosophila* ortholog. *Mob1* is known to be required for the abscission of the midbody during cytokinesis. Other than this, little is known about *Mob1*.

Both *Yap* and *Taz* are mammalian orthologs of *Yki*, with *Yap* being more structurally similar to *Yki*. Yap has two *WW*-domains while *Taz* has only one [57]. *Taz* lacks an SH3-domain, which is present in *Yap*. The structural difference suggests that *Yap* but not *Taz* may be the predominant effecter of the mammalian Hippo pathway. Like *Yki*, both *Yap* and *Taz* lack a DNA binding domain, and must be associated with transcription factors to regulate target gene transcription. Computational prediction, based on domain-domain interaction, has identified many transcription factors as potential *Yap/Taz* associating-proteins, some of which are already known to be important for cell cycle regulation such as *C/EBP* and *P73*. The predicted transcription factor *TEF/TEAD* has been demonstrated to associate with *Yap/Taz* [58,59,60] and initiate *ctgf* gene expression [61,62]. *Ctgf* is required for chondrocyte proliferation, angiogenesis, extracellular matrix production and turnover. Moreover, *Yap* and *Taz* have distinct partners that regulate expression of different sets of target genes. For instance, *Taz* interacts with *TBX5* [63] and *Smad2/3/4* [64], while *Yap* interacts with *ErbB4* [65] and *Smad7* [66]. Both *Yap* and *Taz* can be phosphorylated and inhibited by *Lats*. They are the only two identified effectors of the mammalian Hippo signaling pathway.

1.3 Liver function and liver development

The liver is the largest solid organ of the body and has essential functions in metabolism, detoxification, and biosynthesis. It is located in the upper right-hand portion of the abdominal cavity, beneath the diaphragm and on top of the stomach and intestines. Nutrients (carbohydrate, fat and protein) from the intestine are further digested in the liver and the products are converted into other energy forms (protein, glucose, vitamins, etc.), which can be either stored or released into blood to meet body consumption. It also filters body wastes (bilirubin, ammonia) and toxins (alcohol, drugs and chemicals) from blood and transforms them into either water-soluble or bile-soluble materials for elimination through kidney or as feces, respectively. Therefore, liver functions as a guardian to keep the body healthy.

The major cell type of the liver is the hepatocyte, which constitute about 70% of the whole liver mass and are the main cell type that performs liver function [67]. The remaining 30% of cells are non-parenchymal cells, including BECs (Biliary Epithelial Cells, also called cholangiocytes), stellate cells, küpffer cells, and sinusoidal endothelial cells. Hepatocytes and BECs are epithelial cells that are derived from embryonic endoderm, while the other cells are from embryonic mesoderm. The development of the liver is a consequence of reciprocal tissue interactions between endoderm and nearby mesoderm. It originates from the ventral foregut endoderm around embryonic day 8.0 (E8.0) of gestation [68,69]. Hepatic diverticulum forms around E9.0 when it is adjacent to the developing heart. At E9.5, the hepatoblasts (progenitor cells of both hepatocytes and BECs) delaminate from the anterior portion of the hepatic diverticulum and invade the adjacent mesenchyme to form the liver bud

[70,71,72]. The reciprocal interactions between endoderm and mesoderm promote hepatoblast proliferation and stellate cell formation from the adjacent mesenchyme [73,74,75,76]. Between E10.5 to E15, the liver bud grows tremendously due to hepatoblast proliferation and latter on differentiation. Biliary epithelial cells emerge early on E11.5 [77] adjacent to the portal vein, and keep on differentiating and growing while interacting with adjacent endothelial cells and mesenchymal cells. Majority of the hepatoblasts differentiate into hepatocytes. The process continues untill the characteristic architecture of the liver comes into being, which is around birth.

Several signaling pathways are known to be important for BEC development and bile duct formation, such as TGFβ signaling, Wnt signaling, and Notch signaling (**Diagram 3**). TGFβ signaling forms a gradient with a higher level in the portal region and a lower level in the parenchymal region [78,79]. This gradient is important for biliary differentiation as evidenced by suppression of biliary differentiation following TGFβ pathway blockage, and ectopic biliary differentiation following TGFβ pathway activation. Wnt signaling is temporally activated during biliary differentiation, peaking around E12.5 but completely being suppressed after E16.5 [80]. Notch signaling (**Diagram 4**) promotes biliary differentiation and is activated specifically in the portal region by its ligand *jagged1*, which is secreted from portal endothelial cells [81,82,83]. This also explains why the bile ducts only forms close to the portal vein. This interaction between the portal hepatoblasts and the endothelial cells is essential for bile duct development. In human, *Jagged1* mutation is responsible for an autosomal dominant disorder called Alagille syndrome (AGS) [84,85,86]. *Jagged1* and *Notch2*

deleted mouse mimics the human AGS symptom, and therefore being used as a model for the study of bile duct development [81,82,87,88,89,90,91].

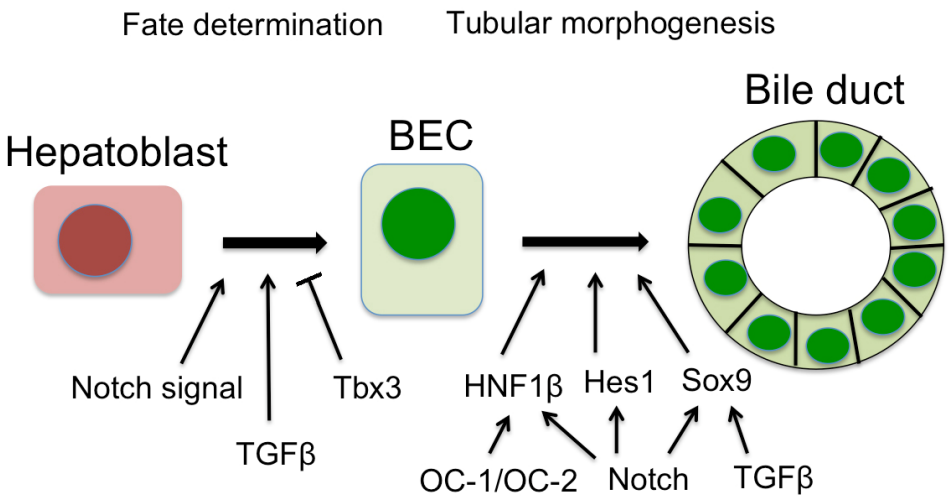

Diagram 3. Molecular signals regulating the bile duct development. The development of the bile duct can be roughly divided into two steps: the BEC fate determination, and the tubular morphogenesis. Some known factors that contribute to the fate determination step are the Notch signaling, *TGFβ* and *Tbx3*. While Notch and *TGFβ* promote BEC differentiation from hepatoblast, *Tbx3* inhibits the process. Notch and *TGFβ* also play a role during the tubular morphogenesis. Notch activates several targets genes that are important for the tubular morphogenesis, such as *HNF1β*, *Hes1* and *Sox9*, making it to be a major signaling that regulates the bile duct tubular morphogenesis.

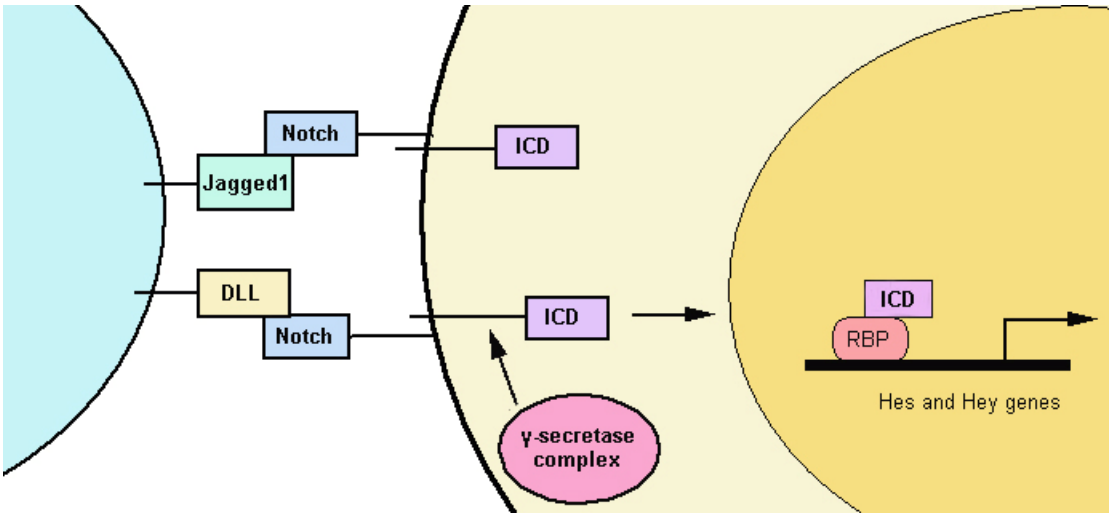

Diagram 4 Notch signaling. Notch signaling is activated via the binding of Notch trans-membrane receptor with ligand *Jagged1* or *DLL* (Delta-like ligand) from adjacent cells. The Notch intracellular domain (*ICD*) is then cleaved by *γ-secretase* and translocates into the nucleus, where it binds to Recombination signal-binding protein (*RBP*) and initiates *Hes* and *Hey* genes expression.

The characteristic architecture of the adult liver is the liver plate. In human and swine, the liver plate is lined up by connective tissues and segregated into a hexagon. However, murine liver plate is not clearly segregated by connective tissues, although it consists of similar anatomic structures: portal triads and a central vein (CV) (**Figure. 1 and Diagram 5**). A portal triad consists of a portal vein (PV), a bile duct and a hepatic artery. The hepatocytes line up as cords connecting the central vein with portal triads. Between the cords are sinusoids that are lined up with endothelial cells. The major liver immune cells, Küpffer cells, reside in the sinusoids. Between the hepatocytes and the endothelial cells is the space of Disse where the hepatic stellate cells reside. Following liver injury, stellate cells can be activated and secrete collagens that contribute to liver fibrosis and cirrhosis [92]. Liver architecture is important for proper liver function and liver homeostasis. Nutrients and biochemical materials from the small intestine enter into liver through the portal vein, and then together with blood from hepatic arteries pass through the sinusoids and empty into the central veins. On the other hand the bile acids secreted by hepatocytes are collected in hepatic canaliculus and flow towards bile ducts. The two flows ensure efficient nutrition transportation and biological material recycling between liver and intestine. Under some disease conditions, when liver architecture is disrupted by infiltrating immune cells or activated liver stem/progenitor cells, the blood and bile acid flows will be perturbed and the resulting hepatic injury may elevate the disease status to tumor development.

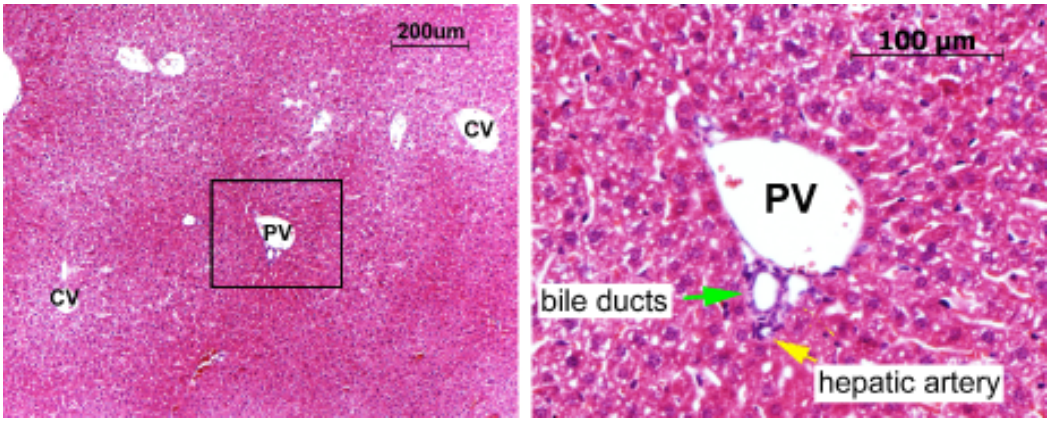

Figure 1. Normal adult mouse liver plate and portal triad structure. (A) HE staining shows typical mouse liver plate structure: central vein (CV) and portal vein (PV) surrounded by hepatocytes. (B) is a higher magnified view of the portal triad as squared in (A). Green arrow points to a bile duct and yellow arrow points to a hepatic artery.

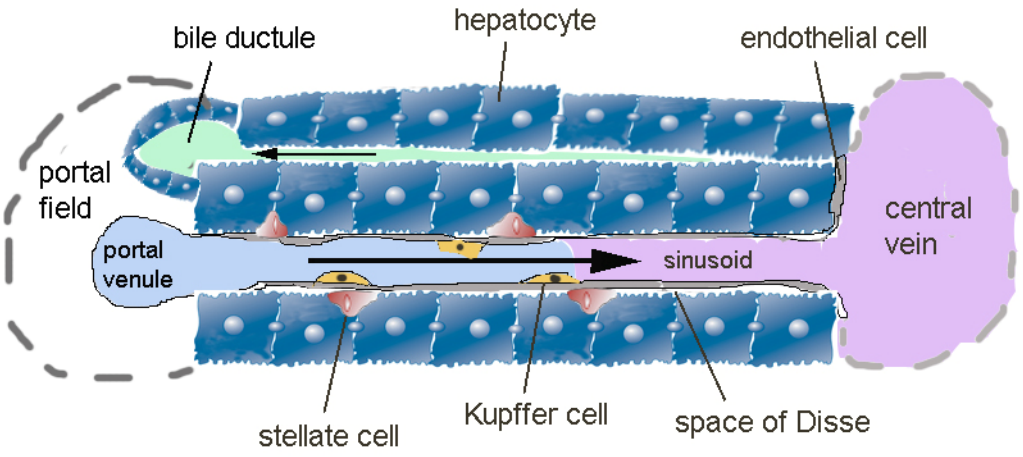

Diagram 5 Cell types and functional structures of the liver.

1.4 Liver cancer

Liver cancer is the third leading cause of cancer-related patient death. The 5-year survival rate of patients with liver cancer is less than 10%. Additionally, over 50% of liver cancer patients have cancer recurrence within 3 years after tumor removal surgery [93,94]. This high mortality is due to both the lack of early diagnosis and the quick malignant aggressive nature of liver cancer [95]. Adult primary liver cancer is highly associated with HBV and HCV infection which induces chronic inflammation, parenchyma regeneration and subsequent liver cirrhosis, dysplastic lesions and eventually liver carcinomas [96]. Heavy alcohol abuse and corrupted food intake can exacerbate disease severity [97]. Liver stem cell and progenitor cell activation due to viral infection, chronic inflammation and cirrhosis can potentially lead to malignant transformation.

Based on the cellular origin, there are two types of primary liver cancers: the hepatocellular carcinoma (HCC) and the cholangiocarcinoma. HCC features uncontrolled hepatocyte proliferation and cytoplasmic content decrease. The cholangiocarcinoma is characterized by the expanding of poorly organized bile ducts due to bile epithelial cell proliferation. The two types of carcinoma cells sometimes co-exist within one liver tumor, which is believed to be originated from common liver stem or progenitor cells which possess dual differentiation abilities into both hepatocytes and cholangiocytes (bile ductal cells, biliary epithelail cells) [98]. Tumors with cancer stem cells are malignant and frequently relapse after treatment [98,99,100,101]. Understanding the roles of cancer stem cells during tumorigenesis may help improve liver cancer treatment. Liver stem cells are believed to reside in the bile ducts or the

periportal area. However, there has been no specific biomarker to identify them. The identification of liver stem cells relies on their morphology of an oval shape (so called oval cells) which can be determined by electron microscopy [102]. By using this technique, several intermediate progenitor cell types between oval cells and mature hepatocytes are identified and classified as Type I, II and III hepatic progenitor cells. The rare oval cells are termed as Type 0 cells [102]. In liver disease models, such as allyl alcohol-induced hepatic necrosis in rat, the activated periportal cell expansion always consists of mixed cell populations of the abovementioned cell types. Since more differentiated cell types (like Type II and Type III) appear at later stage and more undifferentiated progenitor cells (like Type 0 and Type I) appear at early stage, a scheme of dynamic cell differentiation from Type 0 to Type III and finally hepatocytes can be illustrated [102]. The available antibodies such as OV-6, A6, OC2-1D11 and MIC1-1c3 [103] can only recognize a mixture of these cell types but not a designated one.

1.5 Organ size control

Organ size can be determined by the cell number as well as the cell size [104]. For example, an elephant heart is bigger than a mouse heart is because it has more cells [105], whereas a small wing of some *Drosophila* strain is a result of smaller cell size [106]. A certain organ's size, however, is determined at a level of the total organ mass, which is achieved by coordinately regulated cell number and cell size. A good example is that although a tetraploid salamander has twice the cell size of that in a diploid salamander, the corresponding organs' sizes are similar in the two animals because the tetraploid salamander has half cell number of the diploid salamander's

[107]. Also, changes in cell number from deregulated cell proliferation do not necessarily result in changes in organ size [108,109]. These experimental findings suggest that there is a “total mass setting point” mechanism, which functions to link the regulation of cell number (proliferation) and cell size (growth).

In the studies of the “total mass setting point” mechanism, genetic screening has been carried out in *Drosophila* looking for genes whose mutations can decouple the cell number - cell size regulation and result in dramatic organ size changes. The insulin-signaling pathway was identified to be an important organ size control pathway in that it regulates cell growth without affecting cell proliferation (reviewed in [110]). Mutations of its components often affect cell growth and consequently change cell size only and result in changes in organ size. It functions through *PI3K/AKT* pathway and regulates mRNA transcription as well as protein translation. The consequence is the change in RNA:DNA ratio and protein amount, which contributes to the change of cell size [111]. The size control mechanism by the insulin pathway has been further confirmed in mammalian system: in mouse heart, increase or decrease the activity of this pathway results in a corresponding heart size change, and this change is associated with comparable increase or decrease in myocardiocyte size [112]; in mouse liver, transient activation of the insulin pathway by activation of *Akt* triggers a 3-4-fold liver size increase within days due to hepatocyte hypertrophy without significant hepatocyte proliferation [113]. The importance of insulin pathway in determining the “total mass setting point” is further supported by data from liver regeneration experiments, in which it compensates hepatocyte proliferation deficiency through promoting cell growth [114,115]. The most striking phenomenon is that disrupting *PI3-*

K/PDK1/Akt pathway, the main cytoplasmic kinase complex of the insulin pathway, does not affect hepatocyte post-PH mitotic response, rather, significantly ceases liver regeneration due to the inability of cell growth [115]. These findings supports that the insulin-signaling pathway is a conserved organ size control pathway, and it plays important roles in the “total mass setting point” mechanism through regulating cell growth/size.

The recent identified Hippo pathway has been also connected to organ size control mechanism. However, instead of regulating cell growth, the Hippo pathway appears to be important for cell number regulation by balancing cell proliferation and apoptosis. Deregulation of the Hippo pathway in *Drosophila* results in overgrowth of the imaginal discs and enlargement of the corresponding adult organs without affecting cell size and tissue patterning (reviewed in [116]). Several identified Hippo pathway target genes are related with cell cycle progression (*bantam*, *cyclin E*) and cell survival (*diap1*), suggesting a role of the hippo pathway in cell number regulation. However, whether the Hippo pathway is a conserved organ size control pathway in different species and contributes to the “total mass setting point” mechanism needs further investigation.

Studying the mechanisms in organ size control is important not only because the organ size control is a fundamental biological question, but also because the potential genetic linkage between this mechanism and tumorigenesis. Genes contributing to the insulin pathway, the known organ size control pathway, are often mutated in tumorigenesis. *PTEN* affects organ size through negatively regulates cell size [117,118,119]. It negatively regulates the insulin signaling and is one of the most

frequently mutated genes in many types of human tumors [120]. Tuberous sclerosis complex

(TSC), another component of the insulin pathway, is a tumor suppressor [121], whose mutation results in *Drosophila* eye enlargement due to the dramatic increase in cell size [122]. Exploring the organ size control mechanism may help to better understand tumorigenesis.

1.6 Liver regeneration

The liver is a unique organ that maintains its regenerative ability throughout its lifetime [123]. Liver regeneration can be triggered by hepatocyte injury (toxin intake) or hepatic tissue loss (hepatectomy) [124]. While toxins often induce liver inflammatory responses and progenitor cell expansion in addition to hepatocyte proliferation, surgical resection only induces hepatocyte proliferation. Therefore using surgical resection to induce liver regeneration is widely used in studies of liver regeneration. In addition, the reproducibility of partial hepatectomy (PH) in terms of liver mass removal and the precision of ensuing event timing have made PH a preferred approach for experimental liver regeneration study [125,126].

Full liver re-growth by surgical induced liver regeneration takes about 7-10 days in rodents. The whole process is characterized by a synchronous induction of normally quiescent hepatocytes to reenter the cell cycle, which leads to a complete restoration of liver mass [127]. The major cellular events can be briefly divided into three phases: the priming phase (0h-12h after PH), the proliferation phase (12h-72h after PH), and the growth termination phase (72h-7 days after PH) [128]. Right after PH (priming

phase), the non-paranchymal cells (mainly the Küpffer cells and stellate cells) are activated and secrete cytokines (e.g. IL-6) and growth factors (e.g. HGF) to induce hepatocyte proliferation (proliferative phase). The initiation of hepatocytes cell cycle reentry is a complicated process and requires the activity of multiple pathways, which also link to each other in some way and function in a redundant manner. One well-known signaling that activates hepatocyte proliferation is the IL-6 -Jak-Stat pathway. IL-6 accounts for about 40% of the immediate early genes in the priming stage [129,130] and IL-6 KO mice show striking deficit in DNA replication after PH [131]. IL-6 signaling can activate cell cycle regulators, such as *Cycin D1*, a hall maker for hepatocyte cell cycle reentry. Increased expression of *Cyclin D1* activates *Cdk4/6*, which promotes hepatocyte G0-G1 transition. The importance of *Cyclin D1* in hepatocyte cell cycle reentry is affected by: transient expression of *cyclin D1* is sufficient to initiate hepatocyte proliferation [132,133]; diminished expression of *Cyclin D1* is related with impaired liver regeneration [131,134]. Another important factor that regulates hepatocytes cell cycle re-entry is *P21*, which is a universal Cyclin kinase inhibitor and promotes cell cycle exit [135]. Liver regeneration impairment resulting from blockage of the G1/S transition can be restored by *P21* deletion [136], suggesting *P21* plays an pivotal role in suppressing G1/S transition. *P21* expression peaks around 24 hours after PH, when hepatocytes begin to exit the cell cycle. The termination phase mainly involve extracellular matrix synthesis and reestablishment, hepatocyte and bile duct rearrangement [128]. Complete liver function recovery is around 14 days after PH.

Our lab investigated the Hippo pathway function *in vivo* by generating conditional knockout mice for each main component and analyzing the phenotypes of these mutant mice. We found that the Hippo pathway is important for liver homeostasis and tumor suppression. In addition, it may contribute to liver development through controlling the BEC differentiation. Finally, it is not a critical pathway for the “total mass checkpoint”-organ size control mechanism; however, it does play an important role in regulating hepatocyte cell-cycle reentry during the liver regeneration. Our study is among the first ones to address these questions, and the results may help understand the molecular mechanisms of fetal liver development and adult liver homeostasis.

CHAPTER 2: RESEARCH RATIONALE

We hypothesized that the Hippo pathway is a tumor suppressor pathway as well as an organ size control pathway in the mammalian system according to its function in *Drosophila* and the conservation of the components in mammals. In *Drosophila*, deregulation of the Hippo pathway kinase cassette and up-regulation of its nuclear effecter *Yki* causes cell uncontrollable proliferation and organ tumor-like growth. In addition, dysregulation of the Hippo pathway in *Drosophila* decouples the cell proliferation and cell growth in imaginal discs and leads to adult organ size enlargement. The two topics are related in that organ size control is one of the mechanisms for maintaining tissue homeostasis.

2.1 Role of Hippo pathway in mouse liver tumorigenesis.

Genes that affect cell proliferation or growth can be oncogenes (e.g. *myc* [137,138]) or tumor suppressors (e.g. *p53* [139,140]*, pten* [120]). In human, dysregulation of the Hippo pathway main components in tumor tissues has been reported. *Yap* and *Taz* are abnormally expressed in a variety of human cancers, including colonic adenocarcinoma, lung adenocarcinoma , ovarian serous cystadenocarcinoma, HCC, and breast cancer [50,141,142]. Decreased expression of *Mst1* and *Mst2* due to promoter hypermethylation has been reported in soft tissue sarcomas, which suggests their potential roles as tumor suppressors [40]. *Mst* can be activated by forming a heterodimer with members from the tumor suppressor family of Rassf [55] whose expression is often inactivated by epigenetic silencing in human cancers. Given that the Rassf family has at least six members and they do not exist in *Drosophila*, we can assume that the mammalian Hippo signaling pathway could have

distinct and complicated regulatory mechanisms. *Sav1* deletion in human cancer is rare and has only been reported in one colon cancer and two renal cancer cell lines among 52 cancer cell lines [42]. *Lats1* and *Lats2* are believed to be broad governors of cellular homeostasis. Their deregulations have been reported in astrocytoma [43], breast cancer [44], leukemia [143], soft tissue sarcoma [144], lung cancer [145] and prostate cancer [146]. *Taz* is required for kidney and lung organogenesis [147] and breast cancer stem cell quiescence [141,148]. We therefore hypothesized that the Hippo pathway is a tumor suppressor pathway in mammals, and we used several genetically engineered mouse models to test this hypothesis. Uncontrolled cell proliferation and tissue overgrowth are features of tumorigenesis.

The mammalian Hippo pathway is complicated by the paralogs of the main components as they potentiate more regulatory interaction with other factors. Null mutations of the major components of the Hippo pathway have been generated, and results revealed significant functional redundancy between the paralogs. *Mst1* or *Mst2* deficient mice are relatively normal. But *Mst1* and *Mst2* double deficient embryos die around E8.5 due to hematopoietic defects [149], suggesting a strong functional redundancy between *Mst1* and *Mst2*. *Sav1* is also required for embryonic development because its germline deletion causes embryonic lethality at around E17.5 to E18.5 due to defects in placenta vascularization [150]. *Lats1* null mice are viable but lack mammary glands. They are infertile, exhibit growth retardation, and develop soft tissue sarcoma and ovarian tumors [151]. *Lats2* null mice show a more severe phenotype as they die before E12.5 and also exhibit growth retardation [152]. Both observations suggest that *Lats1* and *Lats2* have distinct functions and are both required for

embryonic development. The earlier embryonic lethality of *Lats1/2* double deleted mutants (unpublished data) implies that functional redundancy exists between *Lats1* and *Lats2*. *Yap*-null mice die around E8.5 with defects in yolk sac vasculogenesis, chorioallantonic fusion, and body axis elongation [153]. Viable *Taz* null mice have defects in the kidney [147,154]. On the other hand, potential functional redundancy and a possible synergistic relationship between *Yap* and *Taz* are reflected by the observation that *Yap/Taz* double null embryos die before the 16-cell morula stage [155]. Embryonic lethality hinders further analysis for the potential tumor suppressor function of this pathway in adults, and therefore gene conditional deletion in adult tissues is required. The dissection of how the Hippo pathway contributes to tissue homeostasis and tumorigenesis in the adult is important for uncovering its role during human tumorigenesis and providing valuable information for cancer treatment.

The *Cre/Loxp* recombination system is the most commonly used conditional gene deletion strategy. By crossing the mice bearing loxp-flanked allele(s) in the functional domains of the target genes with the mice bearing either tissue specific promoter-driven *cre* or tetracycline-inducible *cre*, we generated series of tissue-specific/inducible conditional gene knockout mice. Defects were seen in mammary glands terminal end bud (TEB) cell differentiation (**Figure 2A**), intestinal villus development (**Figure 2B**), brain, liver, ovary, and testis epididymis (data not shown). Although the Hippo pathway is involved in the development of almost all examined tissues, the liver seems to be the most susceptible organ to the Hippo pathway deficit. Low-frequency gene deletion of *Mst* or *Sav1* in the liver (as evidenced by low and scattered cre expression driven by non-liver specific *MMTV* [156] and *CAGGS* [157] promoters) led to liver tumorigenesis.

Our finding is consistent with the previous report about *Yap* overexpression resulting in liver cancer [34]. The dramatic phenotypes from altered expression of Hippo pathway components make liver an ideal organ model for studying the *in vivo* function of this pathway. In addition, this study also has clinical significance. In a study consisting of 177 patient liver tumor biopsies, 62% of them show *Yap* over-expression and nuclear accumulation, which significantly correlate with poor differentiated tumor cells. *Yap* nuclear accumulation correlates with tumor relapse after tumor resection and low 5-year patient survival rate [51], which makes *Yap* become a new prognostic marker for HCC. Therefore, figuring out how the Hippo pathway regulates *Yap* activity and contributes to the tumorigenic process may help to develop therapeutic approaches for liver cancer.

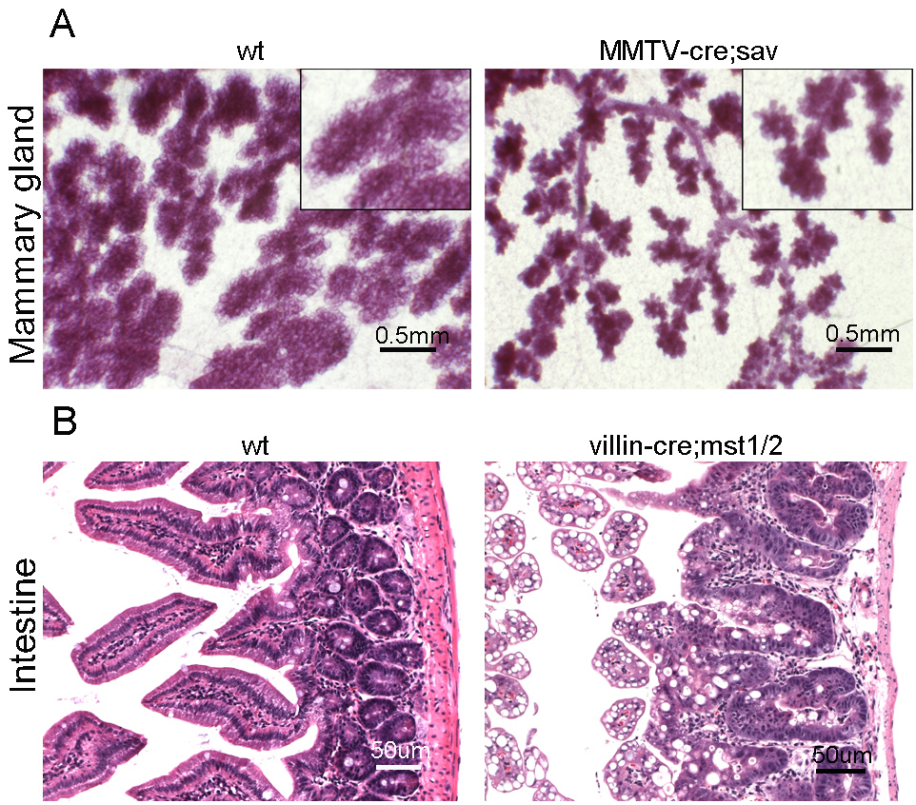

Figure 2. *Sav1* deletion in mammary gland and *Mst1/2* deletion in intestine. (A) On 18th day of mice pregnancy, wild type TEB cells differentiate into milk-secreting alveoli, which are large and plump; but the *MMTV-cre;Sav1* TEB cells do not differentiate well. The mutant alveoli are small and do not contain much milk as compared with the wild type. (B) In intestine, the wild type duodenum has well developed and organized villi and crypt layers, whereas the *villin-cre;mst1/2* duodenum has thinner basal layer and disorganized crypt layers, together with massive cell vacuolation.

To specifically analyze how the Hippo pathway kinase cassette (*Mst/Sav1/Lats*) regulates *Yap/Taz* function in the liver, we used *alb-cre* to delete the Hippo pathway genes in all (>90% [158]) hepatocytes, as well as in the BECs. The *alb-cre* mouse line has been widely used for liver-specific gene knockout studies. The *albumin* promoter activates around E9.5 [159]; however, 90% gene deletion will not be achieved until after birth [158]. In this manner, *alb-cre* mediated gene deletion occurs in both hepatocytes and BECs in a developed liver, and the deletion in the embryonic liver is mosaic. *Alb-cre* mediated gene deletion usually does not cause embryonic lethality, except if the interested genes are essential for liver function. An example is *C/EBP*, an important transcription factor for liver energy homeostasis [160].

2.2 Role of Hippo pathway in mouse liver regeneration

In *Drosophila*, deregulated Hippo pathway results in overgrown imaginal discs and corresponding increase in adult tissue due to enhanced cell proliferation and reduced cell apoptosis. Change of cell size is not found, and the overgrown tissues still maintain normal patterns. Hippo pathway is thus linked to an organ size control mechanism and, unlike the insulin pathway, it may contribute to the “total mass setting point” mechanism by regulating cell number without affecting cell size.

Similar phenomena have been observed in the mammalian system. Enlarged heart [161] and liver [34,37,38,41] sizes due to uncontrolled cell proliferation have been observed when the Hippo pathway is deregulated. In mouse liver, the hepatocyte number but not size shows a correlation with *Yap* amount: liver size dramatically enlarges when *Yap* over-expression is induced to promote hepatocyte proliferation; whereas the liver shrinks towards its normal size due to hepatocyte apoptosis when withdrawing the induction [34]. Pro-proliferation and anti-apoptosis are also observed in *Mst* mutants [41]. However, whether these phenomena are the consequences of the disturbed organ size control mechanism or just a disease symptom need to be clarified.

Previous reports about liver size control suggest that the liver size is well regulated by complicated signaling networks and the majority of gene deletions only impair rather than totally cease the liver regeneration. For example, *myc* functions to promote cell proliferation and is activated during the priming phase of liver regeneration [162]. However, *Myc* deleted liver still can regenerate and grow back to its original size [163,164], implying its function can be compensated by other liver size

control mechanism. However, whether and how much the Hippo pathway accounts for liver size control needs to be further investigated.

Liver size setting point is recognized to be 4~5% of the host's body weight, and it is strictly regulated throughout lifetime by liver's unique regeneration ability. Theoretically the liver regeneration is regulated by the size control mechanism, and any deficit in liver regeneration should reflect disturbances of the size control mechanism. We used partial hepatectomy (PH) technique to induce liver regeneration to test our hypothesis. The benefits of using PH to induce liver regeneration are: first, the PH technique has been well established [165] and extensively studied [128,166,167,168], which technically ensures the project's performance. Second, PH induced liver regeneration is a process of synchronized hepatocyte proliferation with well defined timing of cell cycle events, which eases the analysis by providing plenty of samples for any regeneration phases. Third, PH induced liver regeneration is a normal biological phenomenon happened in an mature organ, therefore excluding the signaling interferences from developmental process or disease effect.

CHAPTER 3: MATERIAL AND METHODS

3.1 Breeding and generation of mice with *sav1* deletion, *mst1*;*mst2* double deletion, *lats1*;*lats2* double deletion, and *Yap;Taz* double deletion

Sav1 $^{fl/fl}$, *mst1* $^{fl/fl}$, *mst2* $^{fl/fl}$**,** *lats1* $^{fl/fl}$, and *lats2* $^{fl/fl}$ mice were designed and generated by Randy Johnson (PhD, MD Anderson Cancer Center). These mice have a mixed genetic background of C57BL/6, 129SvEvTac and CD1. *Yap* $^{fl/fl}$ and *taz* $^{fl/fl}$ mice were design and generated (but not published) by Eric Olsen's lab (PhD, UT Southwestern Medical Center, Dallas, TX). *Yap* $^{fl/fl}$*;taz* $^{fl/fl}$ mice were bred with our mouse colony, and therefore they also have a mixed genetic background. *Sav1* $^{fl/fl}$, *mst1* $^{fl/fl}$, *mst2* $^{fl/fl}$ mice were subsequently bred to *alb-cre*, *MMTV-cre*, *villin-cre* and *CAGGS-creER(T2)* mice followed by backcrossing to homozygous floxed animals. *Lats1* $^{fl/fl}$, *lats2* $^{fl/fl}$, *yap* $^{fl/fl}$;*taz* $^{fl/fl}$ were bred to *alb-cre* mice followed by backcrossing to homozygous floxed animals.

All mice were housed in a conventional facility with a 12-h light/dark schedule and access to food and water ad libitum. All procedures were approved by the University of Texas, M. D. Anderson Cancer Center Animal Care and Use Committee.

* "fl/fl" will be omitted in the following paragraph. For example, "alb-cre;*mst1/2*" represents "*alb-cre*; *mst1* $^{fl/fl}$; *mst2* $^{fl/fl}$ ".

3.2 Genotyping

Genotype of each mouse was analyzed by PCR. Chromosome DNA was extracted from tail lysate from 2~3 weeks old mice using previously described techniques [169,170,171]. Primers (**Table 2.**) were designed to detect the floxed exon in each gene. The PCR conditions were 35 cycles of 95°C for 30 seconds, different annealing temperatures (**Table 2.**) for 30 seconds and 72°C for 1 minute. PCR products were run in agarose gel added with ethidium bromide. Genotypes were determined according to specific bands (**Table 3.**)

Table 2. Primer information

Gene	Primer sequcence (5’ – 3’)		A.T. (°C)
mst1	F	CCTGCTTCAGTGTTGGCTCTTGATTTTCCT	50
	R	TAGACCAGCCAGGGCTAGAGTGAAACCTTG	
mst2	F	GTTCAGGGTCCCACCAAGAGTCGCTTCATT	55
	R	TGTCTAGCTGCTGATGACACTGAACTTCTGGC	
sav1	F	TGTCAGTGTAAAATGGCCACA	50
	R	TTGGGAATGGTTTTACAAGTTT	
lats1	F	TTGTTGCTGGTGTTGTTTCC	55
	R	ATGAATGAACCTGAGGCTGC	
lats2	F	ATCCTAGCACTCAGGAGGCA	55
	R	ACACATTCCCCTCCACTGAC	
yap	F	ACATGTAGGTCTGCATGCCAGAGGAGG	60
	R	TGGTTGAGACAGCGTGCACTATGGAGC	
taz	F	GGCTTGTGACAAAGAACCTGGGGCTATCTGAG	62.5

	R	AACTGCTAACGTCTCCTGCCCCTGACCTCTC	
cre	F	TCCAATTTACTGACCGTACACCAA	55
	R	CCTGATCCTGGAATTTCGGCTA	

F: forward primer

R: reverse primer

A.T. : Annealing Temperature

Table 3. PCR product size

Gene	Allele	PCR product size (bp)
mst1	Wild type	319
	loxP	400
mst2	Wild type	213
	loxP	370
sav1	Wild type	250
	loxP	405
lats1	Wild type	182
	loxP	350
lats2	Wild type	235
	loxP	380
yap	Wild type	457
	loxP	600
taz	Wild type	496

	loxP	655
cre	cre	450

3.3 Tissue processing and paraffin slides preparation

Mice were sacrificed by cervical dislocation. Liver tissues were cut into 5 mm-thick pieces and fixed with 4% PFA overnight at 4°C. The next day, the fixative was washed off with PBS, and then the tissues went through increasing alcohol gradient (70%-90%-100%). After dehydration, tissues were cleared in Xylene for 45 minutes and then put into 65°C liquid paraffin for over 6 hours with three times paraffin change. Lastly, the tissues were put into metal cassette and embedded in paraffin by cooling down to 4°C. Paraffin blocks were cut into 5 μm sections and slides were put on 37°C heater overnight to ensure tissue attachment.

3.4 Immunostaining with paraffin slides

Slides were pre-heated in 65°C oven for 1 hour to melt the paraffin and also enhance tissue attachment. They were then deparaffinized in 3 changes of Xylene with 15 minutes in total, followed by rehydration in decreasing alcohol gradient until into water (100% - 90% - 70% - ddH_2O). Heat antigen retrieval was carried out in sodium citrate buffer (10mM Sodium Citrate, 0.05% Tween 20, PH6.0) for 15 minutes using a steamer. After cooling down for 20 minutes, the antigen retrieval buffer was washed off with PBS for 5 minutes and three times. Endogenous biotin was blocked by putting the slides into 3% H_2O_2 (in Methonal) for 15 minutes, followed by antibody blocking with 5% normal horse (or goat) serum for 1 hour at room temperature. After that, slides were added with primary antibody (**Table 2**) and incubated in a wet chamber at 4°C overnight. The next day, after washing off the primary antibody with

PBST, 5 minutes for 3 times, tissues were incubated with HRP or fluorescence conjugated secondary antibody for 1 hour at RT. The positive staining signal was developed with DAB reagents (Vector Laboratory, SK-4105). The tissues were counter-stained with Mayer's hematoxylin (Fisher Scientific, TA060MH), and then dehydrated in increasing alcohol gradient into Xylene. Slides were then sealed with Permount (Fisher Scientific, S70104) and signals were detected with microscope under bright field.

* *note*: For fluorescent staining, seal the slides with anti-fade mounting solution with DAPI (invitrogen, CEL36935), and the slides are ready to view under microscope.

3.5 Frozen section and immunostaining (only for oval cell markers)

Liver samples were cut into 5 μm-thick pieces and immediately immersed into CRYO-OCT Compound (Fisher Scientific, 14-373-65). After adjusting the tissue position, the OCT cassettes were carefully held and put on top of isopentane, which had been pre-chilled by putting into liquid nitrogen for at least 10 minutes. After about 2 minutes, when the OCT was frozen into a block, the block was either stored in -80°C or directly sectioned. For the staining of the oval cell markers (**Table 2**), slides were briefly fixed in cold acetone (-20°C) for 5 minutes. After washing off acetone with PBS for three times and each time for 2 minutes, slides were added with 5% goat serum and incubated for 10 minutes at room temperature to block non-specific antibody affinity. Slides were then incubated with primary antibody for 30 min. After the primary

antibody was washed off with PBS for 2 minutes in a total of three times, Cy3-conjugated secondary antibody was added and the slides were incubated at room temperature for 15 minutes. Again with PBS wash to get rid of excessive secondary antibody, slides were sealed with anti-fade mounting solution with DAPI (invitrogen, CEL36935), and signals were detected with confocal microscopy.

Table 4. Antibody information

Antibody	**Source**	**Catalog number**	**Applied experiment**	**Dilution ratio**
A6	Dr. Valentina Factor (NIH)		IF	1:500
BrdU	Abcam	ab6326	IHC	1:100
CK19	Dr. Milton Finegold (Texas Children's Hospital)		IF, IHC	1:1000
Cyclin D1	Cell signaling	2922	WB	1:1000
F4/80	BD Biosciences	552958	IF	1:200
HNF4α	Santa Cruz	sc-101059	IF	1:200
Lats1	Cell signaling	9153	WB	1:1000
MIC1-1c3	Dr. Craig Dorrell (Oregon Health Sciences Center)		IF	1:20

Mst1	Cell signaling	3682	WB	1:1000
Mst2	Cell signaling	3952	WB	1:1000
OC2-1D11	Dr. Craig Dorrell (Oregon Health Sciences Center)		IF	1:20
PCNA	Cell signaling	2586	WB	1:1000
Phospho-Lats1	Cell signaling	9159	WB	1:1000
Phospho-STAT3	Cell signaling	4113	WB	1:1000
Phospho-Yap/Taz	Cell signaling	4911	WB	1:1000
P21	Cell signaling	2946	WB	1:1000
Sox9	Millipore	AB5535	IF	1:500
STAT-3	Cell signaling	9139	WB	1:1000
Yap	Cell signaling	4912	WB, IHC	1:1000, 1:500
Taz	BD Pharmingen	560235	WB	1:1000

WB: Western Blot

IHC: Immunohistochemistry

IF: Immunofluorescence

3.6 PAS staining

Paraffin tissue sections were deparaffinized and rehydrated to water, followed by being oxidized in 0.5% periodic acid solution for 5 minutes. After being rinsed with distilled water for three times, slides were put into Schiff's reagent (Sigma-Aldrich, 3952016) and incubated at room temperature for 15 minutes. The color (pink) was developed under running warm tap water for at least 5 minutes. The slides were then counterstained with Mayer's hematoxylin for about 1 minute. After wash and dehydration, the tissues were then sealed with Permount and ready to view under the microscope.

3.7 Quantitative PCR

For each mouse, about one gram liver tissue was cut and put into 1 ml TRIZOL reagent (Invitrogen, 15596-025), followed by being broken down using an electronic homogenizer. Five hundred-microliter chloroform was then added to each sample tube and mixed with TRIZOL well by vortex. The samples were then centrifuged at the highest speed (14000g), and the supernatant was then transferred into Qiagen RNeasy mini column for binding. After centrifuge, the mRNAs binding to the column were washed by the RW buffer (Qiagen RNeasy Mini Kit, 74104), followed by washing with 70% ethanol (prepared in DEPC-treated water). Finally, mRNAs were eluted with into 15 ul RNase-free water. mRNA concentration and purity were checked with NanoDrop 1000. Quantitative RT-PCR analysis was carried out using One-Step TaqMan gene expression assays (Applied Biosystems) according to the manufacturer's instructions.

Gene	Assay ID
lats1	Mm01191883
lats2	Mm01321139
yap	Mm00494237
taz	Mm00513560
gapdh	Mm99999915

3.8 Microarray analysis

Illumina Total Prep RNA Amplification Kit (Ambion) was used for preparation of biotin-labeled cRNA samples. The microarray analysis was previously described [38]. Five hundred nanograms of total RNA was used for the cDNA synthesis, amplification and biotin labeling. 1.5 µg of biotinylated cRNAs was hybridized to the Illumina mouse-6 BeadChip v.2 microarray. Signaling reading is performed by the Microarray Core Laboratory of UT Health Science Center in Houston. Heat-map of expression was generated by Treeview. Gene ontology assay was performed using the DAVID web tool.

3.9 Protein extraction

Fresh harvested liver tissues were broken down into cells using a glass-teflon homogenizer, or underwent perfusion to enrich hepatocytes. Then, cells were forced to pass through a strainer to get rid of the connective tissue, and the hepatocytes were collected into a 50 ml conical tube. The cells then underwent two times wash with PBS and re-suspended in RIPA buffer (Cell signaling, #9806) added with protease inhibitor (Roche, 04693132001) and phosphatase inhibitor (Roche, 04906837001). The cell suspension was then put on ice for at least 30 minutes for sufficient lysate. Cell debris was separated from lysate by centrifuging the tube at the maximum speed (14,000 rpm) for 5 minutes. The supernatant was transferred to a new clean tube, and about 2 ul aliquot was used for protein concentration measurement;

* Cytoplasmic and nuclear portion of proteins were extracted by NE-PER Nuclear and Cytoplasmic Extraction Reagents (Thermal Scientific, #78835) by following manufacture's protocol. Protein concentrations were measured by using BCA Protein Assay Reagents (Thermal Scientific, 23227) according to the manufacture's protocol.

3.10 Western blot:

Protein samples were denatured via boiling for 5 minutes with protein loading buffer containing 5% beta-metheltransferase. Denatured samples were run on 10% acrylamide denatured gels for 2 hours at 80 volts, followed by semi-dry transfer to PVDF membranes (Millipore, IPFL10100) for 2 hours. The membrane containing proteins was blocked from non-specific antibody binding with 5% milk in TBST for 1 hour at room temperature, and then incubated with primary antibody (**Table 4**) in 5% BSA at 4℃ overnight. The next day, secondary antibody was added after the primary

antibody was washed off, and incubated with membrane at room temperature for 30 minutes. After further wash, membranes were developed by enhanced chemiluminescence (ECL, PerkinElmer, NEL103001EA), and signal was detected by X-ray film.

3.11 Hepatocytes enrichment (liver perfusion)

Prepare for the experiment by warming up HBSS (Invitrogen # 14170-11, 0.3mg/ml collagenase D), EBSS (Invitrogen #14155-063, 0.5mM EGTA) and Rinse Medium (Invitrogen # 17704-024) to 37°C in water bath. Mice were then anesthetized with IP injection of avertin (400-500ul/mouse). Mouse anesthetizing status was checked by pinching the mouse toes for pain reflex. The mouse should not respond if anesthetized. The mouse was body stretched by pinning the hand and feet to the working platform. A U-shape incision was made to expose liver and inferior vena cava. Buffer-fly needle was inserted into inferior vena cava. Right after the pump was turned on, portal vein was cut to provide for exit of blood and perfusion liquid, and thus to establish the perfusion reagents flow from the liver central vain to the portal vain. The perfusion with EBSS lasted for 1-2 minutes (about 40 ml with pump set to 6-7, or 7-8 speed) and then switched to HBSS and perfused for 2-3 more minutes. When the liver became soft, the pump was stopped and the liver was cut out. Gallbladder and fat were removed by cutting off. Liver was then put in a 10cm petridish containing 20ml RM and gently squeezed with two cell scrapers to release the hepatocytes from connective tissue. The cells were then passed through a strainer into a 50ml Conical tube. After the cells were rinsed with additional 10ml RM, they were spin at 600 rpm

for 2 minutes and re-suspend in 10-25 ml RM. To remove the dead cells, Percoll solution was prepared by mixing 15ml Percoll (Sigma #P4937) and 10ml DPBS in a new 50ml conical tube, and cell suspension was slowly added into the percoll mixture. The tube was centrifuged at 600rpm for 10 minutes, and dead cells were sucked off from the upper layer. The remaining cell pellet was re-suspended and washed with RM, followed by RNA isolation or protein extraction.

3.12 Partial hepatectomy

Five to 6 week old *alb-cre;mst1/2* mice and 7-8 week old *alb-cre;yap/taz* mice were used for performing 2/3 PH. The wild-type littermates were used as corresponding controls. The mice were anesthetized with IP injection of avertin. After briefly rinsing the feather with 70% ethonal, an excision was made in the middle of the abdomen to expose the whole liver. Cotton tips were used to lift the left lobe and put a 15 cm silk suture under it. The suture was moved towards vena cava and a tie was made close to it. The entire left lobe was removed with scissors. The middle lobe was removed in a similar way but attentions were paid to not tie too close to vena cava. Blood was briefly cleaned by using cotton tips, and the abdomen was closed up by sewing the muscle and then the skin with silk suture. Morphine (5 mg/kg) was injected to reduce pain, and then the mice were put on 37℃ incubator for recovery. Mice were sacrificed at select time intervals: 0 hour (h), 6h, 24h, 48h, 72h, and 7days (7d) after PH and the livers were harvested for protein extractions and paraffin sections. At 14 days, measurements were acquired for liver/body weight ratio. All the animal procedures were performed in accordance with the MD Anderson Cancer Center

institutional guidelines using an approved animal protocol by the Institutional Animal Care and use committee.

3.13 Statistical Analysis

Student T-test was applied in MicroSoft Excel for two-sample comparison. One-way ANOVA was used in SSPS program for three-sample comparison. Survival data was analyzed using Kaplan Meier statistical method, and the survival curve was generated in SSPS program.

CHAPTER 4: RESULTS

4.1 *Mst* and *Sav1* are required for liver tumor suppression

Loxp-floxed alleles for *mst1* and *mst2*, *sav1* were successfully generated [38]. The *mst1*/2 $^{fl/fl}$ and *sav1* $^{fl/fl}$ mice showed no detectable abnormalities. *Alb-cre;mst1* mice and *alb-cre;mst2* mice were also phenotypically normal up to 1 year of age. They eventually developed liver tumors at around 24 months of age, implying they both are required for liver homeostasis. However, a severe phenotype was observed when combining *Mst1* and *Mst2* deletion: *alb-cre;mst1/2* (double deletion) mice developed multiple nodular tumors in the liver within 4 months after birth and died around 6-7 months (**Figure 3C**), implicating that significant functional redundancy exists between *Mst1* and *Mst2* in suppressing liver tumorigenesis. The multiple gray-white nodular tumors were identified as HCC (**Figure 3F**). *Sav1*-deleted livers showed a similar but milder phenotype as compared with *Mst1/2* double deleted livers. A few scattered gray-white nodular tumors developed in the *Sav1*-deleted liver at about 8 months old. The slower progression of liver tumors in *Sav1* mutants allowed the mice to survive longer and the tumors to fully develop (**Figure 3B**). Both HCC (**Figure 3D**) and cholangiocarcinoma (**Figure 3E**) were observed in *Sav1* mutants at around 18 months of age. These observations revealed that both Mst and Sav1 are liver tumor suppressors.

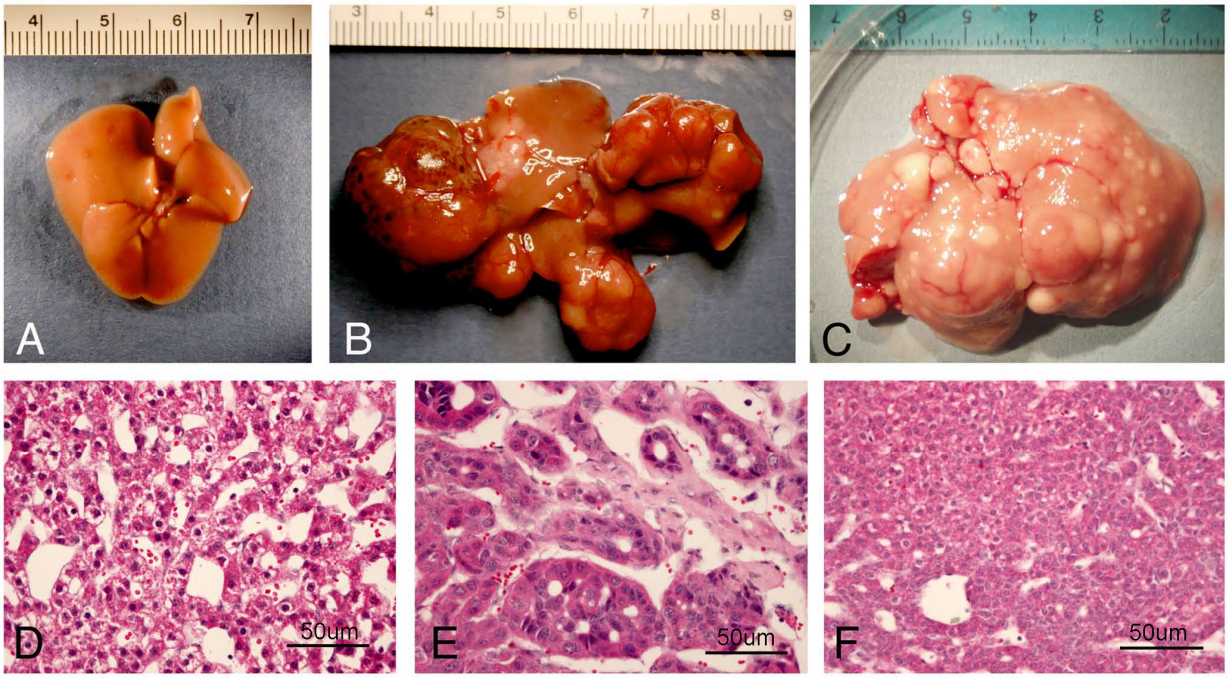

Figure 3. Hepatoma formation in *Mst* and *Sav1* mutants. Wild-type livers display a normal appearance, devoid of tumor foci (A). In contrast, conditional deletion of *sav1* in hepatocytes results in large, multifocal tumors (B). Likewise, *alb-cre;mst1/2* mutant livers are significantly enlarged relative to wild type and display multiple focal tumor nodules (C). Histological examination (D-E) reveals both well and poorly differentiated hepatocellular carcinoma (D and F) and cholangiocarcinoma (E). The data have been published [38].

To find out the cause of tumorigenesis in these mutants, mutants of younger ages were collected and analyzed. In contrast to few sporadic hepatocyte divisions in the wild type with normal low rate hepatocyte turnover (**Figure 4A**), the mutant hepatocyte showed uncontrolled proliferation (**Figure 4B and C**) and mutant liver continuously enlarged and eventually developed tumors (**Figure 4D**).

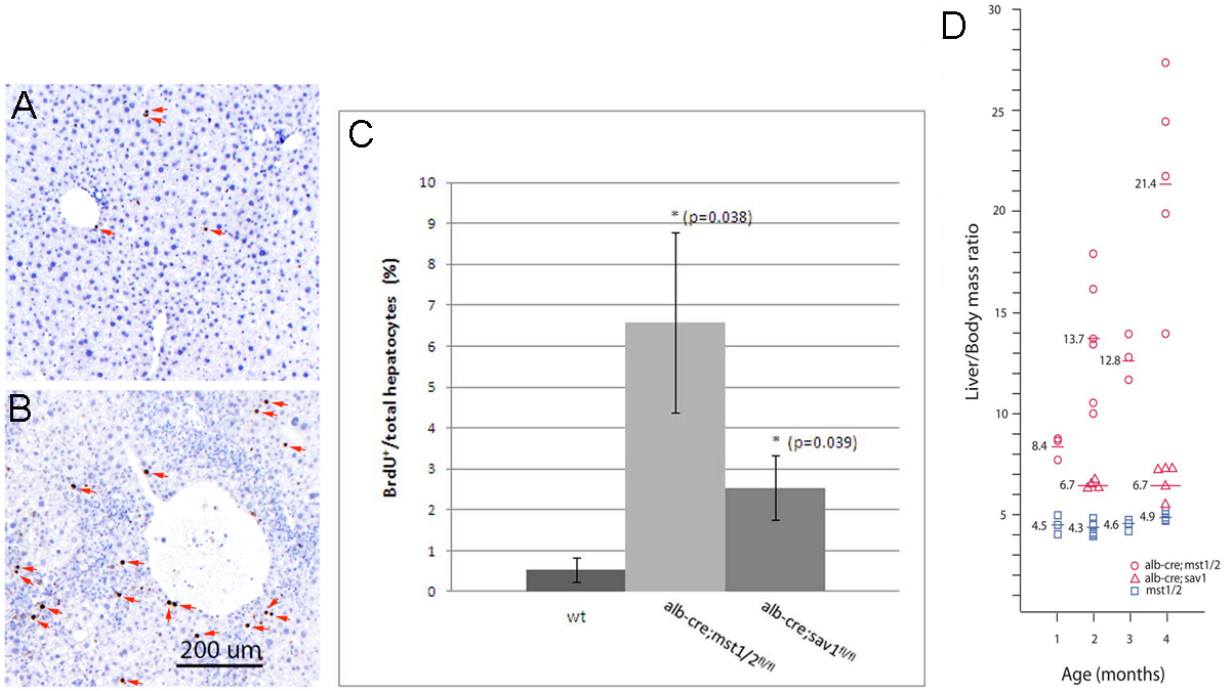

Figure 4. Elevated hepatocyte proliferation contributes to both *Mst* and *Sav* mutants' liver enlargement. According to BrdU staining, in contrast to wild-type (A), *alb-cre;mst1/2* (B) and *alb-cre;sav1* mutants (B) have significantly increased hepatocyte proliferation (C). (D) A plot of liver/body as a function of age shows increased liver size of *mst1/2* mutants at one month. Continued growth is evident at two and three months of age. Modest increases in *alb-cre;sav1* mutant liver sizes is seen at two and four months of age. The data have been published [38].

At 2-month old, there were no visible tumor-like nodules in the *Mst* mutants, although the livers were dramatically enlarged (**Figure 5B**). Further HE Staining revealed that the mutant hepatocytes gradually gained heteromorphism. At 1-month old, there was no obvious difference between the wild-type and mutant hepatocytes; at 2-month old, the mutant hepaotocytes were swollen and their nuclei were smaller and pushed to one side of the cells when compared with wild type (**Figure 5D**). The swollen hepatocytes were not filled with excessive glycogen or fatty acids according to PAS staining and Oil Red staining, respectively. So far, the cause of mutant hepatocyte enlargement is still unknown, as is whether this contributes to liver tumor development.

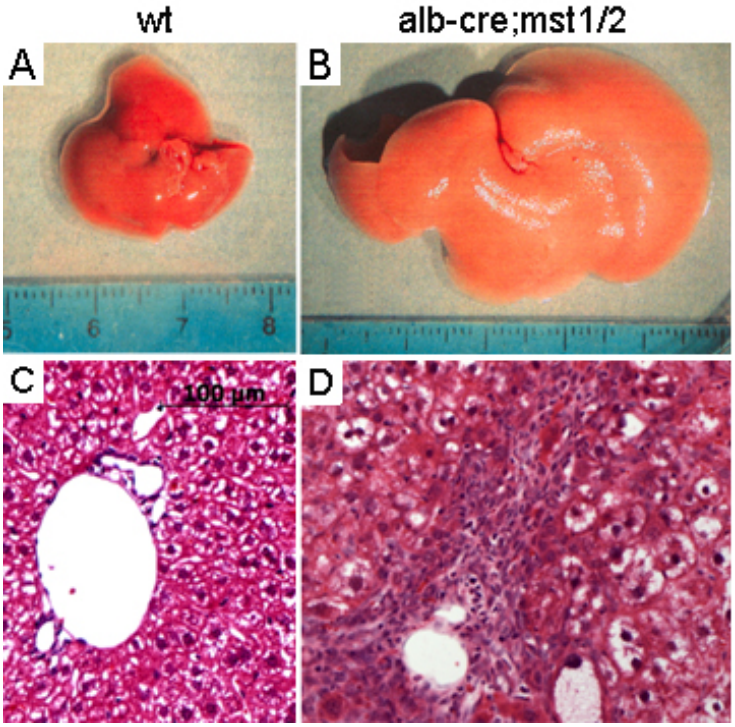

Figure 5. Two-month old *Mst1/2* double deleted liver. At this stage, the mutant liver is dramatically enlarged but no visible tumor-like nodules are seen (B). Compared with the wild type (C), the portal areas of the *Mst1/2* double mutants have many leukocytes expanding and infiltrating into the liver plates (D). The mutant hepatocytes are swollen and their nuclei are more variable and pushed to one side of the cells [38].

4.2 *Yap* is activated in *alb-cre;mst1/2* and *alb-cre;sav1* liver tumor tissues

Yap is a nuclear effecter of the Hippo pathway and its activation is known to promote hepatocyte proliferation and contribute to HCC formation [34]. To see whether *Yap* is activated in *Mst* and *Sav1* mutants, western blots with proteins from enriched hepatocytes before tumor formation were carried out. Results showed decreased phospho-*Lats* and phospho-*Yap* in *alb-cre;mst1/2* liver but not in *alb-cre;sav1* liver (**Figure 6A**). In both mutant tumor tissues, *Yap* was nuclear accumulated and the protein amount was increased (**Figure 6B**), which was possibly due to protein stabilization after decreased phosphorylation.

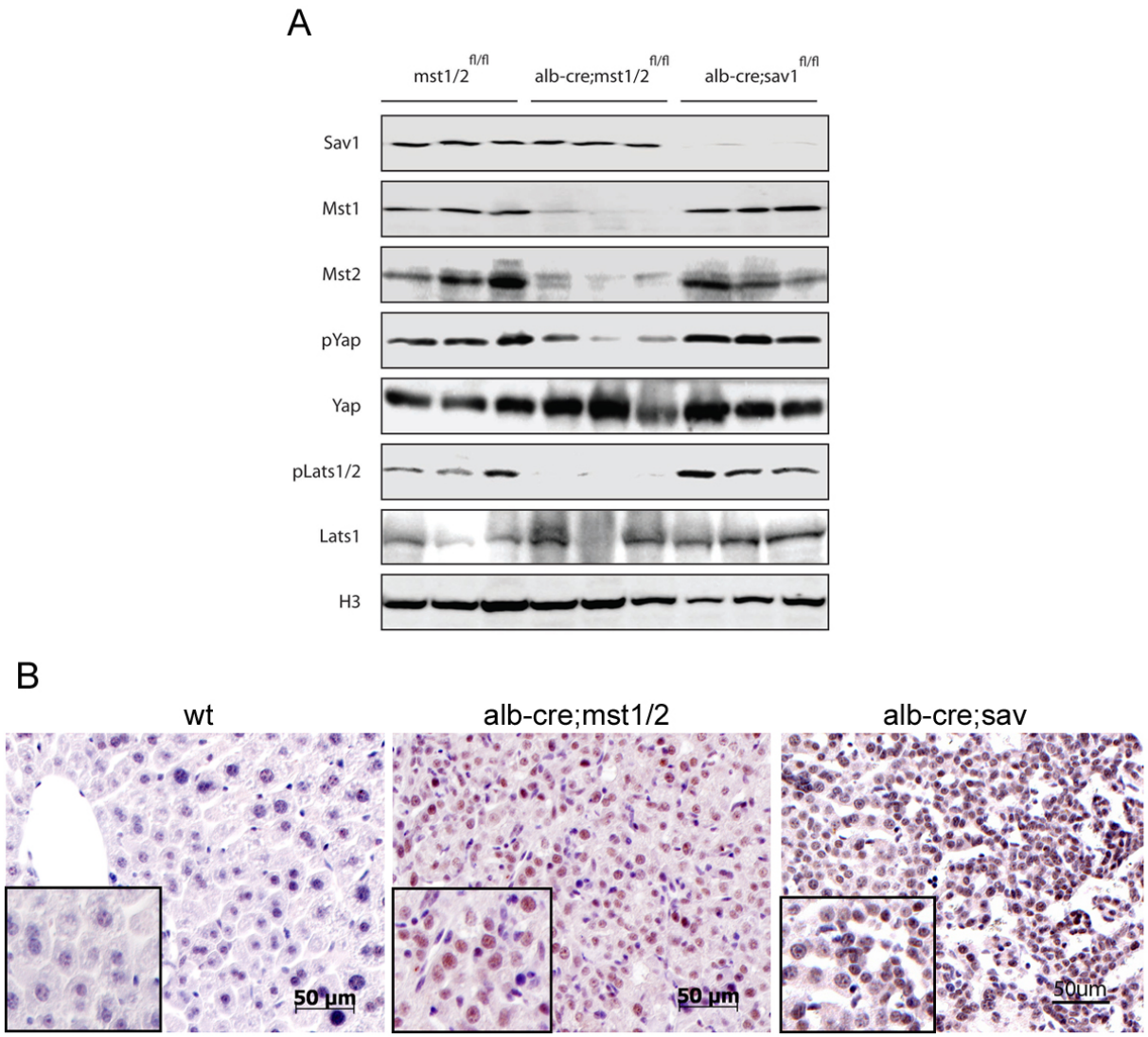

Figure 6. *Yap* activation in *Sav1* and *Mst* mutants. (A) Western analysis (by Wouter Bossuyt) of *alb-cre;sav1* and *alb-cre;mst1/2* double mutant tissues show loss of *sav1* protein in *alb-cre;sav1* mutants and reduced amounts of *mst1* and *mst2* proteins in *alb-cre;mst1/2* mutants. Each lane represents proteins extracted from independent mutant livers. Phosphorylations of *Yap* and *Lats* are reduced in *alb-cre;mst1/2* double mutant hepatocytes but not in *alb-cre;sav1* mutant cells. Histone H3 (H3) is used as a loading control. This datum has been published [38]. *Yap* staining in tumor tissues reveals increased *Yap* protein amount, as well as *Yap* nuclear accumulation in tumor

cells of both mutants (B).

4.3 *Lats* is required for liver development

The loxp-floxed alleles of *lats1* and *lats2* were generated by Randy Johnson (not published). Liver-specific deletions of *Lats1* and *Lats2* were achieved by combining *lats1*$^{fl/fl}$ *lats2*$^{fl/fl}$ homologs with alb-cre. The deletion efficiencies for both genes were about 80% as assessed by quantitative PCR (**Figure 7**).

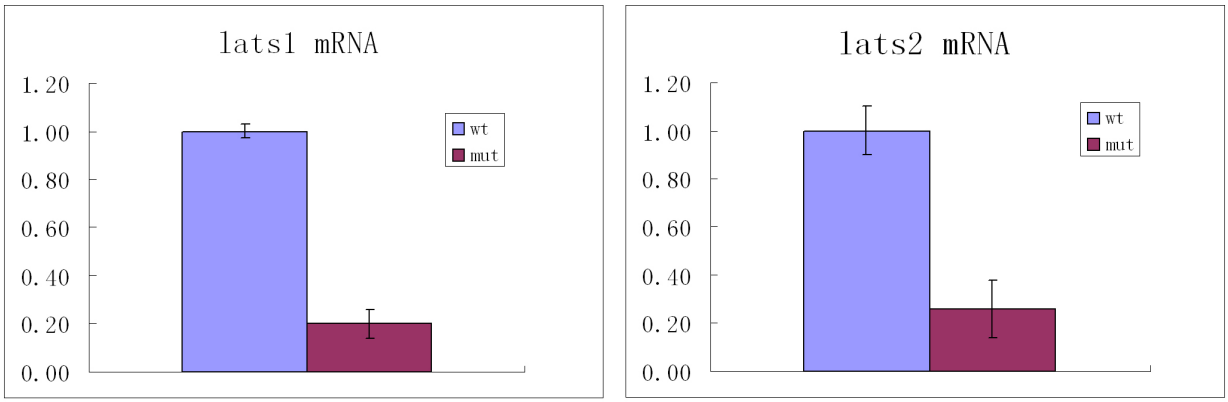

Figure 7 Quantitative analysis of *Lats1* and *lats2* gene deletion efficiency mediated by *alb-cre*.

Lats1/2 double mutants died from severe hypoglycemia on the first day of birth (P0). According to PAS staining (**Figure 8**), two factors contributed to severe hypoglycemia: hepatocyte loss due to hepatic necrosis and decreased glycogen synthesis ability of hepatocytes. G/O assay with microarray data revealed essential liver metabolic functional defects, including catalysis and biosynthesis (**Figure 9C**). Furthermore, many up-regulated genes after Lats deletion were also up regulated in Yap over-expressing liver (**Figure 9B**).

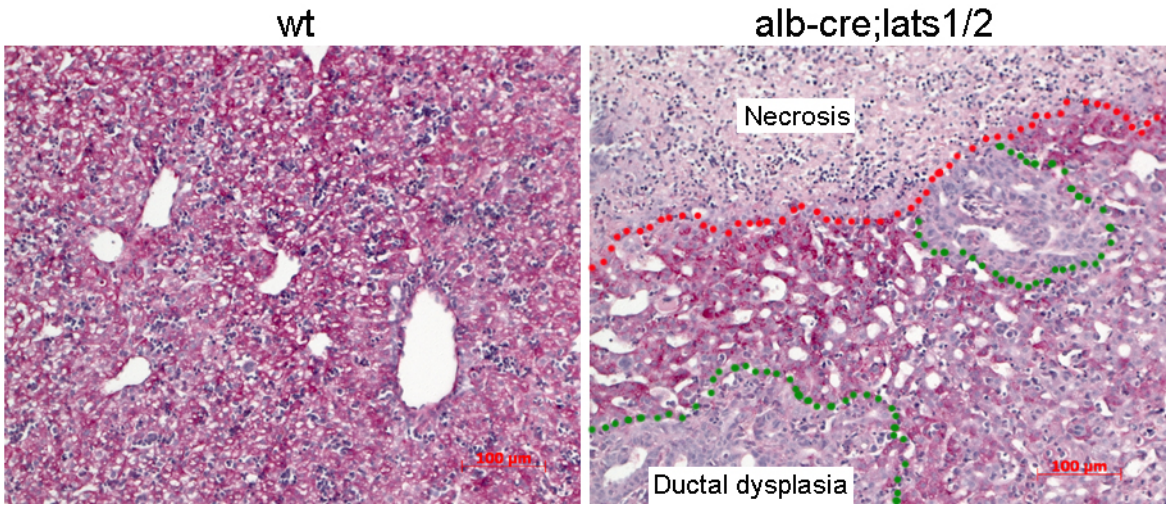

Figure 8. PAS staining on P0 Lats mutant livers. The result shows decreased glycogen synthesis in *Lats1/2* mutant hepatocytes as compared with that in the wild type. The PAS staining is negative in the necrotic area (circled by the red dot line) and ductal hyperplasia areas (circled by green dot lines).

A

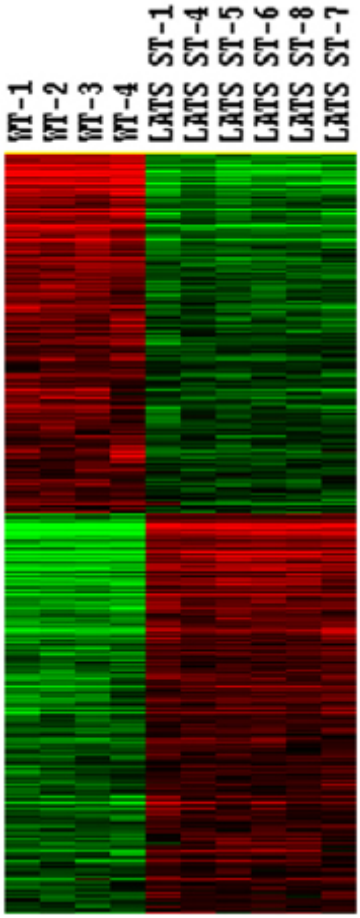

B

SYMBOL	FOLDS	SYMBOL	FOLDS	SYMBOL	FOLDS	SYMBOL	FOLDS
Ctgf	5.54	Oact1	3.38	Gpt2	2.87	Krt1-18	2.63
Fgfbp1	5.36	Ferl13	3.34	Bicc1	2.86	Plk2	2.60
Guca2b	5.04	Tnfrsf12a	3.33	Copeb	2.85	Tacstd2	2.58
Ankrd1	4.85	Pmp22	3.31	Serpinb6b	2.75	Ccl7	2.58
Cyr61	4.74	Cldn2	3.25	Ppl	2.73	Cxcl2	2.57
Ankrd1	4.69	Selenbp2	3.21	Ccl2	2.73	Cyp2s1	2.56
Cldn4	4.35	Slc23a3	3.19	Lrp2	2.72	Map17	2.55
Fos	4.32	Abcb1b	3.16	S100a6	2.72	Gprc5a	2.53
Tubb2b	4.10	Chrnb1	3.14	Spink3	2.70	C9	2.48
Klhl13	3.97	Ager	3.07	Atf3	2.69	Lamc2	2.45
Lmcd1	3.87	Cldn6	3.02	Junb	2.69	Tnfaip3	2.45
Emp1	3.78	Plscr2	3.02	Rragd	2.68	Orm1	2.41
Cxcl10	3.70	Selenbp1	3.01	Sftpd	2.68	Gpx3	2.40
F2rl1	3.70	Ahnak	3.00	Anxa3	2.67	Snx7	2.39
Cxcl1	3.69	Ier3	3.00	Tinagl	2.67	Cav1	2.35
Krt7	3.62	Psca	2.96	Jag1	2.66	Igf2bp1	2.33
Flrt3	3.56	Krt2-8	2.95	Urp	2.66	Kcnk1	2.33
F2rl1	3.56	Krt1-19	2.89	Tmem27	2.64	Gp38	2.32
Itga3	3.55	Esm1	2.88	Spint1	2.63	Ccnd1	1.72

C

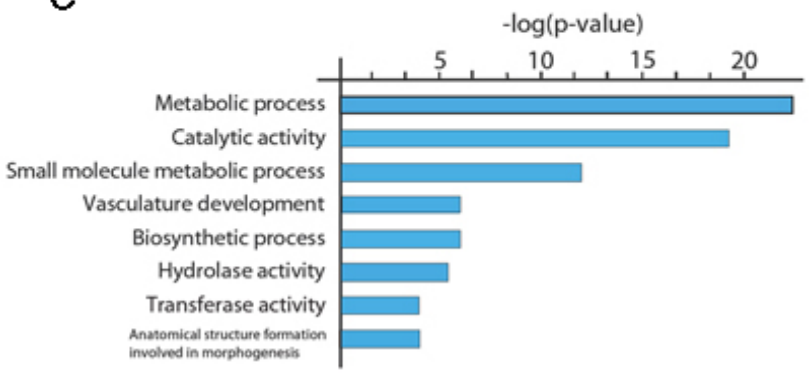

Figure 9. Global gene expression profiles of the *Lats1/2* double mutants on P0. Heat map (A) showed up (red) and down (green) regulated gene expression in *Lats1/2* double deleted livers as compared to wt, among which the most upregulated genes were selected and listed in B. The red highlighted genes are the ones that are also upregulated in *Yap* over-expressed mutant livers. GO assay revealed the *Lats1/2* deletion majorly affected liver metabolic function, together with alterations in vasculature development.

4.4 Biliary hyperplasia and liver stem cell activation in *Mst, Sav1* and *Lats* mutants

A striking phenomenon in all three mutants (*Mst*, *Sav1* and *Lats*) was the expansion of BEC cells. In *Sav1* mutants, BECs showed expansion at around 8 months (**Figure 10C**). In *Mst* mutants, BEC expansion started from 1 month old and dramatically infiltrated into the liver plate at 2 months old (**Figure 10B**). Both mutant livers had inflammatory response represented by increased macrophage population (*F4/80* positive, **Figure 10E and F**), suggesting there was chronic hepatic injury. However, it is not known whether the BEC expansion is activated by hepatic injury (cell non-autonomous) or intrinsic gene deletion (cell autonomous), or both. Similar but more dramatic phenomenon was observed in *Lats* mutants at P0 (**Figure 11 E and G**), suggesting bile duct developmental defects upon Lats deletion.

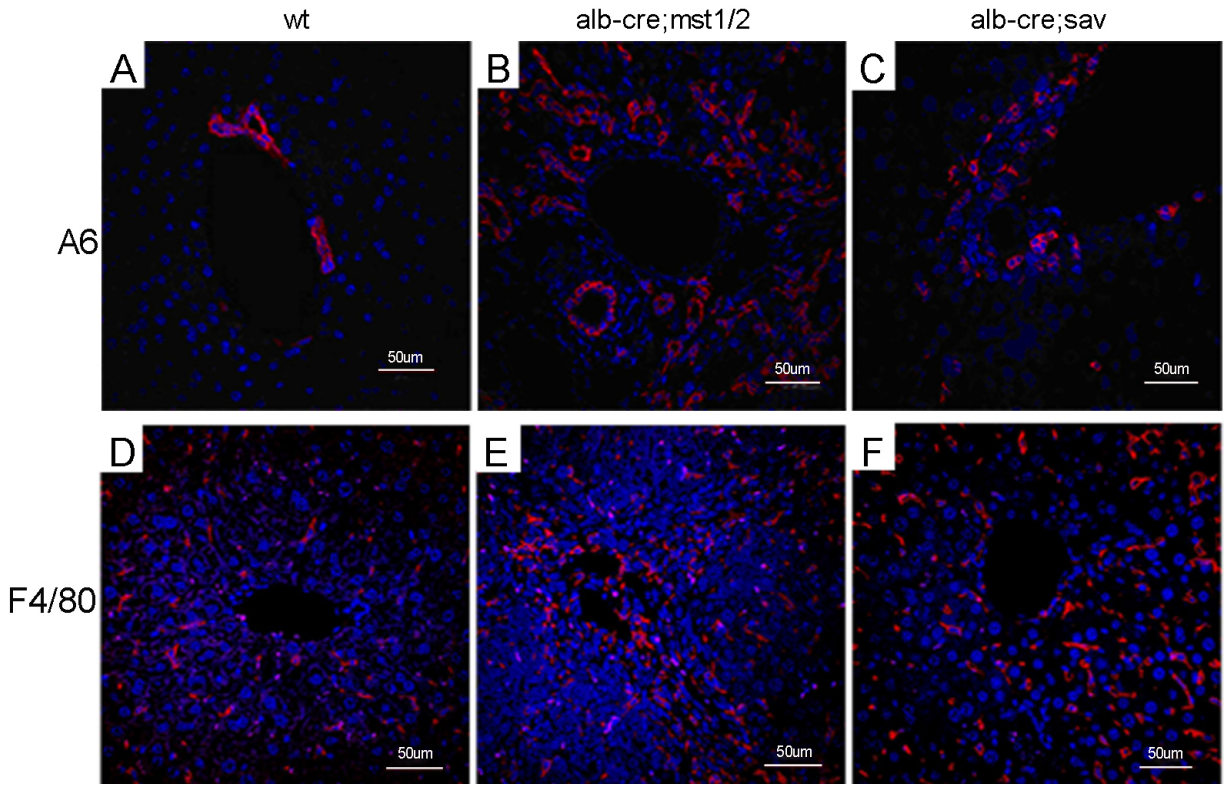

Figure 10. Oval cell activation and inflammatory response in *Mst* and *Sav1 mutants*. The A6 antibody, a marker for oval and ductal cells stains only ductal cells in wild-type tissues (A), but stains both ductal cells and periductal cells in *Mst1/2* mutants (B) and *Sav1* mutants (C). Inflammatory response is revealed by F4/80 staining, a marker for macrophages. Both mutants show elevated macrophage population (E and F) [38].

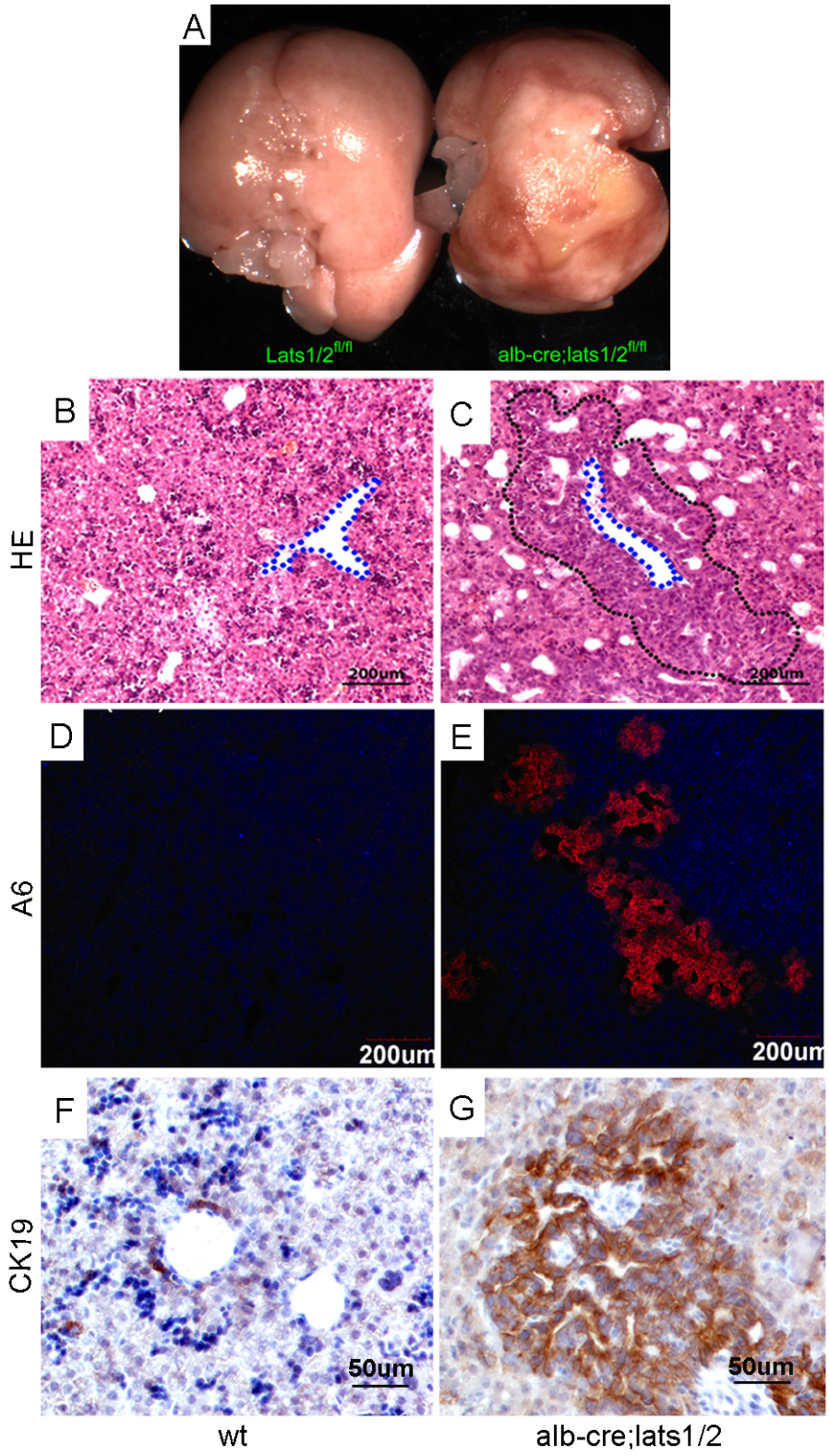

Figure 11. BEC hyperplasia in *Lats1/2* mutants at P0. *Lats1/2* double mutants die from

hypoglycemia on P0. (A) In contrast to the even and smooth surface texture of the wild type liver, *Lats1/2* double deleted liver shows necrotic lesions (A). While BECs are rarely visible in wild types by HE staining, many are found surrounding the portal area in mutants (C). Consistently, both *A6* and *CK19* staining reveal expanded population of oval/ductal cells in mutants (E and G).

As liver stem/progenitor cells are believed to reside in the BECs and/or periportal hepatocyte population [172,173], we used antibody staining to detect whether they were activated together with BECs. Although there is no specific liver stem cell marker, several antibodies (*OC2-1D11, MIC-1c3*, *A6* and *OC-6*) that detect a heterogeneous population of the immature hepatic cells have been generated [103,174,175,176,177] and widely used for detecting immature hepatic cell population. We found liver stem/progenitor cell activation in all three mutants (*Mst, Sav1* and *Lats*) using at least two of these antibodies (**Figure 12,** only one antibody staining is shown here for *Sav1* due to poor image quality).

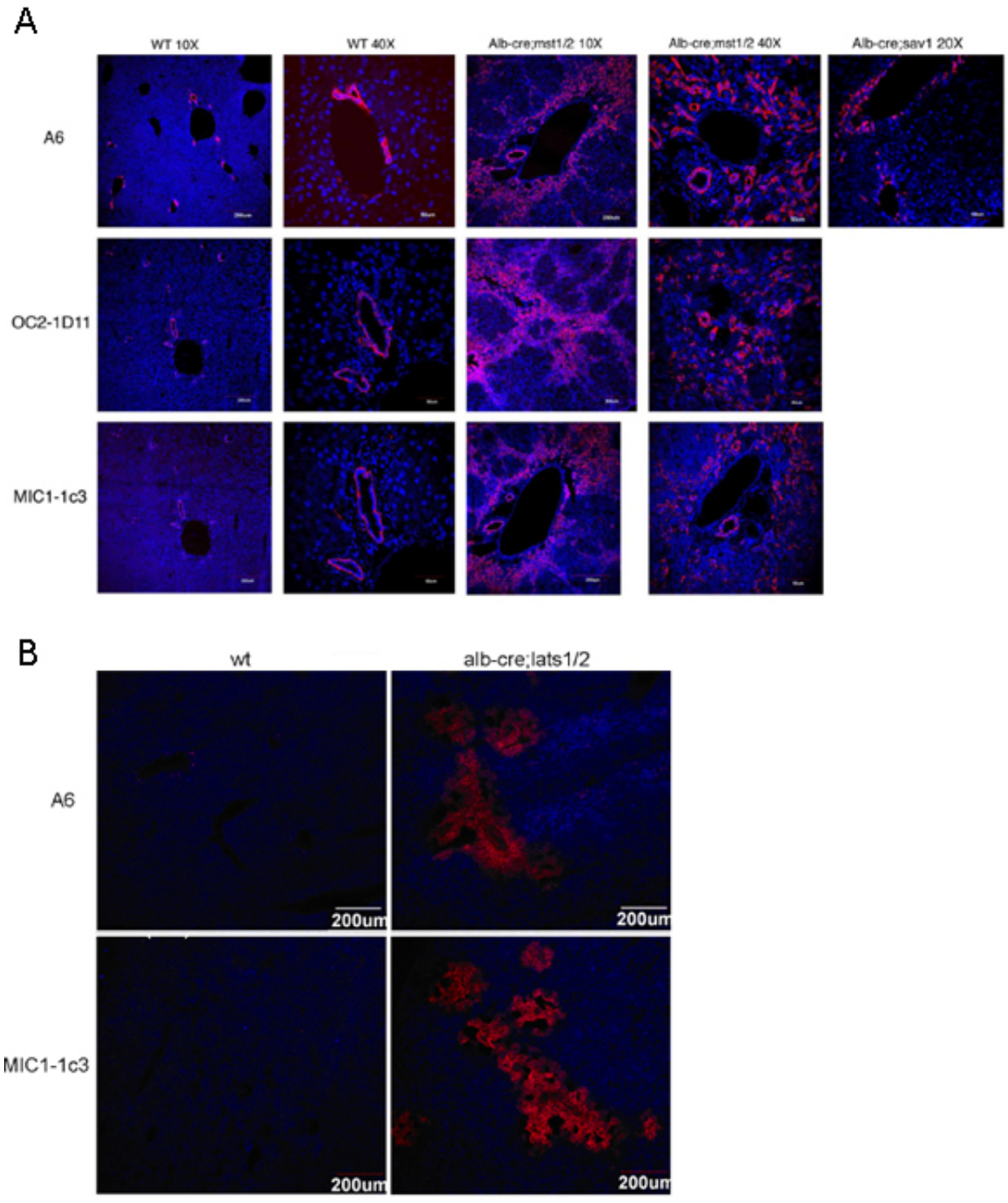

Figure 12. Antibody characterization of liver oval cell. (A) The antibodies *A6*, *OC2-1D11*, and *MIC1-1c3* stain ductal cells in wild-type (see WT 10X and 40X). At 2 months old, *Mst1/2* mutants have increasing *A6*, *OC2-1D11*, and *MIC1-1c3* positive

cells surrounding the portal area and also infiltrating into liver plates. *Sav1* mutants also exhibit enhanced *A6* labeling at four months of age. Antibody *A6* and *MIC1-1c3* recognize a few newly formed ductal cells in E18.5 wt liver. However, more positively stained cells clustered and formed ductal structure in *Lats1/2* mutants. All sections are counterstained with DAPI.

4.5 *Yap* and *Taz* are both dominant downstream inhibition targets of *Lats*

Although *Lats* is a broad governor for cellular homeostasis [53], *Yap* and *Taz* are the only known proteins inhibited by *Lats*. In order to know whether *Yap* and *Taz* are the main *in vivo Lats* interacting proteins that contribute to *Lats* mutant phenotypes, we performed the rescue experiment by introducing floxed-allele *Yap* and *Taz* into the *alb-cre;lats1/2* genetic background. The efficiency of *alb-cre* mediated *Yap* and *Taz* deletions was accessed by both mRNA level and protein level (**Figure 13A**). Results showed over 99% deletion of *Yap* (**Figure 13B**) and approximately 80% deletion of *Taz* (**Figure 13C**).

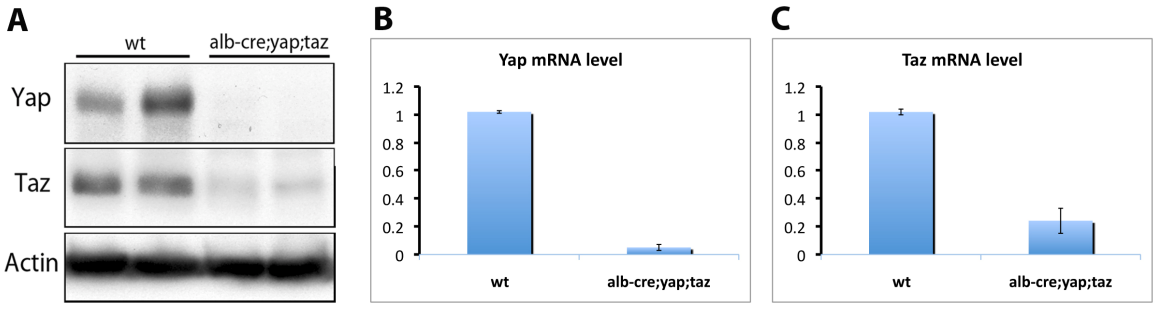

Figure 13. *Yap* and *Taz* deletion efficiencies by *alb-cre*. (A) Western blot shows reduced *Taz* protein level and almost undetectable *Yap* protein level in *Yap/Taz* mutants, which are consistent with the mRNA level detected by real-time PCR, shown in (B, Yap) and (C, Taz).

Yap is required for bile duct formation and hepatocyte survival, but *alb-cre;yap* mice are still viable and tumor free for more than one year [56], which potentiates the outcome of longer lifespan of the *alb-cre;lats1/2;yap* mice if *Yap* activation does contribute to *Lats* mutant phenotype. Our results support this speculation by showing that the medium survival length of the *alb-cre;lats1/2;yap* mice was 12 days (**Figure 14**), which significantly extended *Lats* mutants lifespan (P0) by restoring glycogen synthesis (**Figure 15C**). Deleting even one allele of the *yap* gene significantly rescued the *Lats* mutant phenotype: ductal hyperplasia was reduced (**Figure 16**) and the lifespan was extended with a medium survival length of 5 days (**Figure 14**). Thus, *Yap* is a main Lats downstream inhibition target *in vivo* and its activation contributes significantly to *Lats* mutant phenotype.

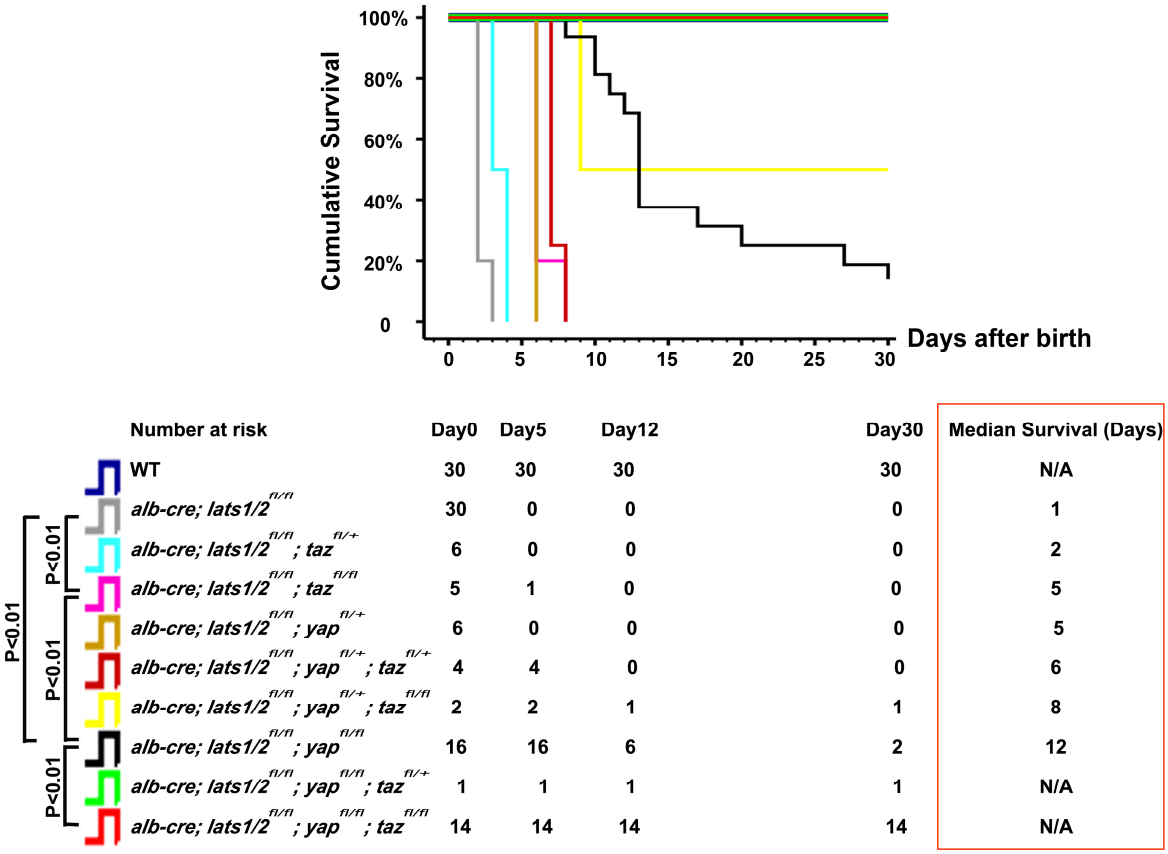

	Number at risk	Day0	Day5	Day12	Day30	Median Survival (Days)
	WT	30	30	30	30	N/A
	alb-cre; lats1/2$^{fl/fl}$	30	0	0	0	1
P<0.01	*alb-cre; lats1/2*$^{fl/fl}$ *; taz*$^{fl/+}$	6	0	0	0	2
P<0.01	*alb-cre; lats1/2*$^{fl/fl}$ *; taz*$^{fl/fl}$	5	1	0	0	5
P<0.01	*alb-cre; lats1/2*$^{fl/fl}$ *; yap*$^{fl/+}$	6	0	0	0	5
P<0.01	*alb-cre; lats1/2*$^{fl/fl}$ *; yap*$^{fl/+}$ *; taz*$^{fl/+}$	4	4	0	0	6
P<0.01	*alb-cre; lats1/2*$^{fl/fl}$ *; yap*$^{fl/+}$ *; taz*$^{fl/fl}$	2	2	1	1	8
	alb-cre; lats1/2$^{fl/fl}$ *; yap*$^{fl/fl}$	16	16	6	2	12
P<0.01	*alb-cre; lats1/2*$^{fl/fl}$ *; yap*$^{fl/fl}$ *; taz*$^{fl/+}$	1	1	1	1	N/A
P<0.01	*alb-cre; lats1/2*$^{fl/fl}$ *; yap*$^{fl/fl}$ *; taz*$^{fl/fl}$	14	14	14	14	N/A

Figure 14. *Yap/Taz* deletion rescues *Lats1/2* mutants in a dose-dependant manner. From the survival curve and the median survival length, *Yap* and *Taz* show dosage effects in rescuing *Lats1/2* double mutants neonatal lethality. While Yap appears to be a major downstream effecter of *Lats1/2* protein as its deletion extends *Lats* mutants lifespan to a great degree, *Taz* is also indispensable for proper liver function, as *Taz* deletion significantly increases *Lats* mutant and *Lats* plus *Yap* tri-deletion mutants' life spans.

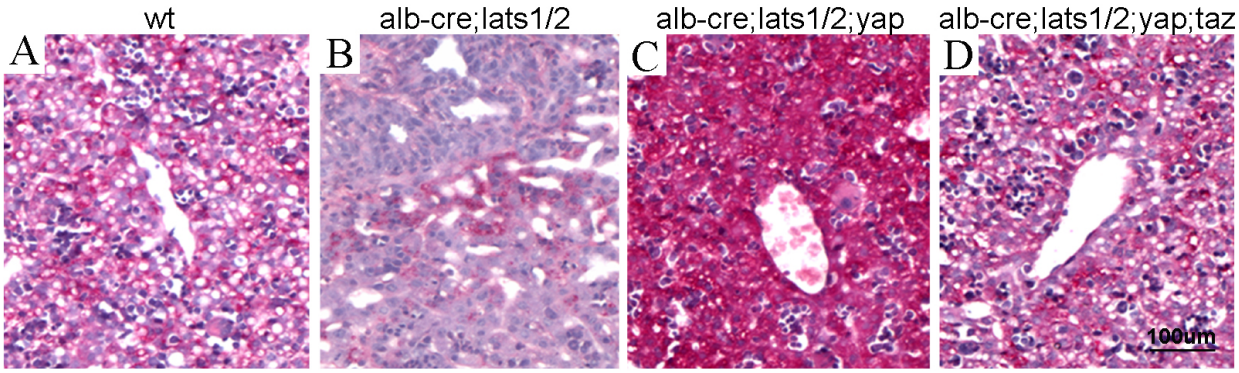

Figure 15. Glycogen level comparison in the rescue experiment by PAS staining. (A) Glycogen level in wild-type P0 liver. *Lats1/2* double mutant have significantly reduced the glycogen level (B). By combining Yap deletion, the liver actually shows an increased glycogen level (C). The glycogen level is totally normal when combining *Yap* and *Taz* deletions with *Lats1/2* double deletion (D).

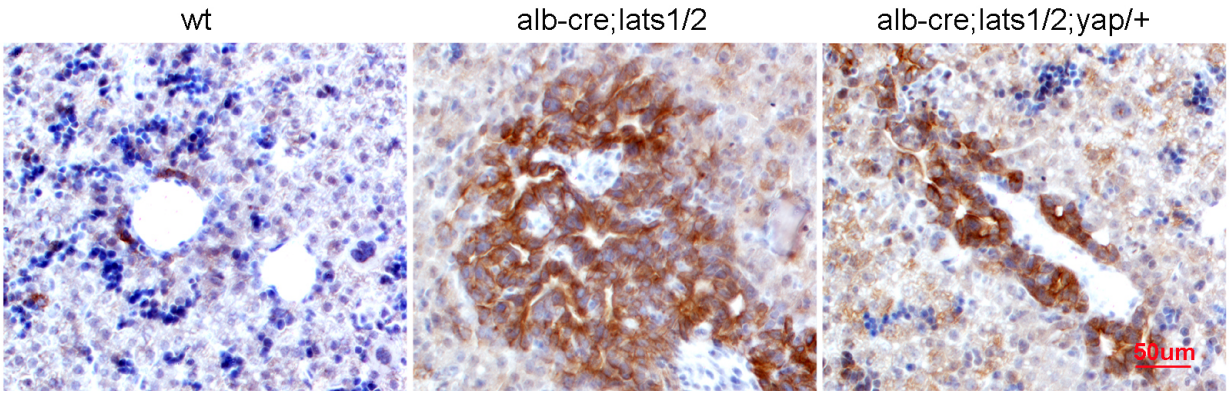

Figure 16. Deletion of one allele of *Yap* decreases *Lats1/2* double mutants' ductal hyperplasia. In P0 wild type liver*, CK19* positive cells are few, surrounding the portal vein. In *alb-cre;lats1/2* liver, *CK19* positive cells show hyperplasia. In *alb-cre;lats1/2;yap/+* liver, the number of *CK19* positive cells is between these of the wild-type and *alb-cre;lats1/2*; Ductal structural can be seen, although slight hyperplasia still exists.

Taz is a paralog of *Yap* and also biochemically phosphorylated and inhibited by *Lats*. So far, there has not been any report about *Taz* function in the liver. In characterizing of *alb-cre;yap;taz* liver, we found that further *Taz* deletion did not significantly elevate the mutant phenotype of the *Yap* deletion. Similar phenotypes showing increased hepatocyte turnover (**Figure 17**) and defects in bile duct development were found (**Figure 18**). The *alb-cre;yap;taz* mice were viable and tumor free up to 1 year old. As with *Yap*, to test whether *Taz* is a down-stream target of *Lats* and contributes to *Lats* mutant phenotype, *Taz* deletion was introduced into a *Lats* mutant genetic background. The significantly extended median survival time (5 days) of the *alb-cre;lats1/2;taz* mutants (**Figure 14**) revealed that *Taz* is also a main *Lats* downstream inhibition target and its activation contributes to *Lats* mutant phenotype.

Moreover, according to the survival curve (**Figure 14**), the mutants' median survival time was extended as one more allele of *Taz* and *Yap* were deleted, suggesting that *Taz* and *Yap* rescued *Lats* mutant lethal phenotype in a dosage-dependent manner on the basis of a single allele. Furthermore, synergistic effect between *Yap* and *Taz* may exist as *Yap* and *Taz* double deletion showed the most dramatic rescue effeciency, which was significantly different from those of either *Yap* or *Taz* deletion.

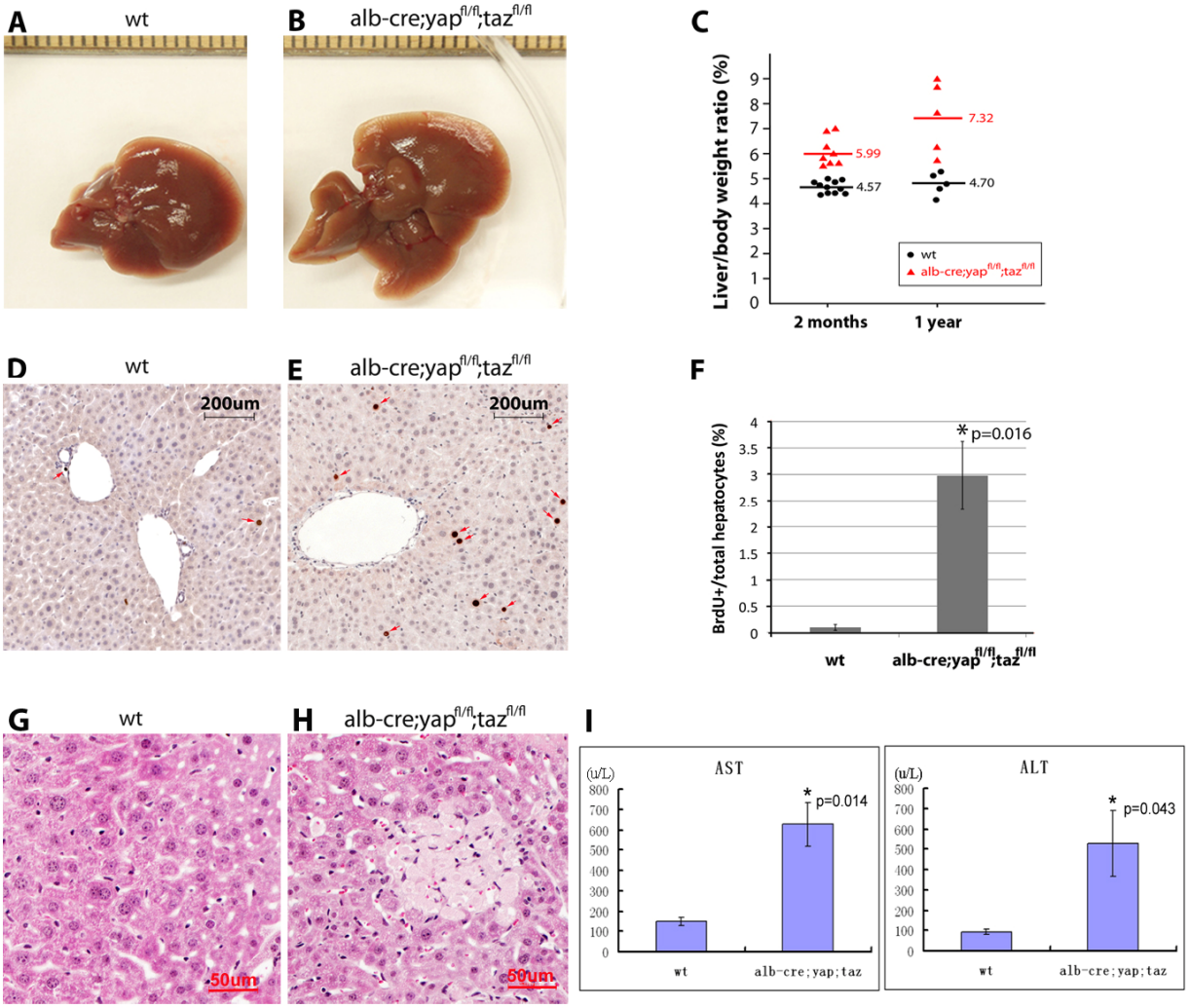

Figure 17. Increased hepatocyte turnover in *Yap/Taz* double deleted liver. The mutant liver is larger (B) as compared to wild type (A). The mutants' mean liver/body weight ratio is slightly higher than wild type (C), which is due to continuous hepatic proliferation (E and F). In addition, the mutant liver shows increased inflammation and engulfment of hepatocytes by macrophages (H). Mutant hepatocyte injury is represented by increased AST and ALT level (I).

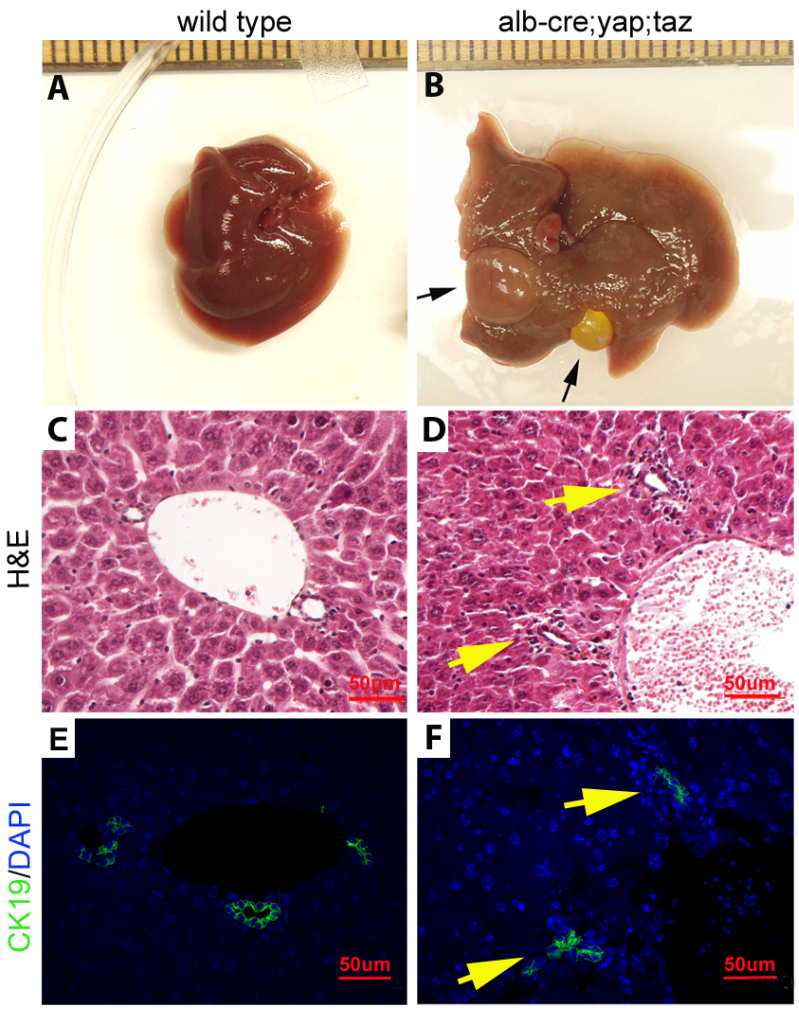

Figure 18. Bile duct malformation in *Yap/Taz* double deleted liver. Mice with liver-specific deletion of *Yap/Taz* are viable, however the liver has a larger gallbladder and develops adenomas at around one year of age (B). Adenoma is a kind of benign tumor that characterized by loss of bile ducts. Though in mutants some areas still develop bile ducts, they are malformed as shown in HE staining (D) and *CK19* staining (G, arrowed). C and F show the morphology of normal bile ducts in wild type.

4.6. *Yap* increase/activation correlates with BEC expansion in *Lats* mutant.

Interesting questions have arisen regarding the cause of biliary hyperplasia in *Mst, Sav1* and *Lats* mutants and whether it is cell autonomous or non-autonomous. As *Mst* (facilitated by *Sav1*) inhibits *Yap/Taz* through *Lats*, it is very likely that the activated *Yap* activity is responsible for the biliary hyperplasia in all three mutants. We further investigated the mechanism of biliary hyperplasia in the *Lats* mutant. Due to the fact that *Lats* functions downstream of *Mst*, and also because *Lats* mutants show the most dramatic biliary hyperplasia, their use will facilitate the detection of abnormalities.

The intrahepatic bile duct (IHBD) plates form around E14.5 [178,179]. Therefore, mutant and wild type livers from E15.5 to E18.5 were collected to investigate the progress of biliary hyperplasia. Double staining of CK19 and Ki67 revealed that elevated BEC proliferation started from E16.5 and became dramatic at E17.5 (**Figure 19**). Interestingly, *Yap* was dominantly expressed in BEC-like cells and increased *Yap*-positive periportal cell population also starting from E16.5 and further elevated afterwards (**Figure 20**). The correlation between these two observations supports our speculation that activated *Yap* is responsible for biliary hyperplasia. Thus, cell autonomous proliferation contributes, at least partially, to the biliary hyperplasia in all three mutants. Furthermore, *Yap* may be a new BEC marker, whose level/activity regulates bile duct development. Double staining of *Yap* with a known BEC marker (e.g. *CK19* and *Sox9*) is required to confirm this theory.

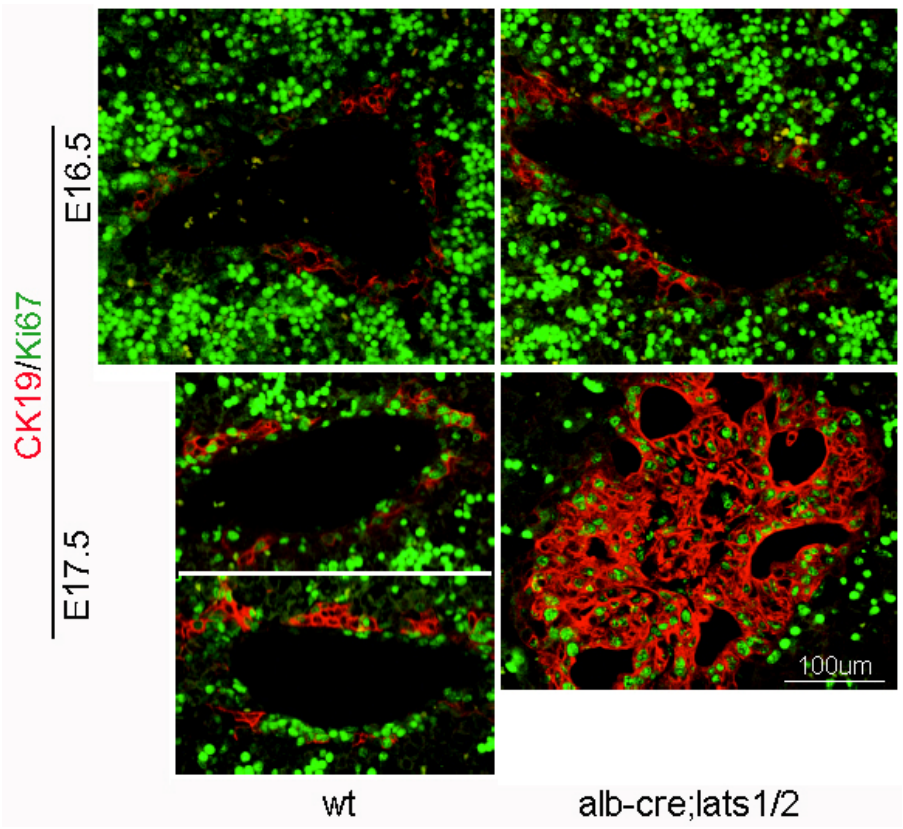

Figure 19. BEC proliferation in Lats mutants starting from E17.5. (By Kilang Yanger, University of Pennsylvania)

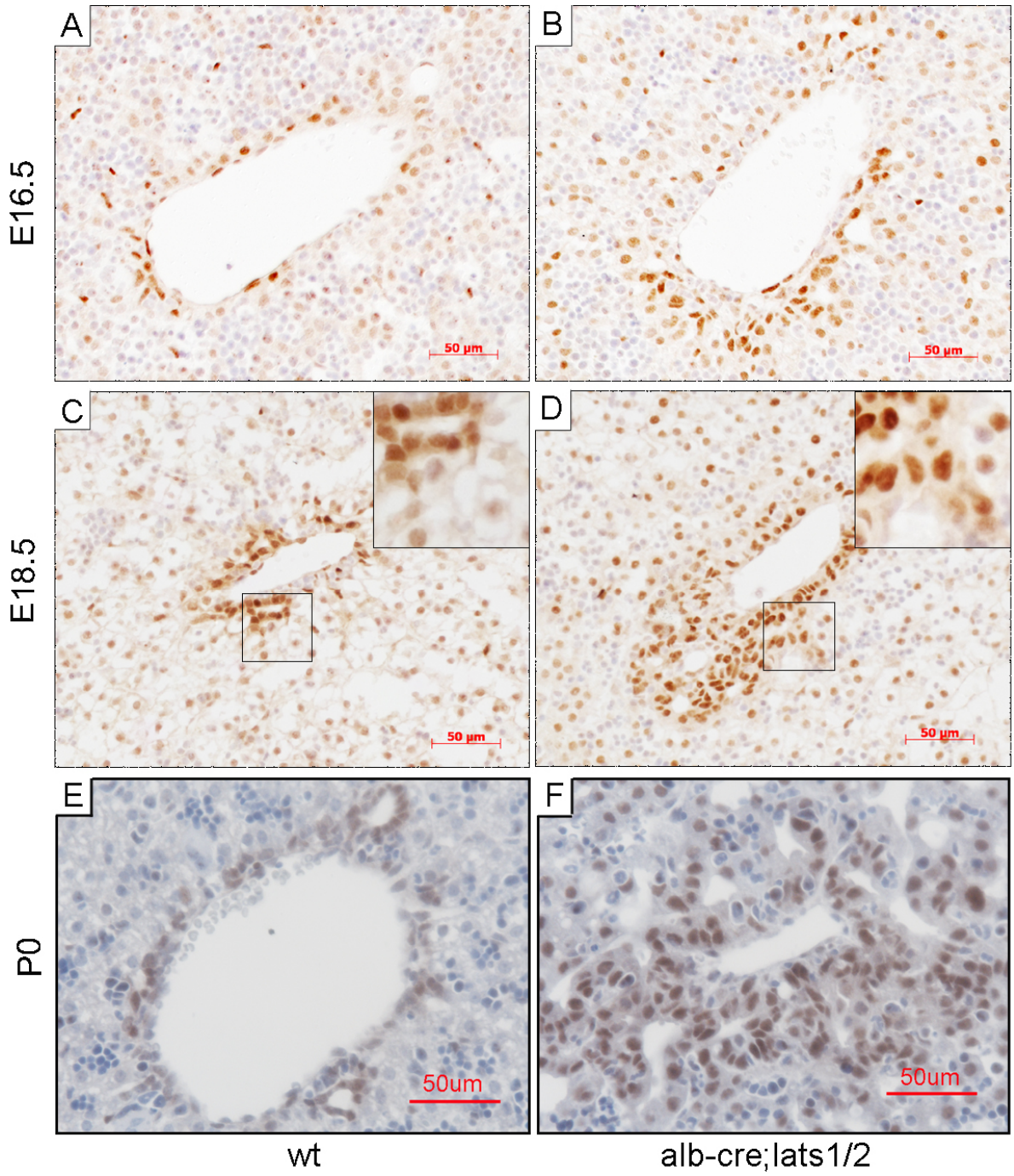

Figure 20. *Yap* positive cells expand in *Lats* mutant. *Yap* antibody positively stains bile ductal-like cells in wild-type livers (A, C and E). *Yap* positive cells in *Lats1/2* double mutants are dysplasic and show progressive hyperplasia, and their nuclei are pleomorphic (B, D and F).

4.7 Notch signaling is activated in *Lats* mutant periportal area

We further investigated whether the dysregulation of the Hippo pathway has impact on classic signaling pathways that are essential for bile duct development. As *Jagged1* gene expression is significantly increased in both *Lats* deleted liver (**Figure 9**) and *Yap* overexpression liver [34], Notch signaling becomes a promising target candidate for our investigation. By double staining of *Jagged1* and *CK19*, a close association between *Jagged1* positive cells and expanding *CK19* positive cells was revealed. Moreover, known Notch signaling downstream gene targets (*Hes1* and *Ostp*) were activated surrounding the portal area with biliary hyperplasia (**Figure 21**). These results revealed that Notch signaling was elevated upon *Lats* deletion in the portal region, and thus contributed to biliary hyperplasia by enhancing BEC-fate determination and promoting bile duct tubular morphogenesis.

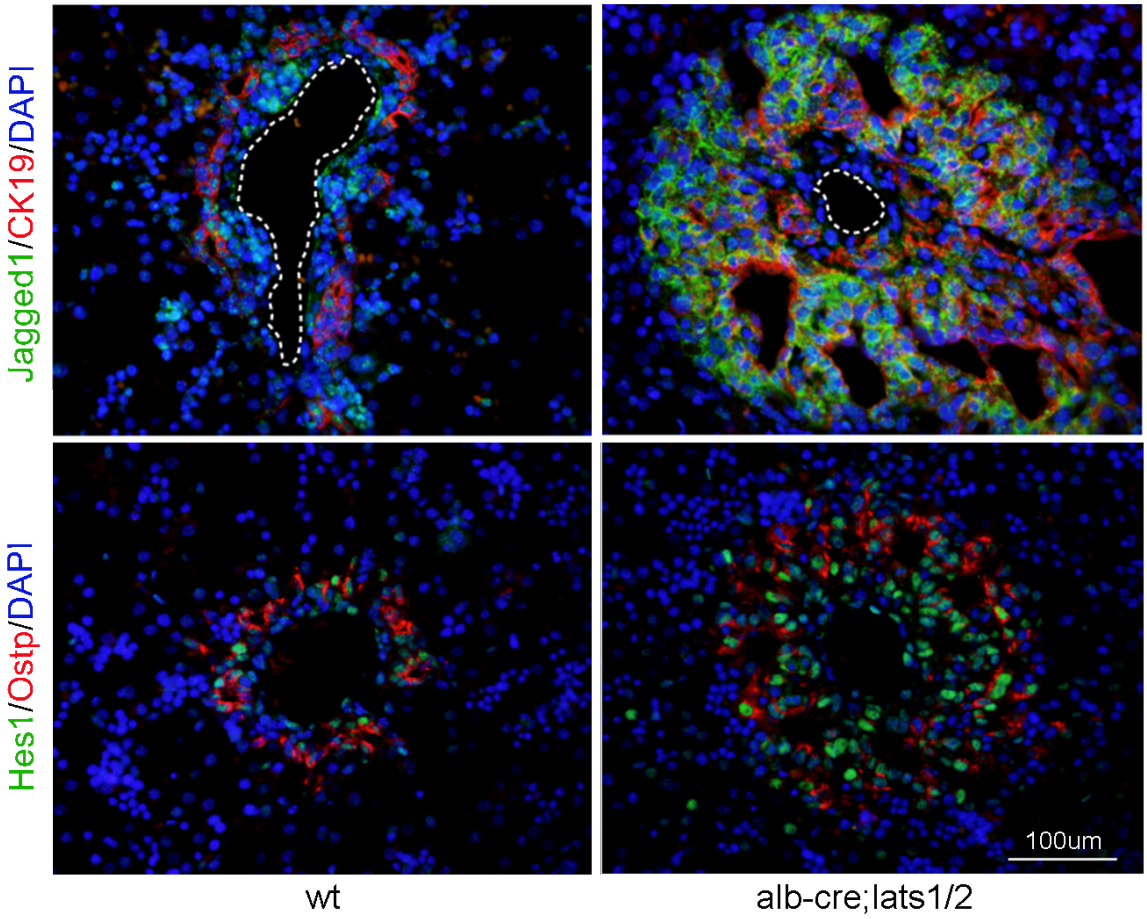

Figure 21. Notch signaling activation in the periportal area of E18.5 *Lats* mutants. (By Kilang Yanger, University of Pennsylvania)

4.8 *Yap* and *Taz* are activated during liver regeneration

Because *Yap* and *Taz* are nuclear effectors of the Hippo pathway, their activities can manifest Hippo pathway activity. *Yap* and *Taz* phosphorylation and protein levels were analyzed during liver regeneration as indicators of potential correlation between Hippo pathway activity and liver re-growth.

To cover all three liver regeneration phases, six time points were chosen for protein analysis: 0h (hour), 6h, 24h, 48h, 72h and 7 days. Western blot analysis showed a correlation between *Taz* activity and regeneration progress: nuclear unphosphorylated *Taz* increased in the priming and proliferative phases (evidenced by decreased cytoplasmic phospho-*Taz* and increased total *Taz,* **Figure 22A**), and decreased in the termination phase (evidenced by increased cytoplasmic phospho-*Taz* and decreased total *Taz*). However, phospho-*Yap* and total *Yap* changed in the same direction, therefore we were unable to determine the coupling between nuclear unphosphorylated *Yap* and liver regeneration based on total protein analysis (**Figure 22B**). For this reason, we further used nuclei-cytoplasm protein extracts to detect the active form of *Yap* (unphosphorylated) in the nuclei. Results showed a slight increase of nuclear *Yap* levels during the proliferative phase (**Figure 22C**), suggesting that Yap was also activated. To exclude any artificial results from the surgery procedure, pseudo-surgery (sham) were carried out and mice were sacrificed at exactly the same time points with that of the PHx mice. Phospho-*Yap*, *P21* and *PCNA* protein levels were checked, and the results showed no change along all the time points that tested, implying the surgical procedure does not affect the proteins' activities or levels (**Figure 22D**).

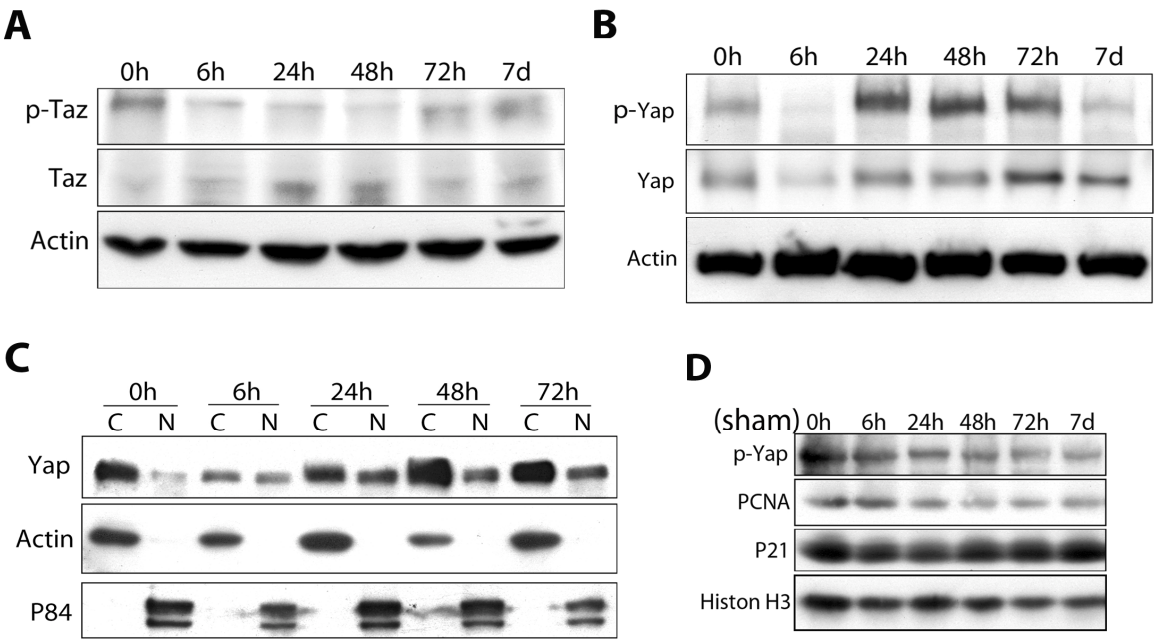

Figure 22. *Yap* and *Taz* activities during normal liver regeneration. During regeneration, *Taz* phosphorylation is decreased while its total protein level is increased (A). *Yap* phosphorylation is decreased at 6h after PH, however increases afterwards. The total *Yap* amount shows a similar trend during regeneration (B). Further nuclear and cytoplasmic localization examination show increased *Yap* nuclei localization along regeneration (C). *Yap* phosphorylation, *PCNA*, and *P21* expressions are not altered in pseudo-surgery (sham) group (D).

4.9 *Yap/Taz* null and *Mst1/2* null livers show impaired regeneration

In order to further investigate whether *Yap/Taz* is required and sufficient to promote liver regeneration, *Yap/Taz* deletion (*alb-cre;yap/taz*) and *Yap/Taz* activation (*alb-cre;mst1/2*) mice were subjected to PH. To reduce the original liver size variation of the *Mst1/2* mutant, PH was performed in young mice (5- to 6-week old). According to our previous report, *Mst1/2* mutant liver size variation at 1 month is much less than at 2 months [38].

Re-growth percentage and hepatocyte proliferation were accessed as parameters for liver regeneration ability. While wild-type livers could fully (100%) re-grow back to their original sizes, both *Yap/Taz* and *Mst1/2* mutants re-grew to approximately 70% of their original sizes (**Figure 23A**). Decreased hepatocyte proliferation was likely the main reason according to BrdU incorporation assay (**Figure 23B**). As *Yap* and *Taz* are the main effecters of Hippo signaling and their pro-proliferation functions are the theoretical basis for the hypothesis that Hippo pathway regulates organ size, the 70% regeneration ability of the *Yap/Taz* null liver suggests that the Hippo pathway is not critically required for liver regeneration. The impaired regeneration is possibly due to the disease effect from early embryonic deletion of *Yap/Taz.* For the same reason, it remains unknown whether activated Yap/Taz (Mst null) can promote the liver to a larger setting point. It should be tested in a way that allows avoidance of the disease effect of *Mst* by deleting the genes prior to PH surgery, possibly, by introducing cre-recombinase adenovirus through tail-vein injection. From the fact that the liver can still regenerate without *Yap* and *Taz*, it can be concluded that Hippo signaling is not a sole

determinant for liver regeneration, or for liver size setting point. Another interactive network must compensate the Hippo pathway's role in liver regeneration.

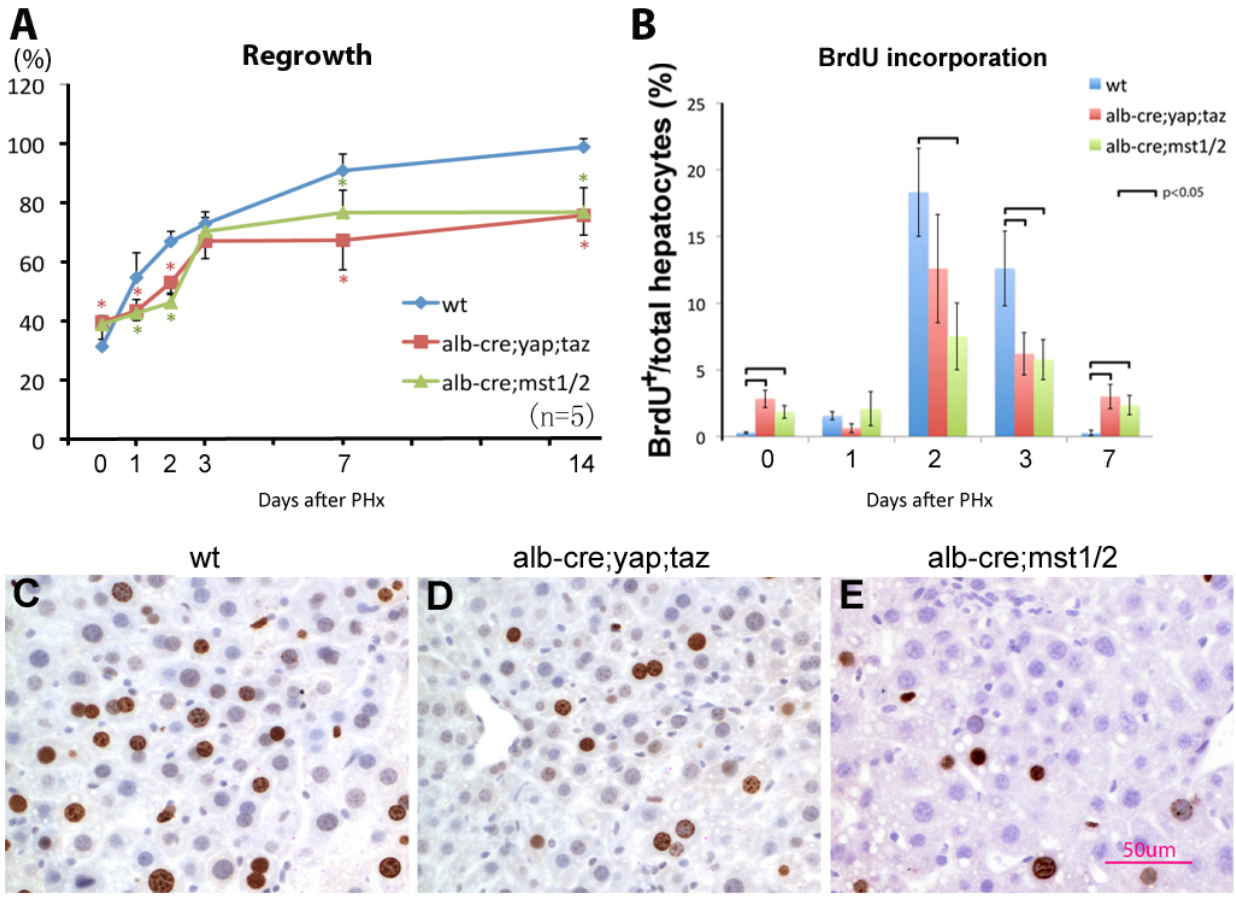

Figure 23. Both *Mst1/2* double mutants and *Yap/Taz* double mutants can regenerate to approximately 70% of their original sizes. (A). Neither mutants' hepatocytes can fully proliferate responding to regeneration signals. *Mst1/2* mutants have significantly retarded hepatocytes proliferation at the peaking time point (2 days after PH). The represented BrdU staining of samples of day-2 after PH shows decreased *Yap/Taz* mutant hepatocyte proliferation (D), as well as decreased *Mst1/2* mutant hepatocyte proliferation (E), as compared to normal hepatocyte proliferation(C).

4.10 Hippo signaling regulates the timing of hepatocyte proliferation

Liver regeneration is indeed a process of synchronized hepatocyte cell-cycle progression [166,180]. Although many genes' loss-of-function do not completely inhibit liver regeneration, they often affect the timing of hepatocyte cell-cycle progression [131,164,181,182]. We therefore also investigated the timing of the *Yap/Taz*-null and *Mst*-null hepatocyte cell-cycle progression, specifically, the timing of the cell-cycle reentry.

A critical step of cell cycle progression is cell cycle initiation, in which cells pass through the G1 phase cell cycle checkpoint and enter the DNA-synthesizing S phase. *Yap/Taz* double mutants had higher *Cyclin D1*, *P21* and *PCNA* baseline levels before PH (0h), which were likely due to cell non-autonomous compensatory growth. After PH, however, a synchronized but delayed expression pattern was seen (**Figure 24A**). Specifically, *Cyclin D1* expression peaked at 72 h after PH in mutants, which was 2 days later than the wild-type littermates. The timing of *STAT3* signaling (known to be a master regulator for the timing of hepatocyte cell-cycle reentry [183]) was unchanged although enhanced at the 24h time point (**Figure 25A**), suggesting the *Yap/Taz* deletion may affect the downstream of STAT3 signaling and caused the delay of CyclinD1 expression.

The same analysis was performed in *Mst1/2* double mutants. Instead of delayed cell cycle re-entry, *Mst* null hepatocytes showed a persistent proliferation pattern (**Figure 24B**). Similar to *Yap/Taz* null hepatocytes, the timing of the *STAT3* activity in *Mst* null hepatocytes was unchanged, but slightly elevated at the 24h time point

(**Figure 25B**), suggesting that the *Mst* deletion also caused effects downstream of *STAT3* signaling and disrupted the synchronization of cell cycle re-entry.

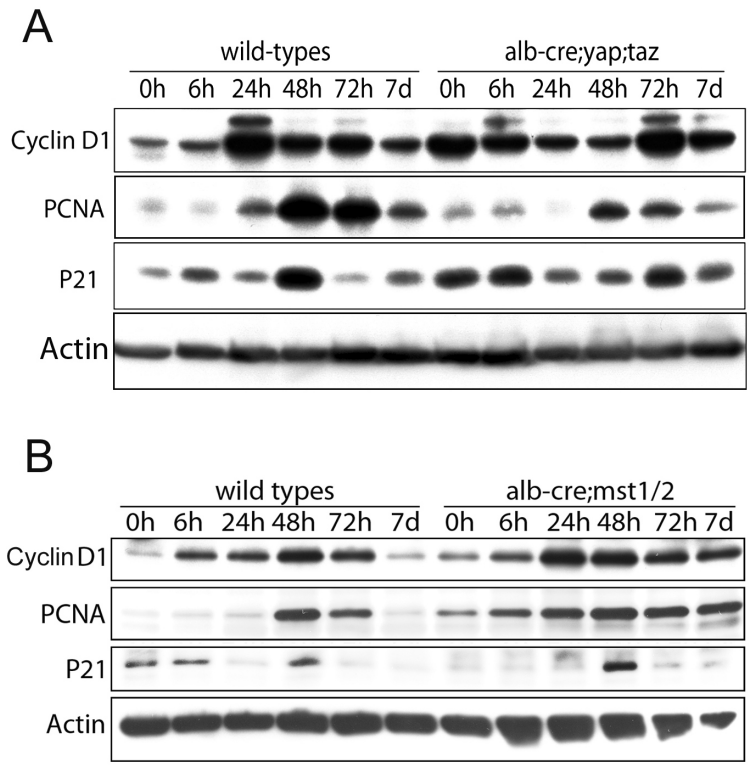

Figure 24. Cell cycle progression is delayed during *Yap/Taz* double mutants' regeneration. (A), and advanced during *Mst1/2* double mutants' regeneration (B).

Yap/Taz double mutants (A) have higher *Cyclin D1*, *PCNA* and *P21* basal level before regeneration (0h). Responding to the regeneration signal, *Cyclin D1* in mutants shows maximal expression at 72 h, which is 2 days later than the wild-type littermates' (24h). Peaking expression of *PCNA* in mutants is still at 48h, but the level is lower than that of wild type. Peaking expression of *P21* in *Yap/Taz* mutants is at 72h, which is one-day delayed as compared to the wild-type littermates. In *Mst1/2* double mutants (B), the basal levels of *PCNA* and *Cyclin D1* are higher, however, *P21* was lower as compared with wild-type littermates'. *Cyclin D1* peak level is at 24h in *Mst1/2* mutants, but occurs at 48h in the wild type littermates. *PCNA* level increases immediately after PH and remains persistently high afterwards, even at 7d after PH. *P21*'s peak time in

mutants is the same as in the wild-type littermate's (48h after PH); however, the protein level is higher as compared to wild-type littermates. Actin is used to show relatively equal loading among samples.

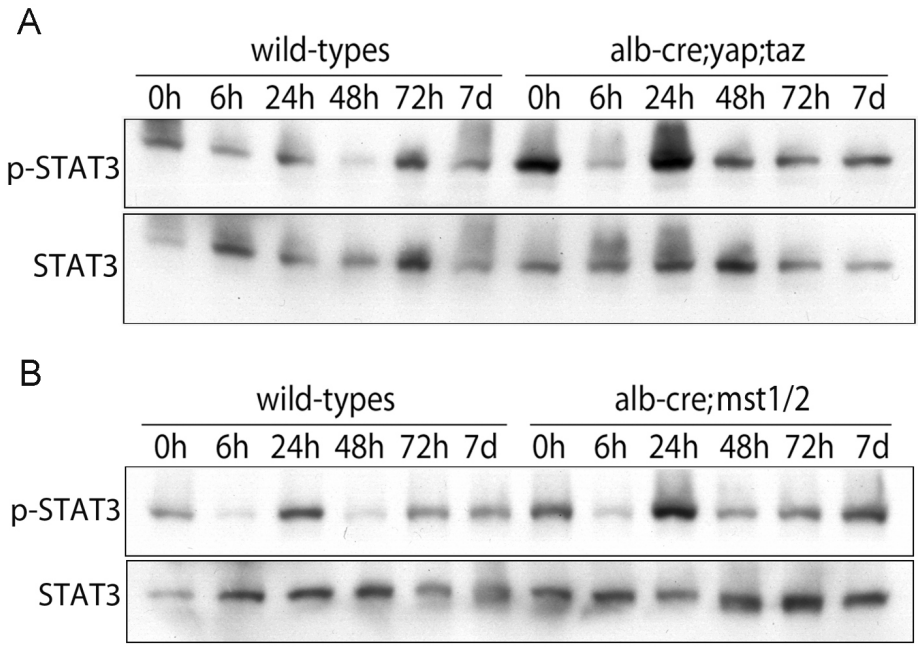

Figure 25. *STAT3* activity during regeneration. In wild type liver regeneration, *STAT3* peaks at 24 h after PH. In both *Yap/Taz* and *Mst1/2* double mutants, *STAT3* still peaks at 24h time point, but the levels are higher than at the same time point in wild types.

CHAPTER 5: DISCUSSION

Our study is among the first ones that address the Hippo pathway function in a mammalian system. We have shown that although the Hippo pathway functions ubiquitously in regulating tissue homeostasis, it has certain tissue specificity in the liver. Our work has addressed how the main components function individually in the live. Results show that the Hippo pathway is not only involved in maintaining liver homeostasis, but is also required for the liver development. Furthermore, we found evidence that the Hippo pathway interacts with Notch signaling in regulating the biliary system. However, in terms of the organ size control function, it is not the sole determinant of the organ size setting point, but does influence the timing of hepatocyte cell cycle progression. As tumor development is often associated with disturbances of the cell cycle regulation, the Hippo pathway may suppress liver tumor development through surveilling the hepatocyte cell cycle progression. Our study is significant in advancing understanding of the tumor suppression mechanism and in helping to develop potential therapeutic approaches for liver cancer.

5.1 *Mst* in liver tumor suppression

Before *Mst* was recognized as the "*Hpo*" kinase in the Hippo pathway, it was known for its role in mediating the apoptosis induced by cellular stress [184,185,186,187]. Except for its ability to form complexes with members of the *Rassf* family [52,188], which are known to be tumor suppressors, no direct evidence supported *Mst* being a tumor suppressor. When its *Drosophila* ortholog, the *Hpo* kinase, was characterized, new insights into the role of the Hippo pathway as a suppressor of tissue growth were gained. *Mst* was hypothesized to be a tumor suppressor in the mammals. To test this hypothesis, several groups, including our lab,

generated *Mst1* and *Mst2* conditional knockout mice and analyzed their phenotypes [37,38,41]. While the other groups studied *Mst* function only in the liver as inspired by the first report about *Yap* over-expression in liver resulting in HCC ([34]), we tested *Mst* function in several tissues by using both tissue specific (*villin-cre*) and widely-active *cre* (*MMTV-cre*, and *Caggs-cre*) lines. We found that *Mst* most likely has a ubiquitous function in tissue homeostasis, but also has certain tissue specific functions in the liver. The underlying mechanism is yet not known.

Different research groups consistently reported that HCC developed as a consequence of *Mst* deletion, suggesting that the *Mst* is an important liver tumor suppressor. Before tumor development, *Mst* null livers were bigger than normal due to increased hepatocyte proliferation and suppressed apoptosis [38,41,189], a feature reminiscent of the *Hpo* mutant phenotype in *Drosophila*. *Yap* activation was also consistently observed in the *Mst* null liver, which supported our hypothesis that the mammalian Hippo pathway is a tumor suppressor pathway. However, several inconsistencies exist between the *Mst* null livers generated by different labs. First of all, there is controversy of whether *Lats* mediates Yap inhibition by *Mst*: we found that the *Lats* phosphorylation was depleted in the *Mst* null hepatocytes [38]; another group claimed that *Lats* phosphorylation was unaffected upon *Mst* deletion [189]. The reason for this disagreement may be due to different cell types used in each experiment. We used the enriched hepatocytes, and the other group used *Mst* null MEFs. Whether *Mst* inhibits *Yap* through different mediators in different tissue contexts or cell types may be addressed by testing in other tissue types or in different cell lines.

Another disparity is in the histology results of *Mst*-null livers generated by different labs. Dr. Yingzi Yang's group and our group observed systematically inflammatory response in the *Mst* deleted liver resulting in infiltration of the macrophages together with liver progenitor cells into the periportal area [38,41]. This phenotype was not obvious in the *Mst*-null liver mouse model generated by Dr. Nabeel Bardeesy's lab [189]. In addition, mutant liver with systematic inflammatory response developed tumors in multifoci or a diffuse fashion [38,41], while the one without obvious inflammatory response developed tumor in unifoci [189]. By looking into the way these mutants were generated, we believe that the genetic differences contribute to these phenotypic inconsistencies. Dr. Yingzi Yang's group and our group used *alb-cre* to deletion both *Mst1* and *Mst2* at the same time (*alb-cre;mst1/2fl/fl*), while Dr. Nabeel Bardeesy's group deleted *Mst1* in the germline and later deleted *Mst2* in liver by *alb-cre* (*alb-cre;mst1Δ/Δ;mst2Δ/fl*). *Mst1* is an important regulator of T-cell maturation, adhesion and migration [190,191]. Under pathological conditions, such as bacterial and viral infection, liver immune cells including küpffer cells, NK cells, NKT cells, and T-cells are activated in a positive feedback loop to protect the host from bacterial and viral infections [192]. As the fetal liver is a major site of development of the immune system [193], germline deletion of the *Mst1* may impair the development of T-cells, disrupt the immune response loop and disable the inflammatory response that would occur when *Mst2* is further deleted by *alb-cre*. Persistent inflammation is the main cause of liver cirrhosis and subsequent development of HCC (reviewed in [194,195]). The systematic inflammatory response in the *alb-cre; mst1/2fl/fl* mice is very likely the main reason for the early development of multifocal cancerous lesions, which

accelerates the liver disease progression from the genetic alteration (i.e. *Mst* deletion). As a consequence, *alb-cre;mst1/2*$^{fl/fl}$ mice have a shorter lifespan (6-7 months) [38,41] compared with the *alb-cre;mst1Δ/Δ;mst2Δ/fl* mice (12-15 months) [189].

While the detailed mechanism of inflammatory response and tumor initiation in *Mst*-null liver is still not clear, there are several possibilities may apply. One is epigenetic alteration caused by *Mst* gene deletion. There are accumulating evidence that epigenetic mechanisms are essential for both normal development and cellular homeostasis. Global changes in the epigenetic landscape are a hallmark of cancer [196]. *Mst* can indirectly affect gene expression through inhibiting *Yap*, but also can directly regulate gene expression through interacting with chromatin. Over-expression of *Mst* can induce chromatin condensation through phosphorylation of histon *H2B* and *H2AX* [197,198] [199] and may thus regulate gene expression at the epigenetic level. Another possibility is the accumulation of DNA damage during mutant hepatocyte proliferation. One of *Mst* phosphorylation targets, the *γH2AX*, plays an important role in DNA double-strand break (DSB) repair [200,201,202] and has become a biomarker for measuring DNA damage [203]. Deletion of *Mst* may impair the DNA-repair mechanism through inhibiting *γH2AX*, resulting in DNA damage accumulation. DNA damage contributes to cell necrosis and release of dead cell cytosol, which triggers the inflammatory reaction and promotes tumorigenesis. A good example is the HCC induction by the carcinogen diethylnitrosamine (DEN) [204,205].

In conclusion, *Mst* is a liver tumor suppressor. It suppresses liver tumor formation by maintaining hepatocyte quiescence and liver homeostasis. It may provide a good model for studying inflammatory response and testing the corresponding treatments.

5.2 *Lats* in liver development

Lats is believed to be a broad governor of cellular homeostasis because of its involvement in many important cellular processes, including proliferation, apoptosis, senescence, transformation, and migration (reviewed in [53]). At the molecular level, multiple domains enable diverse functions such as protein-protein interaction and phosphorylation. Therefore, although *Yap* and *Taz* are so far the only known substrates of *Lats*, multiple substrates are predicted and there is ongoing research that aims to identify other *Lats* substrates by using consensus phosphorylation sequence of *Lats*. However, our *in vivo* genetic analysis about the relationship between *Yap/Taz* and *Lats* revealed that *Yap* and *Taz* are the main substrates of *Lats* (**Figure 14**). This close relationship between *Yap/Taz* and *Lats* may have liver-tissue specificity since *Lats* specific transcriptional targets identified in Hela cells suggest that the *Lats* functions through multiple pathways [53,206].

Although *Lats* contributes to many cellular events, how it functions *in vivo* and contributes to organ function is not known. Our work is the first one to study the *Lats* function *in vivo* by double deletion of the two *Lats* paralogs (*Lats1* and *Lats2*). We found that *Lats* may participate in governing the cholangiocyte-lineage formation through restricting both *Yap* activity and *Yap* protein levels. Through microarray analysis and immunostaining, we found that upon *Lats* deletion, the Notch signaling required for biliary differentiation and morphogenesis [81,82,83,87,88] was activated (**Figure 21)** while *Tbx3*, which globally inhibits the biliary differentiation [207], was suppressed. These changes may thus switch a normal liver developmental

environment to the one that favors the biliary development. Although hepatocytes still developed, microarray data on postnatal day 0 liver showed a global decrease in all most all the hepatocyte functions (**Figure 9**). This may be a result of immature hepatocyte development due to *Lats* deletion.

The mechanism of *Lats* control of hepatic lineage differentiation is yet unknown. One of the possible mechanisms is through interaction with the Notch signaling pathway. Elevation of *Jagged1* gene expression in both *Lats*-deletion mutants and *Yap*-over-expression mutants suggests that *Jagged1* may be a direct gene target of *Yap*. If so, *Lats-Yap(/Taz)* may affect the bile duct development by regulating the *Jagged1* expression and its downstream Notching signaling. In addition, *Sox9* is also up regulated in both *Lats* deficient mutants and *Yap*-over-expression mutants, which suggests that *Sox9* could be a direct target gene of *Yap*. *Sox9* is a BEC marker regulated by Notch signaling during biliary morphogenesis [77,82]. These results point towards a certain interactive relationship between the Hippo pathway and the Notch signaling. **Diagram 5** shows the possible relationship between the two pathways based on the assumption that *jagged1* and *sox9* are direct gene targets of *Yap*. How the two pathways together regulate bile duct development is particularly interesting because it may help advance understanding of the mechanism of human Alaggille syndrome (AGS). AGS is a genetic disorder characterized by abnormalities in liver, heart, eye, skeletal, craniofacial and kidney [208]. It is caused by a null mutation in Jagged1. In liver, Jagged1 deletion results in bile duct paucity and chronic cholestasis [84,86], which is one of the life-threatening symptoms in AGS patients. Obviously,

Jagged1 plays an important role in bile duct development, and understanding its regulation will be of course important for developing the treatments for AGS patients.

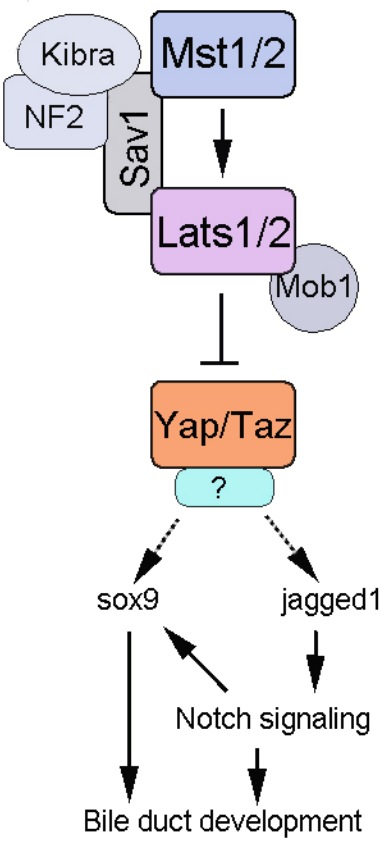

Diagram 5. Potential Hippo pathway function in bile duct development. The Hippo pathway inhibits *Yap/Taz* through phosphorylation. Unphosphorylated *Yap* (and likely *Taz* too) is likely to associate with some unknown transcription factor, and activating *jagged1* and *sox9* transcription, which contributes to the activation of Notch signaling and subsequent bile duct development. The relationships marked by dashed arrow lines need to be experimentally confirmed.

A major conclusion from the above discussion of the phenotypes of *Mst* and *Lats* mutants is that, *Mst* is important for the liver homeostasis because of its ability in reducing the inflammatory response; while *Lats* more closely interacts with *Yap* and regulates cellular behavior through controlling the hepatic transcription profile. Although the *Mst-Lats-Yap* linear kinase cascade is still present, the function of the mammalian Hippo pathway is complicated by the diverse individual functions of its components. Moreover, existence of multiple versions of Hippo pathway proteins may complicate the pathway further by adding other regulatory inputs. There is emerging evidence that *Mst3/4* interacts with *Ndr1/2* (*Lats* family proteins) in regulating *Yap* activity [209,210]. Despite the complexity of the pathway's upstream regulation, *Yap* and *Taz* are so far the only known nuclear effecters of Hippo signaling. The significant rescue effect of *Yap/Taz* deletion on *Lats* mutants (**Figure 14**) and *Mst* mutants (by other lab members) clearly suggested that *Yap/Taz* is the key element of the Hippo pathway in regulating liver homeostasis. As *Yap* activation is highly associate with the poorly differentiated HCC and a low patient survival rate [51], *Yap* may be a promising therapeutic target for HCC treatment.

5.3 The Hippo pathway in liver size control

How organ size is controlled is a fundamental biological question. The prevailing opinion is that organ size is regulated by an intrinsic “total mass checkpoint” mechanism (reviewed in [211]). This mechanism ensures that organs maintain an inherited size through modulating the number and the size of their constituting cells. Classic *Drosophila* genetic screening for genes involved in this mechanism has identified the *Insulin-PI3K-Akt* signaling pathway and *dTOR* (*Drosophila target of rapamycin*) pathway as playing central roles. The two pathways merge at *S6K*, which regulates a cell’s overall mRNA transcription and thus affects cell growth/size (reviewed in [211,212,213]). In contrast, the Hippo pathway appears to mainly affect cell proliferation and survival, and thus regulates organ size via the number of cells.

Liver is known for its unique ability of regeneration, by which it is able to keep a constant size through a checkpoint, or setting point. The regeneration process is strictly controlled by signaling networks with functionally redundant intracellular components, and thus loss of an individual gene rarely leads to complete inhibition of liver regeneration. Therefore it is not surprising to see that *Yap/Taz* null liver still can regenerate to about 70%. Actually, there is speculation that *Yap/Taz* null liver may be able to regenerate 100% of its original size if *Yap/Taz* is deleted right before surgery, which prevents the disease effect from embryonic gene deletion. The impaired regeneration in both *Yap/Taz*-null and Mst-null livers may be a result of this disease effect. To avoid the disease effect, recombinant adenovirus-*cre* recombinase can be introduced into liver through tail-vain injection right before surgery. However this technique modification will not change our current conclusion that the Hippo signaling

is not a critical determinant for liver size control, because the deletion of *Yap/Taz* does not dramatically inhibit liver re-growth.

Although individual component deletion rarely inhibits liver regeneration, it often impairs hepatocyte proliferation [183,214] or delays the timing of regeneration phases [181,182,215,216]. In our study, *Mst* null liver had a disrupted synchronization of hepatocyte cell cycle progression, while *Yap/Taz* null liver showed a delayed hepatocyte cell cycle re-entry. Because *Mst*-null liver and *Yap/Taz*-null liver are supposed to have opposite effects on *Yap/Taz* activity, and *Yap/Taz* is known to promote cell proliferation, the difference between the two cell-cycle progression patterns suggests a dominant role of *Yap/Taz* in promoting cell cycle re-entry, i.e. the G1/S transition. It is likely that the activated *Yap/Taz* (in *Mst*-null liver) overrides the normal regenerative rhythm and activates the G1/S transition regardless of the normal timing; whereas in the absence of *Yap/Taz* (*Yap/Taz*-null liver), the intrinsic regenerative mechanism may lack the proliferative inducing signal at the beginning, but this lacking can be eventually compensated for by other signals and therefore the regeneration rhythm appears to be delayed. The point here is that although *Yap/Taz* regulates cell cycle re-entry, there are compensatory mechanisms during liver regeneration that substitute when the *Yap/Taz* function is not available. Our finding complies with the general thinking that liver regeneration is well controlled by signaling networks with functionally redundant components, and loss of an individual component rarely leads to complete inhibition of liver regeneration.

Emerging evidence suggests that the Hippo pathway may interact with the mTOR pathway and the *PI3K/Akt* pathway, both of which are known to be important for liver

regeneration. Evidences for the interaction between the Hippo and mTOR pathways includes: 1) deletion of *Mer/NF2* results in activation of *mTORC1* [217,218], which is an *mTOR* kinase inhibitor complex; 2) loss of *Mst* activates *mTORC1* [189] and affects *mTORC2* downstream signaling [219]; and 3) *Yap* regulates *IGF-1*, which is a known activator of the mTOR pathway [220]. Furthermore, the transcription factor *Myc* has been identified as a gene target of *Yki* [221,222], and it has also been shown to affect the transcription of *TSC2* by binding to its promoter [223]. It has been reported that activation of the TOR pathway leads to increased cell growth and cell cycle re-entry [224,225,226]. In a liver subjected to partial hepatectomy, mTOR pathway appears to regulate liver regeneration by modulating cell growth and proliferation in response to the energy demands of the remaining liver [227,228,229]. The interaction between the Hippo and *PI3K/Akt* pathways is more direct: *Akt* directly phosphorylates *Yap* to induce interaction with *14-3-3* and result in functional inhibition [230]. *Akt* also indirectly activates mTOR pathway by regulating cellular ATP levels and *AMPK* activity [231,232]. The three pathways form a network and may compensate for each other in regulating liver regeneration and liver size. In the *Yap/Taz* null liver, *PI3K/Akt* may elevate *mTOR* pathway activity in response to insufficient cell proliferation, resulting in liver mass re-growth with a delayed timing of cell cycle progression. The diagram below illustrates the possible regulatory mechanism of liver regeneration by the three pathways (**Diagram 6**).

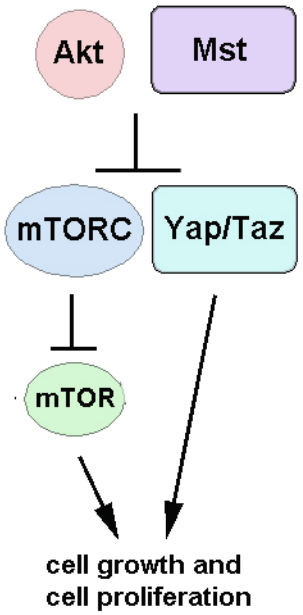

Diagram 6. Both *Akt* and *Mst* can inhibit either *mTORC* or *Yap/Taz*. *mTORC* inhibits *mTOR* kinase, which otherwise promote cell growth and cell proliferation. *Akt* and *Mst* control both *mTOR* activity and *Yap/Taz* activity, and may thus modulate the two pathways to achieve liver size control.

CHAPTER 5: FUTURE STUDIES

In mouse, *Yap* over-expression drives liver tumor development [34]. In human liver cancer patients, *Yap* hyper-activation is correlated with tumor malignancy and low patient survival rate [51]. Study *Yap* function in liver is therefore important for understanding liver cancer initiation, and may help to develop strategies for liver cancer diagnosis and treatments.

Yap is a transcription cofactor that regulates target gene expression by binding to transcription factors. Domain analysis revealed that *Yap* has the potential of binding to a variety of transcription factors via its WW-domain [57,233]. Several *Yap*-interacting transcription factors have been reported [65,66,230]. However, their interactions with *Yap* have not been tested *in vivo*, nor do they give a systematic view about *Yap* function in liver. Microarray data of the *Lats* deficient liver and the *Yap* over-expression liver provide an overview on the gene population affected by *Yap*, but the ones directly regulated by *Yap* and contributing to liver homeostasis are not known. To address the above questions, it is important to find out the transcription factors that *Yap* directly associated with in liver.

Functional protein arrays are emerging as a new tool for studying protein-protein interaction in a large scale (reviewed in [234]) and can be used to identify the *Yap*-binding transcription factors. Potential candidates should be verified by IP (immuno-precipitation) assay and their functional contribution to *Yap* can be tested in cell culture system or mouse. Below shows an example of studying the interaction between *Yap* and one of its potential interacting transcription factors in regulating bile duct development.

In our study, *Yap* up-regulation correlates with biliary hyperplasia and decreased hepatocyte function, suggesting a possible mechanism that Yap activates a gene profile in favor of BEC differentiation and bile duct development. If this is true, then the *Yap* function is opposite to the transcription factor *C/EBP (CCAAT/enhancer-binding protein),* specifically, *C/EBP*α*,* which plays an important role in promoting hepatocyte differentiation and inhibiting biliary cell differentiation [235,236,237,238]. Analysis of the protein domains of *C/EBP*α and *Yap* predicts a possible physical interaction between the two. This suggests a role for *Yap* in promoting bile duct development through inhibiting *C/EBP*α (**Diagram 7**).

C/EBP is a leucine zipper transcription factor widely expressed but primarily in tissues known to metabolize lipid and cholesterol-related compounds at uncommonly high rates, such as liver, fat and intestine [239]. Six isoforms of the *C/EBP* have been isolated (*C/EBP*α to ς), among which the *C/EBP*α is the first one cloned [239,240] and has been extensively studied. *C/EBP*α is detected only in differentiated tissues [239,241], and therefore being implicated in regulating the terminal differentiation of mammalian cells, including hepatocytes. *C/EBP*α is expressed at high levels in hepatocytes, where it regulates a variety of hepatocyte-specific genes, such as serum *albumin* [242], *haptoglobin [243]*, *phosphoenolpyruvate carboxykinase (GTP) (PEPCK*) [244], etc. Its importance for hepatocyte function is also reflected by its inhibitory effect on biliary cell differentiation [236,237]. Suppression of *C/EBP*α expression increases *Hnf6* and *Hnf1b*, two important transcription factors in biliary cell differentiation, [245,246]. Over-expression of *C/EBP*α can even cause trans-differentiation of

pancreatic cells to hepatocytes [247], demonstrating its essential role in hepatocyte fate determination.

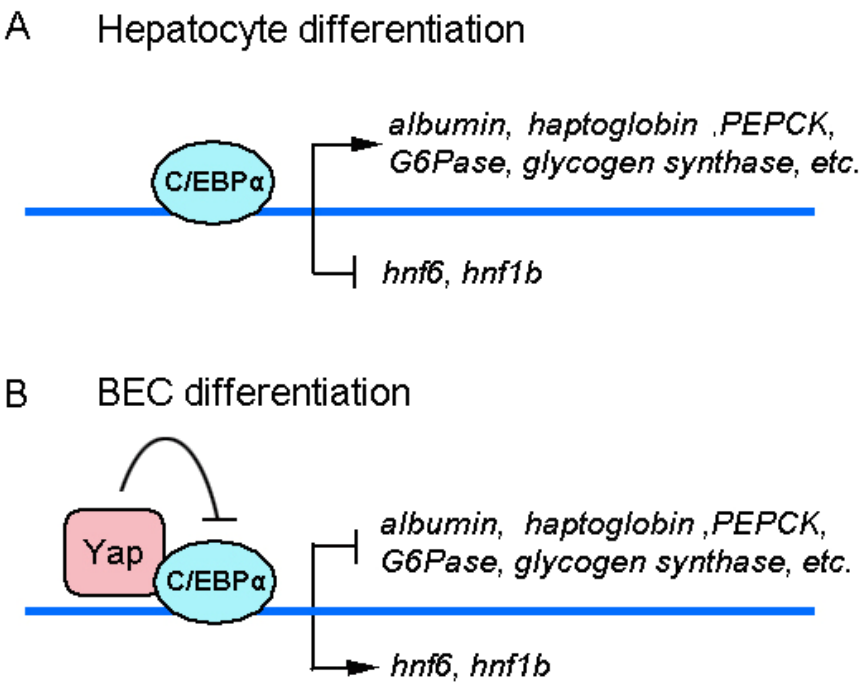

Diagram 7 Hypothesized *Yap* function in biliary cell differentiation. (A) With low level or no *Yap* expression, *C/EBPα* activates genes essential for hepatocyte differentiation while suppressing BEC essential genes. (B) In the presence of *Yap*, *C/EBPα* transcriptional activity is suppressed, leading to a switch of the downstream gene expression pattern from hepatocyte differentiation to BEC differentiation.

We hypothesized that *Yap* promotes bile duct development through inhibiting *C/EBPα* (**Diagram 7**). To test this hypothesis, three questions can be investigated. First, does *Yap* over-expression suppress the *C/EBPα* activating genes, such as *albumin*, *hepatoglobin*, and urea cycle enzymes, and at the same time induce *Hnf6* and *Hnf1b* expression (**Diagram 7**)? Second, does *Yap* deletion block biliary cell differentiation? Third, would a *C/EBPα* dominant mutation antagonize the biliary differentiation promoted by *Yap* over-expression?

To reduce cell non-autonomous effects, assays and tests can be carried out in a primary hepatoblast culture system. Hepatocyte differentiation can be induced by *Oncostatin M* (OSM) [248,249,250] and the effect of *Yap* and *C/EBPα* interaction on regulating hepatic differentiation can be accessed by detecting the expressions of both hepatocyte and biliary cell-specific genes (**Diagram 6**). To test the direct inhibition effect of *Yap* on *C/EBPα,* mutations can be introduced into the PPXY motif (where it binds to *Yap*) of *C/EBPα* through gene targeting. This mutated form of *C/EBPα* should be unaffected by *Yap* and therefore promoting hepatocyte differentiation regardless of *Yap* activity. The hypothesized *Yap- C/EBPα* interaction in regulating hepatoblast differentiation can be further tested *in vivo* through transplantation into the testes of SCID (severe combined immune deficient) male mice. The testes of SCID male mice provide an ideal *in vivo* environment for cell survival and growth. When liver fragments are transplanted into the testes of SCID mice, normal hepatoblasts can construct mature hepatic tissue accompanied by biliary cell differentiation, whereas the *C/EBPα* deficient hepatoblasts only give rise to biliary cells [237]. If *Yap* do regulate biliary cell differentiation through inhibiting *C/EBPα,* then *Yap* over-expression will promote biliary

cell differentiation but loose this effect on the *C/EBP*α deficient or mutated (at *Yap* binding residues) hepatoblasts.

This study will identify the *Yap*-binding transcription factors and its directly regulating genes in a systematical manner. The results may help to understand the mechanisms of tumor development driven by *Yap* activation.

APPENDIX

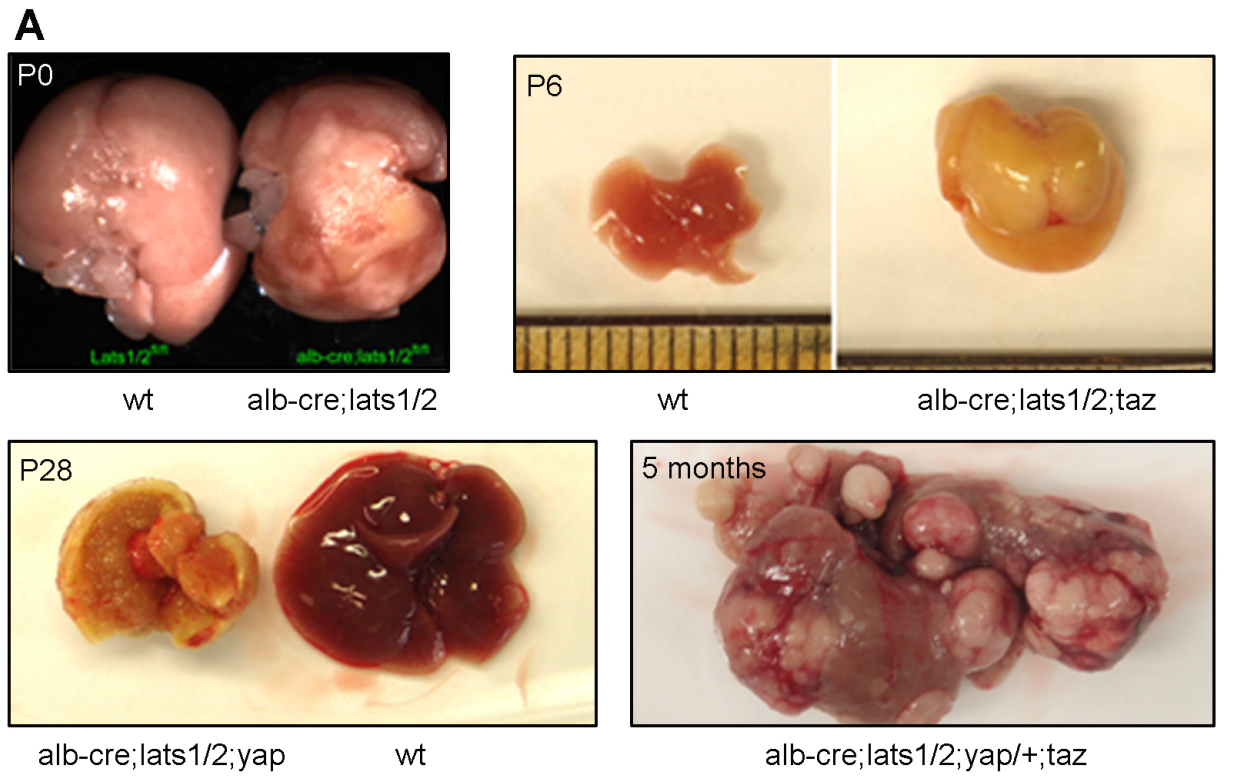

Appendix 1. Liver phenotypes of the mutant mice from the rescue experiment. (A) P0, representative *lats1/2* double deleted liver and the wild-type liver of the same developmental stage. P6, representative *alb-cre;lats1/2;taz* liver and the wild-type littermate's liver. P28, representative *alb-cre;lats1/2;yap* liver and the wild-type littermate's liver. 5 months, representative *alb-cre;lats1/2;yap/taz* liver and the wild-

type littermate's liver. (B) HE staining on liver tissues from the rescue experiment. All of them show ductal-like expansion. Mice with *Lats1/2* and *Taz* deletions die around P5-P6 and show the most dramatic ductal hyperplasia. With *Lats1/2* and *Yaz* deletions, at P11, mutant livers have normal hepatocytes however the liver plates are disrupted by clumps of unrecognized cells. Livers with *Lats1/2* and *Yap/Taz* deletions have normal hepatocytes at 2-months age; however there are still clumps of unrecognized cells penetrating the liver plates.

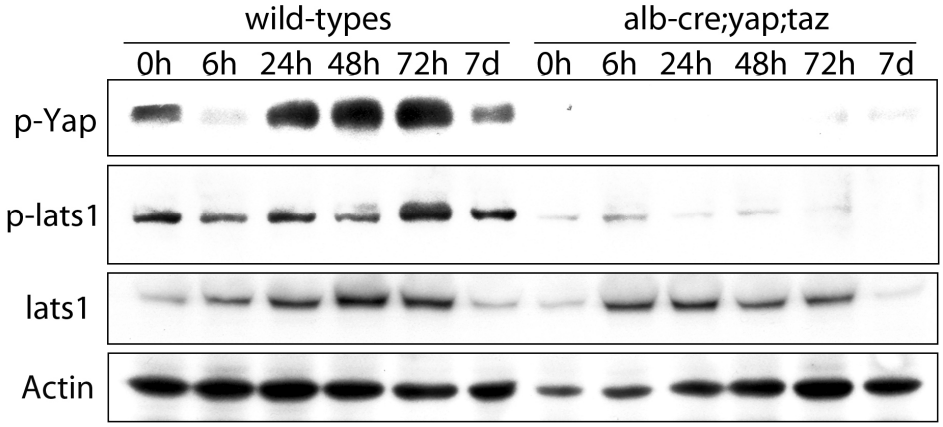

Appendix 2. Decreased phospho-*Lats1* in *Yap/Taz* double mutants. During normal liver regeneration, phosphorylation of *Lats1* decreases at 6h and 48h after PH, and increases at 72h after PH. Total *Lats1* gradiently increases in the first three days of regeneration and returns to normal level at 7d after PH. During *Yap/Taz* double mutants' regeneration, the total *Lats1* shows similar pattern as in normal liver; however, the phosphorylation of *Lats1* is significantly decreased.

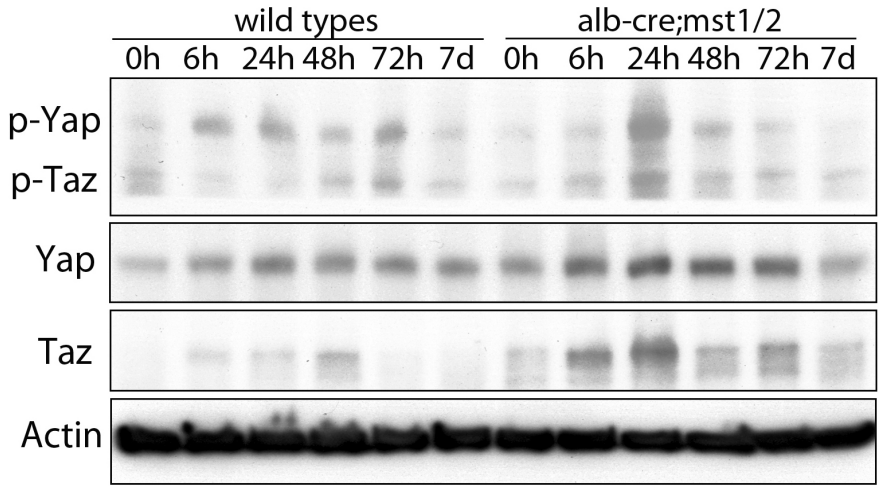

Appendix 3. *Yap* and *Taz* activities during *Mst1/2* double mutants' regeneration. Western blot shows that during normal liver regeneration, the phosphorylation of *Yap* and *Taz* are differentially regulated; however they appear to be similarly regulated during *Mst1/2* double mutants' regeneration. The total protein levels of both *Yap* and *Taz* are increased in *Mst1/2* mutant. *Actin* is used as protein loading controls.

BIBILGRAPHY

1. Justice RW, Zilian O, Woods DF, Noll M, Bryant PJ (1995) The Drosophila tumor suppressor gene warts encodes a homolog of human myotonic dystrophy kinase and is required for the control of cell shape and proliferation. Genes Dev 9: 534-546.
2. Xu T, Wang W, Zhang S, Stewart RA, Yu W (1995) Identifying tumor suppressors in genetic mosaics: the Drosophila lats gene encodes a putative protein kinase. Development 121: 1053-1063.
3. Kango-Singh M, Nolo R, Tao C, Verstreken P, Hiesinger PR, et al. (2002) Shar-pei mediates cell proliferation arrest during imaginal disc growth in Drosophila. Development 129: 5719-5730.
4. Harvey KF, Pfleger CM, Hariharan IK (2003) The Drosophila Mst ortholog, hippo, restricts growth and cell proliferation and promotes apoptosis. Cell 114: 457-467.
5. Pantalacci S, Tapon N, Leopold P (2003) The Salvador partner Hippo promotes apoptosis and cell-cycle exit in Drosophila. Nat Cell Biol 5: 921-927.
6. Jia J, Zhang W, Wang B, Trinko R, Jiang J (2003) The Drosophila Ste20 family kinase dMST functions as a tumor suppressor by restricting cell proliferation and promoting apoptosis. Genes Dev 17: 2514-2519.
7. Udan RS, Kango-Singh M, Nolo R, Tao C, Halder G (2003) Hippo promotes proliferation arrest and apoptosis in the Salvador/Warts pathway. Nat Cell Biol 5: 914-920.

8. Wu S, Huang J, Dong J, Pan D (2003) hippo encodes a Ste-20 family protein kinase that restricts cell proliferation and promotes apoptosis in conjunction with salvador and warts. Cell 114: 445-456.

9. Wei X, Shimizu T, Lai ZC (2007) Mob as tumor suppressor is activated by Hippo kinase for growth inhibition in Drosophila. EMBO J 26: 1772-1781.

10. Glantschnig H, Rodan GA, Reszka AA (2002) Mapping of MST1 kinase sites of phosphorylation. Activation and autophosphorylation. J Biol Chem 277: 42987-42996.

11. Lee KK, Yonehara S (2002) Phosphorylation and dimerization regulate nucleocytoplasmic shuttling of mammalian STE20-like kinase (MST). J Biol Chem 277: 12351-12358.

12. Hamaratoglu F, Willecke M, Kango-Singh M, Nolo R, Hyun E, et al. (2006) The tumour-suppressor genes NF2/Merlin and Expanded act through Hippo signalling to regulate cell proliferation and apoptosis. Nat Cell Biol 8: 27-36.

13. Baumgartner R, Poernbacher I, Buser N, Hafen E, Stocker H The WW domain protein Kibra acts upstream of Hippo in Drosophila. Dev Cell 18: 309-316.

14. Genevet A, Wehr MC, Brain R, Thompson BJ, Tapon N Kibra is a regulator of the Salvador/Warts/Hippo signaling network. Dev Cell 18: 300-308.

15. Yu J, Zheng Y, Dong J, Klusza S, Deng WM, et al. Kibra functions as a tumor suppressor protein that regulates Hippo signaling in conjunction with Merlin and Expanded. Dev Cell 18: 288-299.

16. Tyler DM, Baker NE (2007) Expanded and fat regulate growth and differentiation in the Drosophila eye through multiple signaling pathways. Dev Biol 305: 187-201.

17. Willecke M, Hamaratoglu F, Kango-Singh M, Udan R, Chen CL, et al. (2006) The fat cadherin acts through the hippo tumor-suppressor pathway to regulate tissue size. Curr Biol 16: 2090-2100.

18. Silva E, Tsatskis Y, Gardano L, Tapon N, McNeill H (2006) The tumor-suppressor gene fat controls tissue growth upstream of expanded in the hippo signaling pathway. Curr Biol 16: 2081-2089.

19. Cho E, Feng Y, Rauskolb C, Maitra S, Fehon R, et al. (2006) Delineation of a Fat tumor suppressor pathway. Nat Genet 38: 1142-1150.

20. Bennett FC, Harvey KF (2006) Fat cadherin modulates organ size in Drosophila via the Salvador/Warts/Hippo signaling pathway. Curr Biol 16: 2101-2110.

21. Enomoto M, Igaki T Deciphering tumor-suppressor signaling in flies: genetic link between Scribble/Dlg/Lgl and the Hippo pathways. J Genet Genomics 38: 461-470.

22. Grusche FA, Richardson HE, Harvey KF Upstream regulation of the hippo size control pathway. Curr Biol 20: R574-582.

23. Huang J, Wu S, Barrera J, Matthews K, Pan D (2005) The Hippo signaling pathway coordinately regulates cell proliferation and apoptosis by inactivating Yorkie, the Drosophila Homolog of YAP. Cell 122: 421-434.

24. Oh H, Irvine KD (2008) In vivo regulation of Yorkie phosphorylation and localization. Development 135: 1081-1088.

25. Oh H, Irvine KD (2009) In vivo analysis of Yorkie phosphorylation sites. Oncogene 28: 1916-1927.

26. Badouel C, Gardano L, Amin N, Garg A, Rosenfeld R, et al. (2009) The FERM-domain protein Expanded regulates Hippo pathway activity via direct interactions with the transcriptional activator Yorkie. Dev Cell 16: 411-420.

27. Oh H, Reddy BV, Irvine KD (2009) Phosphorylation-independent repression of Yorkie in Fat-Hippo signaling. Dev Biol 335: 188-197.

28. Goulev Y, Fauny JD, Gonzalez-Marti B, Flagiello D, Silber J, et al. (2008) SCALLOPED interacts with YORKIE, the nuclear effector of the hippo tumor-suppressor pathway in Drosophila. Curr Biol 18: 435-441.

29. Zhang L, Ren F, Zhang Q, Chen Y, Wang B, et al. (2008) The TEAD/TEF family of transcription factor Scalloped mediates Hippo signaling in organ size control. Dev Cell 14: 377-387.

30. Oh H, Irvine KD Cooperative regulation of growth by Yorkie and Mad through bantam. Dev Cell 20: 109-122.

31. Peng HW, Slattery M, Mann RS (2009) Transcription factor choice in the Hippo signaling pathway: homothorax and yorkie regulation of the microRNA bantam in the progenitor domain of the Drosophila eye imaginal disc. Genes Dev 23: 2307-2319.

32. Nicolay BN, Bayarmagnai B, Islam AB, Lopez-Bigas N, Frolov MV Cooperation between dE2F1 and Yki/Sd defines a distinct transcriptional program necessary to bypass cell cycle exit. Genes Dev 25: 323-335.

33. Chan EH, Nousiainen M, Chalamalasetty RB, Schafer A, Nigg EA, et al. (2005) The Ste20-like kinase Mst2 activates the human large tumor suppressor kinase Lats1. Oncogene 24: 2076-2086.

34. Dong J, Feldmann G, Huang J, Wu S, Zhang N, et al. (2007) Elucidation of a universal size-control mechanism in Drosophila and mammals. Cell 130: 1120-1133.

35. Zhao B, Wei X, Li W, Udan RS, Yang Q, et al. (2007) Inactivation of YAP oncoprotein by the Hippo pathway is involved in cell contact inhibition and tissue growth control. Genes Dev 21: 2747-2761.

36. Cinar B, Fang PK, Lutchman M, Di Vizio D, Adam RM, et al. (2007) The pro-apoptotic kinase Mst1 and its caspase cleavage products are direct inhibitors of Akt1. EMBO J 26: 4523-4534.

37. Lee KP, Lee JH, Kim TS, Kim TH, Park HD, et al. The Hippo-Salvador pathway restrains hepatic oval cell proliferation, liver size, and liver tumorigenesis. Proc Natl Acad Sci U S A 107: 8248-8253.

38. Lu L, Li Y, Kim SM, Bossuyt W, Liu P, et al. Hippo signaling is a potent in vivo growth and tumor suppressor pathway in the mammalian liver. Proc Natl Acad Sci U S A 107: 1437-1442.

39. Minoo P, Zlobec I, Baker K, Tornillo L, Terracciano L, et al. (2007) Prognostic significance of mammalian sterile20-like kinase 1 in colorectal cancer. Mod Pathol 20: 331-338.

40. Seidel C, Schagdarsurengin U, Blumke K, Wurl P, Pfeifer GP, et al. (2007) Frequent hypermethylation of MST1 and MST2 in soft tissue sarcoma. Mol Carcinog 46: 865-871.

41. Song H, Mak KK, Topol L, Yun K, Hu J, et al. Mammalian Mst1 and Mst2 kinases play essential roles in organ size control and tumor suppression. Proc Natl Acad Sci U S A 107: 1431-1436.

42. Tapon N, Harvey KF, Bell DW, Wahrer DC, Schiripo TA, et al. (2002) salvador Promotes both cell cycle exit and apoptosis in Drosophila and is mutated in human cancer cell lines. Cell 110: 467-478.

43. Jiang Z, Li X, Hu J, Zhou W, Jiang Y, et al. (2006) Promoter hypermethylation-mediated down-regulation of LATS1 and LATS2 in human astrocytoma. Neurosci Res 56: 450-458.

44. Takahashi Y, Miyoshi Y, Takahata C, Irahara N, Taguchi T, et al. (2005) Down-regulation of LATS1 and LATS2 mRNA expression by promoter hypermethylation and its association with biologically aggressive phenotype in human breast cancers. Clin Cancer Res 11: 1380-1385.

45. Kosaka Y, Mimori K, Tanaka F, Inoue H, Watanabe M, et al. (2007) Clinical significance of the loss of MATS1 mRNA expression in colorectal cancer. Int J Oncol 31: 333-338.

46. Lai ZC, Wei X, Shimizu T, Ramos E, Rohrbaugh M, et al. (2005) Control of cell proliferation and apoptosis by mob as tumor suppressor, mats. Cell 120: 675-685.

47. Sasaki H, Kawano O, Endo K, Suzuki E, Yukiue H, et al. (2007) Human MOB1 expression in non-small-cell lung cancer. Clin Lung Cancer 8: 273-276.

48. Lei QY, Zhang H, Zhao B, Zha ZY, Bai F, et al. (2008) TAZ promotes cell proliferation and epithelial-mesenchymal transition and is inhibited by the hippo pathway. Mol Cell Biol 28: 2426-2436.

49. Overholtzer M, Zhang J, Smolen GA, Muir B, Li W, et al. (2006) Transforming properties of YAP, a candidate oncogene on the chromosome 11q22 amplicon. Proc Natl Acad Sci U S A 103: 12405-12410.

50. Steinhardt AA, Gayyed MF, Klein AP, Dong J, Maitra A, et al. (2008) Expression of Yes-associated protein in common solid tumors. Hum Pathol 39: 1582-1589.

51. Xu MZ, Yao TJ, Lee NP, Ng IO, Chan YT, et al. (2009) Yes-associated protein is an independent prognostic marker in hepatocellular carcinoma. Cancer 115: 4576-4585.

52. Praskova M, Khoklatchev A, Ortiz-Vega S, Avruch J (2004) Regulation of the MST1 kinase by autophosphorylation, by the growth inhibitory proteins, RASSF1 and NORE1, and by Ras. Biochem J 381: 453-462.

53. Visser S, Yang X LATS tumor suppressor: a new governor of cellular homeostasis. Cell Cycle 9: 3892-3903.

54. Callus BA, Verhagen AM, Vaux DL (2006) Association of mammalian sterile twenty kinases, Mst1 and Mst2, with hSalvador via C-terminal coiled-coil domains, leads to its stabilization and phosphorylation. FEBS J 273: 4264-4276.

55. Polesello C, Huelsmann S, Brown NH, Tapon N (2006) The Drosophila RASSF homolog antagonizes the hippo pathway. Curr Biol 16: 2459-2465.

56. Zhang N, Bai H, David KK, Dong J, Zheng Y, et al. The Merlin/NF2 tumor suppressor functions through the YAP oncoprotein to regulate tissue homeostasis in mammals. Dev Cell 19: 27-38.

57. Kanai F, Marignani PA, Sarbassova D, Yagi R, Hall RA, et al. (2000) TAZ: a novel transcriptional co-activator regulated by interactions with 14-3-3 and PDZ domain proteins. EMBO J 19: 6778-6791.

58. Vassilev A, Kaneko KJ, Shu H, Zhao Y, DePamphilis ML (2001) TEAD/TEF transcription factors utilize the activation domain of YAP65, a Src/Yes-associated protein localized in the cytoplasm. Genes Dev 15: 1229-1241.

59. Mahoney WM, Jr., Hong JH, Yaffe MB, Farrance IK (2005) The transcriptional co-activator TAZ interacts differentially with transcriptional enhancer factor-1 (TEF-1) family members. Biochem J 388: 217-225.

60. Wu S, Liu Y, Zheng Y, Dong J, Pan D (2008) The TEAD/TEF family protein Scalloped mediates transcriptional output of the Hippo growth-regulatory pathway. Dev Cell 14: 388-398.

61. Chan SW, Lim CJ, Huang C, Chong YF, Gunaratne HJ, et al. WW domain-mediated interaction with Wbp2 is important for the oncogenic property of TAZ. Oncogene 30: 600-610.

62. Xu MZ, Chan SW, Liu AM, Wong KF, Fan ST, et al. AXL receptor kinase is a mediator of YAP-dependent oncogenic functions in hepatocellular carcinoma. Oncogene 30: 1229-1240.

63. Murakami M, Nakagawa M, Olson EN, Nakagawa O (2005) A WW domain protein TAZ is a critical coactivator for TBX5, a transcription factor implicated in Holt-Oram syndrome. Proc Natl Acad Sci U S A 102: 18034-18039.

64. Varelas X, Sakuma R, Samavarchi-Tehrani P, Peerani R, Rao BM, et al. (2008) TAZ controls Smad nucleocytoplasmic shuttling and regulates human embryonic stem-cell self-renewal. Nat Cell Biol 10: 837-848.

65. Komuro A, Nagai M, Navin NE, Sudol M (2003) WW domain-containing protein YAP associates with ErbB-4 and acts as a co-transcriptional activator for the carboxyl-terminal fragment of ErbB-4 that translocates to the nucleus. J Biol Chem 278: 33334-33341.

66. Ferrigno O, Lallemand F, Verrecchia F, L'Hoste S, Camonis J, et al. (2002) Yes-associated protein (YAP65) interacts with Smad7 and potentiates its inhibitory activity against TGF-beta/Smad signaling. Oncogene 21: 4879-4884.

67. blouin A BR, Weibei ER. (1977) Distribution of organelles and membranes between hepatocytes and nonhepatocytes in the rat liver parenchyma. A stereological study. J cell Biol 72: 5.

68. Tremblay KD, Zaret KS (2005) Distinct populations of endoderm cells converge to generate the embryonic liver bud and ventral foregut tissues. Dev Biol 280: 87-99.

69. Zaret KS, Grompe M (2008) Generation and regeneration of cells of the liver and pancreas. Science 322: 1490-1494.

70. Houssaint E (1980) Differentiation of the mouse hepatic primordium. I. An analysis of tissue interactions in hepatocyte differentiation. Cell Differ 9: 269-279.

71. Tadei A, Geslin P, Delhumeau A, Victor J, Le Douarin L, et al. (1975) [Phentolamine in treatment of acute left ventricular insufficiancies]. Arch Mal Coeur Vaiss 68: 877-885.

72. Medlock ES, Haar JL (1983) The liver hemopoietic environment: I. Developing hepatocytes and their role in fetal hemopoiesis. Anat Rec 207: 31-41.

73. Giroux S, Charron J (1998) Defective development of the embryonic liver in N-myc-deficient mice. Dev Biol 195: 16-28.

74. Hentsch B, Lyons I, Li R, Hartley L, Lints TJ, et al. (1996) Hlx homeo box gene is essential for an inductive tissue interaction that drives expansion of embryonic liver and gut. Genes Dev 10: 70-79.

75. Porter FD, Drago J, Xu Y, Cheema SS, Wassif C, et al. (1997) Lhx2, a LIM homeobox gene, is required for eye, forebrain, and definitive erythrocyte development. Development 124: 2935-2944.

76. Wandzioch E, Kolterud A, Jacobsson M, Friedman SL, Carlsson L (2004) Lhx2-/- mice develop liver fibrosis. Proc Natl Acad Sci U S A 101: 16549-16554.

77. Antoniou A, Raynaud P, Cordi S, Zong Y, Tronche F, et al. (2009) Intrahepatic bile ducts develop according to a new mode of tubulogenesis regulated by the transcription factor SOX9. Gastroenterology 136: 2325-2333.

78. Clotman F, Jacquemin P, Plumb-Rudewiez N, Pierreux CE, Van der Smissen P, et al. (2005) Control of liver cell fate decision by a gradient of TGF beta

signaling modulated by Onecut transcription factors. Genes Dev 19: 1849-1854.

79. Clotman F, Lemaigre FP (2006) Control of hepatic differentiation by activin/TGFbeta signaling. Cell Cycle 5: 168-171.

80. Micsenyi A, Tan X, Sneddon T, Luo JH, Michalopoulos GK, et al. (2004) Beta-catenin is temporally regulated during normal liver development. Gastroenterology 126: 1134-1146.

81. Tanimizu N, Miyajima A (2004) Notch signaling controls hepatoblast differentiation by altering the expression of liver-enriched transcription factors. J Cell Sci 117: 3165-3174.

82. Zong Y, Panikkar A, Xu J, Antoniou A, Raynaud P, et al. (2009) Notch signaling controls liver development by regulating biliary differentiation. Development 136: 1727-1739.

83. Tchorz JS, Kinter J, Muller M, Tornillo L, Heim MH, et al. (2009) Notch2 signaling promotes biliary epithelial cell fate specification and tubulogenesis during bile duct development in mice. Hepatology 50: 871-879.

84. Li L, Krantz ID, Deng Y, Genin A, Banta AB, et al. (1997) Alagille syndrome is caused by mutations in human Jagged1, which encodes a ligand for Notch1. Nat Genet 16: 243-251.

85. McDaniell R, Warthen DM, Sanchez-Lara PA, Pai A, Krantz ID, et al. (2006) NOTCH2 mutations cause Alagille syndrome, a heterogeneous disorder of the notch signaling pathway. Am J Hum Genet 79: 169-173.

86. Oda T, Elkahloun AG, Pike BL, Okajima K, Krantz ID, et al. (1997) Mutations in the human Jagged1 gene are responsible for Alagille syndrome. Nat Genet 16: 235-242.

87. Flynn DM, Nijjar S, Hubscher SG, de Goyet Jde V, Kelly DA, et al. (2004) The role of Notch receptor expression in bile duct development and disease. J Pathol 204: 55-64.

88. Kodama Y, Hijikata M, Kageyama R, Shimotohno K, Chiba T (2004) The role of notch signaling in the development of intrahepatic bile ducts. Gastroenterology 127: 1775-1786.

89. Loomes KM, Taichman DB, Glover CL, Williams PT, Markowitz JE, et al. (2002) Characterization of Notch receptor expression in the developing mammalian heart and liver. Am J Med Genet 112: 181-189.

90. Louis AA, Van Eyken P, Haber BA, Hicks C, Weinmaster G, et al. (1999) Hepatic jagged1 expression studies. Hepatology 30: 1269-1275.

91. McCright B, Lozier J, Gridley T (2002) A mouse model of Alagille syndrome: Notch2 as a genetic modifier of Jag1 haploinsufficiency. Development 129: 1075-1082.

92. Moreira RK (2007) Hepatic stellate cells and liver fibrosis. Arch Pathol Lab Med 131: 1728-1734.

93. Parkin DM, Bray F, Ferlay J, Pisani P (2001) Estimating the world cancer burden: Globocan 2000. Int J Cancer 94: 153-156.

94. Befeler AS, Di Bisceglie AM (2002) Hepatocellular carcinoma: diagnosis and treatment. Gastroenterology 122: 1609-1619.

95. Bruix J, Sherman M (2005) Management of hepatocellular carcinoma. Hepatology 42: 1208-1236.

96. Liu JH, Chen PW, Asch SM, Busuttil RW, Ko CY (2004) Surgery for hepatocellular carcinoma: does it improve survival? Ann Surg Oncol 11: 298-303.

97. Beasley RP (1988) Hepatitis B virus. The major etiology of hepatocellular carcinoma. Cancer 61: 1942-1956.

98. Roskams T (2006) Liver stem cells and their implication in hepatocellular and cholangiocarcinoma. Oncogene 25: 3818-3822.

99. Magee JA, Piskounova E, Morrison SJ Cancer stem cells: impact, heterogeneity, and uncertainty. Cancer Cell 21: 283-296.

100. Sell S, Leffert HL (2008) Liver cancer stem cells. J Clin Oncol 26: 2800-2805.

101. Dan YY, Yeoh GC (2008) Liver stem cells: a scientific and clinical perspective. J Gastroenterol Hepatol 23: 687-698.

102. Sell S (1997) Electron microscopic identification of putative liver stem cells and intermediate hepatocytes following periportal necrosis induced in rats by allyl alcohol. Stem Cells 15: 378-385.

103. Dorrell C, Erker L, Lanxon-Cookson KM, Abraham SL, Victoroff T, et al. (2008) Surface markers for the murine oval cell response. Hepatology 48: 1282-1291.

104. Conlon I, Raff M (1999) Size control in animal development. Cell 96: 235-244.

105. Raff MC (1996) Size control: the regulation of cell numbers in animal development. Cell 86: 173-175.

106. Prout T, Barker JS (1989) Ecological aspects of the heritability of body size in Drosophila buzzatii. Genetics 123: 803-813.

107. Fankhauser G (1952) Nucleo-cytoplasmic relations in amphibian development. INt Rev Cytol 1: 29.

108. Neufeld TP, de la Cruz AF, Johnston LA, Edgar BA (1998) Coordination of growth and cell division in the Drosophila wing. Cell 93: 1183-1193.

109. Weigmann K, Cohen SM, Lehner CF (1997) Cell cycle progression, growth and patterning in imaginal discs despite inhibition of cell division after inactivation of Drosophila Cdc2 kinase. Development 124: 3555-3563.

110. Weinkove D, Leevers SJ (2000) The genetic control of organ growth: insights from Drosophila. Curr Opin Genet Dev 10: 75-80.

111. Schmidt EE, Schibler U (1995) Cell size regulation, a mechanism that controls cellular RNA accumulation: consequences on regulation of the ubiquitous transcription factors Oct1 and NF-Y and the liver-enriched transcription factor DBP. J Cell Biol 128: 467-483.

112. Shioi T, Kang PM, Douglas PS, Hampe J, Yballe CM, et al. (2000) The conserved phosphoinositide 3-kinase pathway determines heart size in mice. EMBO J 19: 2537-2548.

113. Mullany LK, Nelsen CJ, Hanse EA, Goggin MM, Anttila CK, et al. (2007) Akt-mediated liver growth promotes induction of cyclin E through a novel translational mechanism and a p21-mediated cell cycle arrest. J Biol Chem 282: 21244-21252.

114. Haga S, Ogawa W, Inoue H, Terui K, Ogino T, et al. (2005) Compensatory recovery of liver mass by Akt-mediated hepatocellular hypertrophy in liver-specific STAT3-deficient mice. J Hepatol 43: 799-807.

115. Haga S, Ozaki M, Inoue H, Okamoto Y, Ogawa W, et al. (2009) The survival pathways phosphatidylinositol-3 kinase (PI3-K)/phosphoinositide-dependent protein kinase 1 (PDK1)/Akt modulate liver regeneration through hepatocyte size rather than proliferation. Hepatology 49: 204-214.

116. Pan D (2007) Hippo signaling in organ size control. Genes Dev 21: 886-897.

117. Huang H, Potter CJ, Tao W, Li DM, Brogiolo W, et al. (1999) PTEN affects cell size, cell proliferation and apoptosis during Drosophila eye development. Development 126: 5365-5372.

118. Goberdhan DC, Paricio N, Goodman EC, Mlodzik M, Wilson C (1999) Drosophila tumor suppressor PTEN controls cell size and number by antagonizing the Chico/PI3-kinase signaling pathway. Genes Dev 13: 3244-3258.

119. Gao X, Neufeld TP, Pan D (2000) Drosophila PTEN regulates cell growth and proliferation through PI3K-dependent and -independent pathways. Dev Biol 221: 404-418.

120. Cantley LC, Neel BG (1999) New insights into tumor suppression: PTEN suppresses tumor formation by restraining the phosphoinositide 3-kinase/AKT pathway. Proc Natl Acad Sci U S A 96: 4240-4245.

121. Borkowska J, Schwartz RA, Kotulska K, Jozwiak S Tuberous sclerosis complex: tumors and tumorigenesis. Int J Dermatol 50: 13-20.

122. Potter CJ, Pedraza LG, Huang H, Xu T (2003) The tuberous sclerosis complex (TSC) pathway and mechanism of size control. Biochem Soc Trans 31: 584-586.

123. Michalopoulos GK, DeFrances MC (1997) Liver regeneration. Science 276: 60-66.

124. Higgins GM AR (1931) Experimental pathology of the liver, 1:Restoration of the liver of the white rat following partial surgical removal. Arch Pathol: 7.

125. Matsuo T, Yamaguchi S, Mitsui S, Emi A, Shimoda F, et al. (2003) Control mechanism of the circadian clock for timing of cell division in vivo. Science 302: 255-259.

126. Schibler U (2003) Circadian rhythms. Liver regeneration clocks on. Science 302: 234-235.

127. Ehrenfried JA, Ko TC, Thompson EA, Evers BM (1997) Cell cycle-mediated regulation of hepatic regeneration. Surgery 122: 927-935.

128. Mohammed FF, Khokha R (2005) Thinking outside the cell: proteases regulate hepatocyte division. Trends Cell Biol 15: 555-563.

129. Su AI, Guidotti LG, Pezacki JP, Chisari FV, Schultz PG (2002) Gene expression during the priming phase of liver regeneration after partial hepatectomy in mice. Proc Natl Acad Sci U S A 99: 11181-11186.

130. White P, Brestelli JE, Kaestner KH, Greenbaum LE (2005) Identification of transcriptional networks during liver regeneration. J Biol Chem 280: 3715-3722.

131. Cressman DE, Greenbaum LE, DeAngelis RA, Ciliberto G, Furth EE, et al. (1996) Liver failure and defective hepatocyte regeneration in interleukin-6-deficient mice. Science 274: 1379-1383.

132. Nelsen CJ, Rickheim DG, Timchenko NA, Stanley MW, Albrecht JH (2001) Transient expression of cyclin D1 is sufficient to promote hepatocyte replication and liver growth in vivo. Cancer Res 61: 8564-8568.

133. Albrecht JH, Hansen LK (1999) Cyclin D1 promotes mitogen-independent cell cycle progression in hepatocytes. Cell Growth Differ 10: 397-404.

134. Desbois-Mouthon C, Wendum D, Cadoret A, Rey C, Leneuve P, et al. (2006) Hepatocyte proliferation during liver regeneration is impaired in mice with liver-specific IGF-1R knockout. Faseb J 20: 773-775.

135. Xiong Y, Hannon GJ, Zhang H, Casso D, Kobayashi R, et al. (1993) p21 is a universal inhibitor of cyclin kinases. Nature 366: 701-704.

136. Stepniak E, Ricci R, Eferl R, Sumara G, Sumara I, et al. (2006) c-Jun/AP-1 controls liver regeneration by repressing p53/p21 and p38 MAPK activity. Genes Dev 20: 2306-2314.

137. Lutz W, Leon J, Eilers M (2002) Contributions of Myc to tumorigenesis. Biochim Biophys Acta 1602: 61-71.

138. Dang CV MYC on the path to cancer. Cell 149: 22-35.

139. Baker SJ, Fearon ER, Nigro JM, Hamilton SR, Preisinger AC, et al. (1989) Chromosome 17 deletions and p53 gene mutations in colorectal carcinomas. Science 244: 217-221.

140. Koshland DE, Jr. (1993) Molecule of the year. Science 262: 1953.

141. Chan SW, Lim CJ, Guo K, Ng CP, Lee I, et al. (2008) A role for TAZ in migration, invasion, and tumorigenesis of breast cancer cells. Cancer Res 68: 2592-2598.

142. Zhou Z, Hao Y, Liu N, Raptis L, Tsao MS, et al. TAZ is a novel oncogene in non-small cell lung cancer. Oncogene 30: 2181-2186.

143. Jimenez-Velasco A, Roman-Gomez J, Agirre X, Barrios M, Navarro G, et al. (2005) Downregulation of the large tumor suppressor 2 (LATS2/KPM) gene is associated with poor prognosis in acute lymphoblastic leukemia. Leukemia 19: 2347-2350.

144. Hisaoka M, Tanaka A, Hashimoto H (2002) Molecular alterations of h-warts/LATS1 tumor suppressor in human soft tissue sarcoma. Lab Invest 82: 1427-1435.

145. Strazisar M, Mlakar V, Glavac D (2009) LATS2 tumour specific mutations and down-regulation of the gene in non-small cell carcinoma. Lung Cancer 64: 257-262.

146. Powzaniuk M, McElwee-Witmer S, Vogel RL, Hayami T, Rutledge SJ, et al. (2004) The LATS2/KPM tumor suppressor is a negative regulator of the androgen receptor. Mol Endocrinol 18: 2011-2023.

147. Makita R, Uchijima Y, Nishiyama K, Amano T, Chen Q, et al. (2008) Multiple renal cysts, urinary concentration defects, and pulmonary emphysematous changes in mice lacking TAZ. Am J Physiol Renal Physiol 294: F542-553.

148. Cordenonsi M, Zanconato F, Azzolin L, Forcato M, Rosato A, et al. The Hippo transducer TAZ confers cancer stem cell-related traits on breast cancer cells. Cell 147: 759-772.

149. Oh S, Lee D, Kim T, Kim TS, Oh HJ, et al. (2009) Crucial role for Mst1 and Mst2 kinases in early embryonic development of the mouse. Mol Cell Biol 29: 6309-6320.

150. Lee JH, Kim TS, Yang TH, Koo BK, Oh SP, et al. (2008) A crucial role of WW45 in developing epithelial tissues in the mouse. EMBO J 27: 1231-1242.

151. St John MA, Tao W, Fei X, Fukumoto R, Carcangiu ML, et al. (1999) Mice deficient of Lats1 develop soft-tissue sarcomas, ovarian tumours and pituitary dysfunction. Nat Genet 21: 182-186.

152. Yabuta N, Okada N, Ito A, Hosomi T, Nishihara S, et al. (2007) Lats2 is an essential mitotic regulator required for the coordination of cell division. J Biol Chem 282: 19259-19271.

153. Morin-Kensicki EM, Boone BN, Howell M, Stonebraker JR, Teed J, et al. (2006) Defects in yolk sac vasculogenesis, chorioallantoic fusion, and embryonic axis elongation in mice with targeted disruption of Yap65. Mol Cell Biol 26: 77-87.

154. Hossain Z, Ali SM, Ko HL, Xu J, Ng CP, et al. (2007) Glomerulocystic kidney disease in mice with a targeted inactivation of Wwtr1. Proc Natl Acad Sci U S A 104: 1631-1636.

155. Nishioka N, Inoue K, Adachi K, Kiyonari H, Ota M, et al. (2009) The Hippo signaling pathway components Lats and Yap pattern Tead4 activity to

distinguish mouse trophectoderm from inner cell mass. Dev Cell 16: 398-410.

156. Wagner KU, Wall RJ, St-Onge L, Gruss P, Wynshaw-Boris A, et al. (1997) Cre-mediated gene deletion in the mammary gland. Nucleic Acids Res 25: 4323-4330.

157. Mao J, Ligon KL, Rakhlin EY, Thayer SP, Bronson RT, et al. (2006) A novel somatic mouse model to survey tumorigenic potential applied to the Hedgehog pathway. Cancer Res 66: 10171-10178.

158. Postic C, Magnuson MA (2000) DNA excision in liver by an albumin-Cre transgene occurs progressively with age. Genesis 26: 149-150.

159. Shiojiri N (1981) Enzymo- and immunocytochemical analyses of the differentiation of liver cells in the prenatal mouse. J Embryol Exp Morphol 62: 139-152.

160. Wang ND, Finegold MJ, Bradley A, Ou CN, Abdelsayed SV, et al. (1995) Impaired energy homeostasis in C/EBP alpha knockout mice. Science 269: 1108-1112.

161. Heallen T, Zhang M, Wang J, Bonilla-Claudio M, Klysik E, et al. Hippo pathway inhibits Wnt signaling to restrain cardiomyocyte proliferation and heart size. Science 332: 458-461.

162. Pistoi S, Morello D (1996) Liver regeneration 7. Prometheus' myth revisited: transgenic mice as a powerful tool to study liver regeneration. FASEB J 10: 819-828.

163. Sanders JA, Schorl C, Patel A, Sedivy JM, Gruppuso PA Postnatal liver growth and regeneration are independent of c-myc in a mouse model of conditional hepatic c-myc deletion. BMC Physiol 12: 1.

164. Li F, Xiang Y, Potter J, Dinavahi R, Dang CV, et al. (2006) Conditional deletion of c-myc does not impair liver regeneration. Cancer Res 66: 5608-5612.

165. Mitchell C, Willenbring H (2008) A reproducible and well-tolerated method for 2/3 partial hepatectomy in mice. Nat Protoc 3: 1167-1170.

166. Fausto N, Campbell JS, Riehle KJ (2006) Liver regeneration. Hepatology 43: S45-53.

167. Zerrad-Saadi A, Lambert-Blot M, Mitchell C, Bretes H, Collin de l'Hortet A, et al. GH receptor plays a major role in liver regeneration through the control of EGFR and ERK1/2 activation. Endocrinology 152: 2731-2741.

168. Taub R (2004) Liver regeneration: from myth to mechanism. Nat Rev Mol Cell Biol 5: 836-847.

169. Malumbres M, Mangues R, Ferrer N, Lu S, Pellicer A (1997) Isolation of high molecular weight DNA for reliable genotyping of transgenic mice. Biotechniques 22: 1114-1119.

170. Attal J, Cajero-Juarez M, Houdebine LM (1995) A simple method of DNA extraction from whole tissues and blood using glass powder for detection of transgenic animals by PCR. Transgenic Res 4: 149-150.

171. Lin CS, Magnuson T, Samols D (1989) A rapid procedure to identify newborn transgenic mice. DNA 8: 297-299.

172. Cantz T, Manns MP, Ott M (2008) Stem cells in liver regeneration and therapy. Cell Tissue Res 331: 271-282.

173. Gaudio E, Carpino G, Cardinale V, Franchitto A, Onori P, et al. (2009) New insights into liver stem cells. Dig Liver Dis 41: 455-462.

174. Crosby HA, Hubscher SG, Joplin RE, Kelly DA, Strain AJ (1998) Immunolocalization of OV-6, a putative progenitor cell marker in human fetal and diseased pediatric liver. Hepatology 28: 980-985.

175. Crosby HA, Hubscher S, Fabris L, Joplin R, Sell S, et al. (1998) Immunolocalization of putative human liver progenitor cells in livers from patients with end-stage primary biliary cirrhosis and sclerosing cholangitis using the monoclonal antibody OV-6. Am J Pathol 152: 771-779.

176. Engelhardt NV, Factor VM, Medvinsky AL, Baranov VN, Lazareva MN, et al. (1993) Common antigen of oval and biliary epithelial cells (A6) is a differentiation marker of epithelial and erythroid cell lineages in early development of the mouse. Differentiation 55: 19-26.

177. Factor VM, Radaeva SA (1993) Oval cells--hepatocytes relationships in Dipin-induced hepatocarcinogenesis in mice. Exp Toxicol Pathol 45: 239-244.

178. Lemaigre FP (2003) Development of the biliary tract. Mech Dev 120: 81-87.

179. Raynaud P, Carpentier R, Antoniou A, Lemaigre FP Biliary differentiation and bile duct morphogenesis in development and disease. Int J Biochem Cell Biol 43: 245-256.

180. Michalopoulos GK (2007) Liver regeneration. J Cell Physiol 213: 286-300.

181. Espeillac C, Mitchell C, Celton-Morizur S, Chauvin C, Koka V, et al. S6 kinase 1 is required for rapamycin-sensitive liver proliferation after mouse hepatectomy. J Clin Invest 121: 2821-2832.

182. Liao Y, Shikapwashya ON, Shteyer E, Dieckgraefe BK, Hruz PW, et al. (2004) Delayed hepatocellular mitotic progression and impaired liver regeneration in early growth response-1-deficient mice. J Biol Chem 279: 43107-43116.

183. Li W, Liang X, Kellendonk C, Poli V, Taub R (2002) STAT3 contributes to the mitogenic response of hepatocytes during liver regeneration. J Biol Chem 277: 28411-28417.

184. Ahn SH, Cheung WL, Hsu JY, Diaz RL, Smith MM, et al. (2005) Sterile 20 kinase phosphorylates histone H2B at serine 10 during hydrogen peroxide-induced apoptosis in S. cerevisiae. Cell 120: 25-36.

185. Graves JD, Draves KE, Gotoh Y, Krebs EG, Clark EA (2001) Both phosphorylation and caspase-mediated cleavage contribute to regulation of the Ste20-like protein kinase Mst1 during CD95/Fas-induced apoptosis. J Biol Chem 276: 14909-14915.

186. Lee KK, Ohyama T, Yajima N, Tsubuki S, Yonehara S (2001) MST, a physiological caspase substrate, highly sensitizes apoptosis both upstream and downstream of caspase activation. J Biol Chem 276: 19276-19285.

187. Oh HJ, Lee KK, Song SJ, Jin MS, Song MS, et al. (2006) Role of the tumor suppressor RASSF1A in Mst1-mediated apoptosis. Cancer Res 66: 2562-2569.

188. Khokhlatchev A, Rabizadeh S, Xavier R, Nedwidek M, Chen T, et al. (2002) Identification of a novel Ras-regulated proapoptotic pathway. Curr Biol 12: 253-265.

189. Zhou D, Conrad C, Xia F, Park JS, Payer B, et al. (2009) Mst1 and Mst2 maintain hepatocyte quiescence and suppress hepatocellular carcinoma development through inactivation of the Yap1 oncogene. Cancer Cell 16: 425-438.

190. Katagiri K, Imamura M, Kinashi T (2006) Spatiotemporal regulation of the kinase Mst1 by binding protein RAPL is critical for lymphocyte polarity and adhesion. Nat Immunol 7: 919-928.

191. Zhou D, Medoff BD, Chen L, Li L, Zhang XF, et al. (2008) The Nore1B/Mst1 complex restrains antigen receptor-induced proliferation of naive T cells. Proc Natl Acad Sci U S A 105: 20321-20326.

192. Seki S, Nakashima H, Nakashima M, Kinoshita M Antitumor immunity produced by the liver Kupffer cells, NK cells, NKT cells, and CD8 CD122 T cells. Clin Dev Immunol 2011: 868345.

193. Gale RP (1987) Development of the immune system in human fetal liver. Thymus 10: 45-56.

194. Berasain C, Castillo J, Perugorria MJ, Latasa MU, Prieto J, et al. (2009) Inflammation and liver cancer: new molecular links. Ann N Y Acad Sci 1155: 206-221.

195. Karin M (2006) Nuclear factor-kappaB in cancer development and progression. Nature 441: 431-436.

196. Sharma S, Kelly TK, Jones PA Epigenetics in cancer. Carcinogenesis 31: 27-36.

197. Wen W, Zhu F, Zhang J, Keum YS, Zykova T, et al. MST1 promotes apoptosis through phosphorylation of histone H2AX. J Biol Chem 285: 39108-39116.

198. Cheung WL, Ajiro K, Samejima K, Kloc M, Cheung P, et al. (2003) Apoptotic phosphorylation of histone H2B is mediated by mammalian sterile twenty kinase. Cell 113: 507-517.

199. Watabe M, Kakeya H, Onose R, Osada H (2000) Activation of MST/Krs and c-Jun N-terminal kinases by different signaling pathways during cytotrienin A-induced apoptosis. J Biol Chem 275: 8766-8771.

200. Lowndes NF, Toh GW (2005) DNA repair: the importance of phosphorylating histone H2AX. Curr Biol 15: R99-R102.

201. Pinto DM, Flaus A Structure and function of histone H2AX. Subcell Biochem 50: 55-78.

202. Celeste A, Petersen S, Romanienko PJ, Fernandez-Capetillo O, Chen HT, et al. (2002) Genomic instability in mice lacking histone H2AX. Science 296: 922-927.

203. Lobrich M, Shibata A, Beucher A, Fisher A, Ensminger M, et al. gammaH2AX foci analysis for monitoring DNA double-strand break repair: strengths, limitations and optimization. Cell Cycle 9: 662-669.

204. Maeda S, Kamata H, Luo JL, Leffert H, Karin M (2005) IKKbeta couples hepatocyte death to cytokine-driven compensatory proliferation that promotes chemical hepatocarcinogenesis. Cell 121: 977-990.

205. Sakurai T, He G, Matsuzawa A, Yu GY, Maeda S, et al. (2008) Hepatocyte necrosis induced by oxidative stress and IL-1 alpha release mediate carcinogen-induced compensatory proliferation and liver tumorigenesis. Cancer Cell 14: 156-165.

206. Visser S, Yang X Identification of LATS transcriptional targets in HeLa cells using whole human genome oligonucleotide microarray. Gene 449: 22-29.

207. Suzuki A, Sekiya S, Buscher D, Izpisua Belmonte JC, Taniguchi H (2008) Tbx3 controls the fate of hepatic progenitor cells in liver development by suppressing p19ARF expression. Development 135: 1589-1595.

208. Alagille D, Odievre M, Gautier M, Dommergues JP (1975) Hepatic ductular hypoplasia associated with characteristic facies, vertebral malformations, retarded physical, mental, and sexual development, and cardiac murmur. J Pediatr 86: 63-71.

209. Record CJ, Chaikuad A, Rellos P, Das S, Pike AC, et al. Structural comparison of human mammalian ste20-like kinases. PLoS One 5: e11905.

210. Stegert MR, Hergovich A, Tamaskovic R, Bichsel SJ, Hemmings BA (2005) Regulation of NDR protein kinase by hydrophobic motif phosphorylation mediated by the mammalian Ste20-like kinase MST3. Mol Cell Biol 25: 11019-11029.

211. Potter CJ, Xu T (2001) Mechanisms of size control. Curr Opin Genet Dev 11: 279-286.

212. Thomas G, Hall MN (1997) TOR signalling and control of cell growth. Curr Opin Cell Biol 9: 782-787.

213. Schmelzle T, Hall MN (2000) TOR, a central controller of cell growth. Cell 103: 253-262.

214. Jackson LN, Larson SD, Silva SR, Rychahou PG, Chen LA, et al. (2008) PI3K/Akt activation is critical for early hepatic regeneration after partial hepatectomy. Am J Physiol Gastrointest Liver Physiol 294: G1401-1410.

215. Natarajan A, Wagner B, Sibilia M (2007) The EGF receptor is required for efficient liver regeneration. Proc Natl Acad Sci U S A 104: 17081-17086.

216. Wustefeld T, Rakemann T, Kubicka S, Manns MP, Trautwein C (2000) Hyperstimulation with interleukin 6 inhibits cell cycle progression after hepatectomy in mice. Hepatology 32: 514-522.

217. James MF, Han S, Polizzano C, Plotkin SR, Manning BD, et al. (2009) NF2/merlin is a novel negative regulator of mTOR complex 1, and activation of mTORC1 is associated with meningioma and schwannoma growth. Mol Cell Biol 29: 4250-4261.

218. Lopez-Lago MA, Okada T, Murillo MM, Socci N, Giancotti FG (2009) Loss of the tumor suppressor gene NF2, encoding merlin, constitutively activates integrin-dependent mTORC1 signaling. Mol Cell Biol 29: 4235-4249.

219. Lehtinen MK, Yuan Z, Boag PR, Yang Y, Villen J, et al. (2006) A conserved MST-FOXO signaling pathway mediates oxidative-stress responses and extends life span. Cell 125: 987-1001.

220. Xin M, Kim Y, Sutherland LB, Qi X, McAnally J, et al. Regulation of insulin-like growth factor signaling by Yap governs cardiomyocyte proliferation and embryonic heart size. Sci Signal 4: ra70.

221. Ziosi M, Baena-Lopez LA, Grifoni D, Froldi F, Pession A, et al. dMyc functions downstream of Yorkie to promote the supercompetitive behavior of hippo pathway mutant cells. PLoS Genet 6.

222. Neto-Silva RM, de Beco S, Johnston LA Evidence for a growth-stabilizing regulatory feedback mechanism between Myc and Yorkie, the Drosophila homolog of Yap. Dev Cell 19: 507-520.

223. Ravitz MJ, Chen L, Lynch M, Schmidt EV (2007) c-myc Repression of TSC2 contributes to control of translation initiation and Myc-induced transformation. Cancer Res 67: 11209-11217.

224. Soucek T, Pusch O, Wienecke R, DeClue JE, Hengstschlager M (1997) Role of the tuberous sclerosis gene-2 product in cell cycle control. Loss of the tuberous sclerosis gene-2 induces quiescent cells to enter S phase. J Biol Chem 272: 29301-29308.

225. Soucek T, Rosner M, Miloloza A, Kubista M, Cheadle JP, et al. (2001) Tuberous sclerosis causing mutants of the TSC2 gene product affect proliferation and p27 expression. Oncogene 20: 4904-4909.

226. Oldham S, Montagne J, Radimerski T, Thomas G, Hafen E (2000) Genetic and biochemical characterization of dTOR, the Drosophila homolog of the target of rapamycin. Genes Dev 14: 2689-2694.

227. Volarevic S, Stewart MJ, Ledermann B, Zilberman F, Terracciano L, et al. (2000) Proliferation, but not growth, blocked by conditional deletion of 40S ribosomal protein S6. Science 288: 2045-2047.

228. Jiang YP, Ballou LM, Lin RZ (2001) Rapamycin-insensitive regulation of 4e-BP1 in regenerating rat liver. J Biol Chem 276: 10943-10951.

229. Goggin MM, Nelsen CJ, Kimball SR, Jefferson LS, Morley SJ, et al. (2004) Rapamycin-sensitive induction of eukaryotic initiation factor 4F in regenerating mouse liver. Hepatology 40: 537-544.

230. Basu S, Totty NF, Irwin MS, Sudol M, Downward J (2003) Akt phosphorylates the Yes-associated protein, YAP, to induce interaction with 14-3-3 and attenuation of p73-mediated apoptosis. Mol Cell 11: 11-23.

231. LoPiccolo J, Blumenthal GM, Bernstein WB, Dennis PA (2008) Targeting the PI3K/Akt/mTOR pathway: effective combinations and clinical considerations. Drug Resist Updat 11: 32-50.

232. Hahn-Windgassen A, Nogueira V, Chen CC, Skeen JE, Sonenberg N, et al. (2005) Akt activates the mammalian target of rapamycin by regulating cellular ATP level and AMPK activity. J Biol Chem 280: 32081-32089.

233. Yagi R, Chen LF, Shigesada K, Murakami Y, Ito Y (1999) A WW domain-containing yes-associated protein (YAP) is a novel transcriptional co-activator. EMBO J 18: 2551-2562.

234. Hu S, Xie Z, Qian J, Blackshaw S, Zhu H (2010) Functional protein microarray technology. Wiley Interdiscip Rev Syst Biol Med 3: 255-268.

235. Tomizawa M, Garfield S, Factor V, Xanthopoulos KG (1998) Hepatocytes deficient in CCAAT/enhancer binding protein alpha (C/EBP alpha) exhibit both hepatocyte and biliary epithelial cell character. Biochem Biophys Res Commun 249: 1-5.

236. Shiojiri N, Takeshita K, Yamasaki H, Iwata T (2004) Suppression of C/EBP alpha expression in biliary cell differentiation from hepatoblasts during mouse liver development. J Hepatol 41: 790-798.

237. Yamasaki H, Sada A, Iwata T, Niwa T, Tomizawa M, et al. (2006) Suppression of C/EBPalpha expression in periportal hepatoblasts may stimulate biliary cell differentiation through increased Hnf6 and Hnf1b expression. Development 133: 4233-4243.

238. Yoshida Y, Hughes DE, Rausa FM, 3rd, Kim IM, Tan Y, et al. (2006) C/EBPalpha and HNF6 protein complex formation stimulates HNF6-dependent transcription by CBP coactivator recruitment in HepG2 cells. Hepatology 43: 276-286.

239. Birkenmeier EH, Gwynn B, Howard S, Jerry J, Gordon JI, et al. (1989) Tissue-specific expression, developmental regulation, and genetic mapping of the gene encoding CCAAT/enhancer binding protein. Genes Dev 3: 1146-1156.

240. Landschulz WH, Johnson PF, Adashi EY, Graves BJ, McKnight SL (1988) Isolation of a recombinant copy of the gene encoding C/EBP. Genes Dev 2: 786-800.

241. Antonson P, Xanthopoulos KG (1995) Molecular cloning, sequence, and expression patterns of the human gene encoding CCAAT/enhancer binding protein alpha (C/EBP alpha). Biochem Biophys Res Commun 215: 106-113.

242. Friedman AD, Landschulz WH, McKnight SL (1989) CCAAT/enhancer binding protein activates the promoter of the serum albumin gene in cultured hepatoma cells. Genes Dev 3: 1314-1322.

243. Dinic S, Bogojevic D, Petrovic M, Poznanovic G, Ivanovic-Matic S, et al. (2005) C/EBP alpha and C/EBP beta regulate haptoglobin gene expression during rat liver development and the acute-phase response. Mol Biol Rep 32: 141-147.

244. Park EA, Roesler WJ, Liu J, Klemm DJ, Gurney AL, et al. (1990) The role of the CCAAT/enhancer-binding protein in the transcriptional regulation of the gene for phosphoenolpyruvate carboxykinase (GTP). Mol Cell Biol 10: 6264-6272.

245. Clotman F, Lannoy VJ, Reber M, Cereghini S, Cassiman D, et al. (2002) The onecut transcription factor HNF6 is required for normal development of the biliary tract. Development 129: 1819-1828.

246. Coffinier C, Gresh L, Fiette L, Tronche F, Schutz G, et al. (2002) Bile system morphogenesis defects and liver dysfunction upon targeted deletion of HNF1beta. Development 129: 1829-1838.

247. Shen CN, Slack JM, Tosh D (2000) Molecular basis of transdifferentiation of pancreas to liver. Nat Cell Biol 2: 879-887.

248. Kinoshita T, Sekiguchi T, Xu MJ, Ito Y, Kamiya A, et al. (1999) Hepatic differentiation induced by oncostatin M attenuates fetal liver hematopoiesis. Proc Natl Acad Sci U S A 96: 7265-7270.

249. Kamiya A, Kinoshita T, Ito Y, Matsui T, Morikawa Y, et al. (1999) Fetal liver development requires a paracrine action of oncostatin M through the gp130 signal transducer. EMBO J 18: 2127-2136.

250. Yoshimura A, Ichihara M, Kinjyo I, Moriyama M, Copeland NG, et al. (1996) Mouse oncostatin M: an immediate early gene induced by multiple cytokines through the JAK-STAT5 pathway. EMBO J 15: 1055-1063.

VITA

Li Lu was born in Taicang, Jiangsu, China in 1977. After completing her work at Shaxi High School, Taicang, Jiangsu in 1996, she entered Nanjing University in Nanjing, Jiangsu. She received the degree of Bachelor of Science with a major in Biology from Nanjing University in July 2000. For the next two years, she worked as a research technician in the Institution of Molecular Medicine at Nanjing University. In September of 2002, she entered Nanjing Medical University in Nanjing. She received the degree of Master of Science with a major in Biomedical Science from Nanjing Medical University in July 2005. For the next two years, she worked as a research assistant in the Department of Neuron-Oncology at MD Anderson Cancer Center. In August of 2007 she entered the University of Texas Health Science Center at Houston Graduate School of Biomedical Sciences.

Permanent address:

Fuqiao Peace Gordon 35-404,

Taicang, Jiangsu, 215434

P.R.China